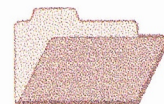




CRCLEME

Cooperative Research Centre for
Landscape Evolution & Mineral Exploration



**OPEN FILE
REPORT
SERIES**



CSIRO
EXPLORATION
AND MINING



Australian Mineral Industries Research Association Limited ACN 004 448 266

MULTI-ELEMENT SOIL SURVEY OF THE MOUNT HOPE AREA, WESTERN AUSTRALIA

M.J. Lintern, H.M. Churchward and C.R.M. Butt

CRC LEME OPEN FILE REPORT 40

October 1998

(CSIRO Division of Exploration Geoscience Report I09R, 1990.
Second impression 1998)

CRC LEME is an unincorporated joint venture between The Australian National University, University of Canberra, Australian Geological Survey Organisation and CSIRO Exploration and Mining, established and supported under the Australian Government's Cooperative Research Centres Program.



MULTI-ELEMENT SOIL SURVEY OF THE MOUNT HOPE AREA, WESTERN AUSTRALIA

M.J. Lintern, H.M. Churchward and C.R.M. Butt

CRC LEME OPEN FILE REPORT 40

October 1998

(CSIRO Division of Exploration Geoscience Report 109R, 1990.
Second impression 1998)

© CSIRO 1990

RESEARCH ARISING FROM CSIRO/AMIRA REGOLITH GEOCHEMISTRY PROJECTS 1987-1993

In 1987, CSIRO commenced a series of multi-client research projects in regolith geology and geochemistry which were sponsored by companies in the Australian mining industry, through the Australian Mineral Industries Research Association Limited (AMIRA). The initial research program, "Exploration for concealed gold deposits, Yilgarn Block, Western Australia" (1987-1993) had the aim of developing improved geological, geochemical and geophysical methods for mineral exploration that would facilitate the location of blind, buried or deeply weathered gold deposits. The program included the following projects:

P240: Laterite geochemistry for detecting concealed mineral deposits (1987-1991). Leader: Dr R.E. Smith.
Its scope was development of methods for sampling and interpretation of multi-element laterite geochemistry data and application of multi-element techniques to gold and polymetallic mineral exploration in weathered terrain. The project emphasised viewing laterite geochemical dispersion patterns in their regolith-landform context at local and district scales. It was supported by 30 companies.

P241: Gold and associated elements in the regolith - dispersion processes and implications for exploration (1987-1991). Leader: Dr C.R.M. Butt.

The project investigated the distribution of ore and indicator elements in the regolith. It included studies of the mineralogical and geochemical characteristics of weathered ore deposits and wall rocks, and the chemical controls on element dispersion and concentration during regolith evolution. This was to increase the effectiveness of geochemical exploration in weathered terrain through improved understanding of weathering processes. It was supported by 26 companies.

These projects represented "an opportunity for the mineral industry to participate in a multi-disciplinary program of geoscience research aimed at developing new geological, geochemical and geophysical methods for exploration in deeply weathered Archaean terrains". This initiative recognised the unique opportunities, created by exploration and open-cut mining, to conduct detailed studies of the weathered zone, with particular emphasis on the near-surface expression of gold mineralisation. The skills of existing and specially recruited research staff from the Floreat Park and North Ryde laboratories (of the then Divisions of Minerals and Geochemistry, and Mineral Physics and Mineralogy, subsequently Exploration Geoscience and later Exploration and Mining) were integrated to form a task force with expertise in geology, mineralogy, geochemistry and geophysics. Several staff participated in more than one project. Following completion of the original projects, two continuation projects were developed.

P240A: Geochemical exploration in complex lateritic environments of the Yilgarn Craton, Western Australia (1991-1993). Leaders: Drs R.E. Smith and R.R. Anand.

The approach of viewing geochemical dispersion within a well-controlled and well-understood regolith-landform and bedrock framework at detailed and district scales continued. In this extension, focus was particularly on areas of transported cover and on more complex lateritic environments typified by the Kalgoorlie regional study. This was supported by 17 companies.

P241A: Gold and associated elements in the regolith - dispersion processes and implications for exploration. Leader: Dr. C.R.M. Butt.

The significance of gold mobilisation under present-day conditions, particularly the important relationship with pedogenic carbonate, was investigated further. In addition, attention was focussed on the recognition of primary lithologies from their weathered equivalents. This project was supported by 14 companies.

Although the confidentiality periods of the research reports have expired, the last in December 1994, they have not been made public until now. Publishing the reports through the CRC LEME Report Series is seen as an appropriate means of doing this. By making available the results of the research and the authors' interpretations, it is hoped that the reports will provide source data for future research and be useful for teaching. CRC LEME acknowledges the Australian Mineral Industries Research Association and CSIRO Division of Exploration and Mining for authorisation to publish these reports. It is intended that publication of the reports will be a substantial additional factor in transferring technology to aid the Australian Mineral Industry.

This report (CRC LEME Open File Report 40) is a Second impression (second printing) of CSIRO, Division of Exploration Geoscience Restricted Report 109R, first issued in 1990, which formed part of the CSIRO/AMIRA Project P241.

Copies of this publication can be obtained from:

The Publication Officer, c/- CRC LEME, CSIRO Exploration and Mining, PMB, Wembley, WA 6014, Australia. Information on other publications in this series may be obtained from the above or from <http://leme.anu.edu.au/>

Cataloguing-in-Publication:

Lintern, M.J.

Multi-element soil survey of the Mount Hope Area, Western Australia

ISBN 0 642 28296 X

1. Soils 2. Soil surveys - Western Australia - Mount Hope Region 3. Geochemistry.

I. Churchward, H.M. II. Butt, C.R.M. III. Title

CRC LEME Open File Report 40.

ISSN 1329-4768

PREFACE

The CSIRO-AMIRA project "Exploration for Concealed Gold Deposits, Yilgarn Block, Western Australia" has as its overall aim the development of improved geological, geochemical and geophysical methods for mineral exploration that will facilitate the location of blind, concealed or deeply weathered gold deposits. This Report presents results of research conducted as part of Module 2 of this project (AMIRA Project 241): "Gold and Associated Elements in the Regolith - Dispersion Processes and Implications for Exploration".

The objectives of this module are, *inter alia*, to suggest improvements in techniques of sampling and data interpretation for gold exploration, and to increase knowledge of the properties and genesis of the regolith. This report is a continuation of an earlier study conducted at Mt.Hope (Lintern, 1989). The results of the present study contribute strongly to these objectives by (i) further investigating the relationship between gold and the alkaline earth metals established in the earlier report (ii) examining the distribution of other geochemical components of the regolith (iii) using a statistical approach to integrate the available data to interpret geochemical distribution patterns. Work is continuing at Mt.Hope and elsewhere to understand the nature of the association between gold and the carbonates.

C.R.M. Butt,
Project Leader.
April, 1990.

ABSTRACT

Composite soil auger samples from the top metre were analysed for elements and compared with similar existing information for Au. Regolith and geomorphological features were mapped from air photo and field studies and, in conjunction with existing geology maps were used to interpret the observed distribution of the elements. Initially, simple distribution maps, selected binary plots, histograms and correlation matrices were used to describe the results. Further statistical treatment using R-Q mode principal component analysis and cluster analysis developed the interpretation. The results demonstrated strong associations between certain elements, soil type and underlying geology. Most notable were the associations between SiO_2 and sediments, transition metals and the laterites, and alkali and alkaline earth metals with the red earth soils. Whilst Au itself did not show any strong associations certain areas have been identified from this integrated approach that warrant further investigation.

CONTENTS

	Page
INTRODUCTION	2
STUDY AREA DESCRIPTION	
Physical setting	5
Geology	6
The Regolith	8
The Soil Pattern	10
SAMPLING and ANALYTICAL METHODS	13
RESULTS and DISCUSSION	14
FURTHER DISCUSSION	53
FURTHER STATISTICAL ANALYSIS	
Introduction and methods	57
Results and discussion	58
SUMMARY	69
ACKNOWLEDGEMENTS	70
REFERENCES	70
APPENDICES	71

INTRODUCTION

The Mt. Hope area, located south of Southern Cross, lies in the narrow Southern Cross-Forrestania Greenstone Belt which extends for over 300km in a near north-south orientation. This greenstone belt is currently undergoing intensive exploration for Au, with the Bounty mine and associated pits the most recent testaments to the potential of the region as a major producer.

Exploration here has involved a variety of techniques including stream sediment and soil sampling, and deep drilling into the regolith. Surface sampling by auger has been particularly successful because Au, where present, commonly occurs within the top metre of the profile. The soil anomaly that existed for Au at the Bounty minesite was a notable example.

Earlier investigations by CSIRO (Lintern, 1989) have revealed a strong correlation between pedogenic alkaline earth carbonates and Au in the top metre of the soil profiles. The relationship appears to be developed most prominently when the total concentration of carbonate exceeds about 0.5 - 1%. Such concentrations are not commonly found within lateritic duricrusts or gravels at Mt. Hope but occur, instead, in adjacent and overlying calcareous red earths that are abundant throughout the lease area. These calcareous earths are widespread throughout the Southern Cross-Forrestania Greenstone Belt and the most important conclusion from the previous work is that the carbonate layer be sampled when exploring for Au. If the carbonate is not sampled, when present, then areas determined to have no Au anomalies cannot be considered to have been explored effectively.

Whereas Au soil anomalies in themselves warrant further investigation (e.g. by drilling) other areas of interest may be indicated by elements other than Au. For example, at Mt. Hope, Mn, Ba and Cu distributions are highly correlated with Au in carbonate profiles (Lintern, 1989). The distribution of these and other elements on a semi-regional basis therefore may make it possible to identify additional areas of interest for exploration. Multi-element geochemistry is a well established exploration technique for deeply weathered terrain. In Western Australia, it has mainly been applied to areas having more or less complete, predominantly residual lateritic profiles. Stripped or eroded landscapes have not been routinely sampled except where particular soil components (e.g. ferruginous lags) are present. The advantage of multi-element geochemistry is that (i) indicator (or pathfinder) elements associated with the target mineralization may be detected and there (ii) may be present

spatially larger or more persistent anomalies than the target element due to different original distributions and/or geochemical behaviour during weathering. Such an approach has been applied to the auger soil survey at Mt. Hope. The Au-carbonate association has been examined in detail to determine whether other elements or combinations of elements provide information additional to that if Au alone was considered.

Initial exploration in the region was by routine soil sampling using shallow auger drilling. This procedure is particularly suitable over much of the area because carbonate development appears to be strongest in the top metre of the soil profile (Figure 1). A pilot study was instigated using approximately 150 samples from around the Bounty minesite to test the usefulness of the approach. The results, incorporated within this current study, indicated areas that were geochemically anomalous in elements other than Au, including Mn and Ba, and suggested that further expansion of the study area was warranted to establish the regional significance. Mapping of major regolith units within the area was also undertaken and, combined with the known geology and topography, provided an integrated approach to the interpretation of geochemical dispersion in the region. This study covers a 6.5 by 1.5 km area mainly to the south of, but including, the Bounty minesite.

Figure 1 (opposite): Map showing the auger sample locations within the area considered in this study.

STUDY AREA DESCRIPTION

Physical setting

The Mt. Hope area is on the Great Plateau of Western Australia and is situated in the upper Avon catchment, close to the regional divide between the west- and east-trending drainages. The terrain is broadly undulating, and dominated by sandy lateritic detritus forming landscapes commonly referred to as sandplains. The elevation is mostly 400 to 450 m a.s.l., rising to about 500 m a.s.l. as occasional summits such as Mt. Holland and North Ironcap, which have developed on banded iron formation (BIF). Broad undulations in this landscape relate to a system of valleys that commence as shallow upland concavities and merge downslope with deeper and broader valley forms. These are tributary to the major drainages which are in part occupied by salt lake systems.

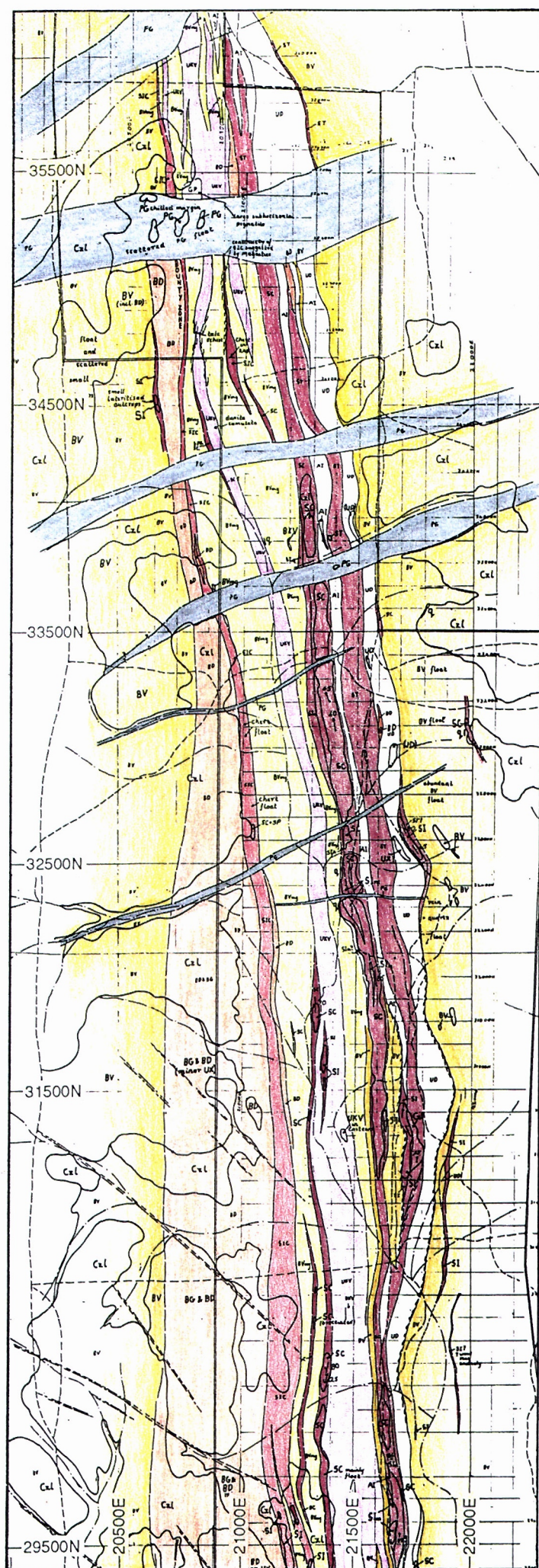
The Bounty mine at Mt. Hope is in a north-south trending valley tract, set some 20 m below a local drainage divide. There are significant topographic changes along this tract related to the presence within it of a divide at about 34500N (Aztec Exploration grid). To the north east, the drainage trends along a broad unchannelled valley floor. At this point, the floor is approximately 20 km from a major salt lake system and the gradient is 1:500 to 1:700. In contrast, drainage southwards from the divide occupies a clearly defined channel flanked by gentle, somewhat linear, slopes. This channel, which is active only after heavy rain, is approximately 8 to 9 km from a salt lake system and has a gradient of 1:300.

Short first-order tributaries of this valley system feed from shallow erosional tracts along the mid to upper valley side. Low breakaway scarps or smoothly rounded convexo-concave slope elements can occur along the upper slope limits of these areas and separate them from the sandy uplands. Each erosional tract is separated by low, gently sloping, sandy spurs that extend

from the uplands towards the valley floor. Amalgamation of adjacent erosional tracts, in the upper slope positions, has ensured isolation of elements of the sandy tract in lower slope positions. These outliers (e.g. as at 20900E 33500N) are often partially flanked by low breakaways. The more active erosional environments of the southern drainage has ensured that chert outcrops, or subcrops, as low elongate north-south stony ridges arrayed approximately parallel to the main drainage channels.

Geology

As part of the Yilgarn Block, this region is underlain by Archaean granitoid rocks with minor interfolded belts of metamorphosed volcanic and sedimentary rocks which have a general north-north west strike (Johnstone et al., 1973). The Mt. Hope project is situated in one such zone of metamorphic rocks, the Forrestania Greenstone Belt, an extension, from the north, of the Southern Cross Greenstone Belt. The Forrestania Greenstone Belt (Chin et al., 1984) is dominated by tholeiitic basalt and occupies wide zones to the east and west of a core of sediments that comprise cherts, siltstones and sandstones. Ultramafic rocks, including komatiites, now occurring as chlorite schists, and serpentized dunites are also present. Some meta-gabbros are associated with the flanking mafic rocks, and several units BIF units are associated with ultramafic rocks. A series of lower Proterozoic gabbroic dykes with a general east-west orientation, cross-cut the greenstone sequence. The Bounty mine currently focuses on a narrow zone of B.I.F.-related Fe-amphibolites and some associated siliceous and pelitic rocks. This is known locally as the "Bounty Zone" and is flanked by dolerite to the west and by high-Mg basalts to the east. The geological map (Figure 2) is based on mapping by J.Martyn and Associates, consultants to Aztec Exploration Ltd., and is presented as an overlay to aid comparison between geochemical, geological and soil data.



CxL	Ferricrete
(UD)	Silcrete & ferricrete over weathered dunite
(UKV)	Silcrete & ferricrete over weathered komatiite
PG	Lower Proterozoic gabbro, granophyre etc. dykes
NB: All Archaean rocks are metamorphosed to amphibolite grade	
q	Quartz veins
GP	Pegmatite, associated muscovite-rich granite
AI	Miscellaneous fine-medium grained felsic to intermediate igneous rocks in RAB and poor outcrop; either porphyry intrusives or volcanic lenses
ST	Siltstone & sandstone (psammitic-semipellitic schist)
SP	Pelitic rocks including graphitic pelite
SIC	Mixed BIF-related assemblage including magnetite, Fe-amphiboles, silica and pelite
SC	Chert, Fe-rich chert, local magnetite bands
SI	BIF - undifferentiated
SIm	Magnetite-rich BIF
BV	Tholeiitic basalt & dolerite - hornblende or actinolite amphibolite
BVmg	High-Mg basalt, actinolite-chlorite-plag. rock
BKV	Pyroxenitic komatiite - mainly nematoblastic amphibole-chlorite rock
UKV	Peridotitic komatiite, spinifex-textured, dunite cumulate zones, talcose schists
BD	Dolerite
BG	Gabbro
UX	Pyroxenite, coarse actinolite-chlorite rock
UD	Intrusive dunite (minor peridotite, pyroxenite & komatiite) coarse bladed metamorphic olivine textures, talc schists
	Drainage lines

Scale 1:25,000

Fig 2. **COMBINED OUTCROP
AND INTERPRETATION
GEOLOGICAL MAP**

Supplied by Aztec Exploration Ltd
(Colours drafted by CSIRO)

The Regolith

A deep regolith derived by long continued weathering is an extensive feature of the study area. As elsewhere in south-west Australia, the upper part of deep weathered mantle comprise a lateritic ferruginous horizon. This merges at depth to a mottled clay (the mottled horizon), thence to a bleached saprolite which in turn merges into unweathered rock. Much of the ferruginous horizon as exposed in the Bounty and North Bounty pits consists of indurated light brown to reddish brown mottled material with incipient pisolitic structures. It ranges in thickness from 2 to 4 m. Horizontal to subhorizontal, slightly convoluted structures (possibly once voids) are occupied by very pale grey sandy clay. Well defined black nodules (10 mm diameter) occur in the brown phase; locally, these are very abundant and form nodular duricrusts one to two metres thick that extend laterally for tens of metres. The full profile is not present over much of the study area and the ferruginous horizon is commonly absent. In these areas, the saprolite and, locally, colluvium/alluvium, are the soil material.

There are four principal soil types in the region; they are as follows: (i) friable yellow to reddish brown clayey sand with abundant brown subangular to sub-rounded gravels. These are developed on duricrust; they are acid in reaction and hence are in marked contrast to the other major group of soils in the area; (ii) red to light brown friable clay loams with much soft carbonate at a shallow depth (i.e. usually less than 15 cm). Some profiles of this general group merge, at depths of about 1-2m, to saprolite derived from mafic rock. However, more commonly, massive dark red brown to dark brown clays appear at 50 to 70 cm and form a continuous substrate below about 100 cm, although some large pockets of soft carbonate continue to about 1.5 m. This clay substrate is very plastic and has a neutral or mildly acid pH. It can merge, over a narrow zone, to weathered rock, at a depth of from five or six

metres; (iii) duplex soils consisting of greyish brown sandy clay, 10-15cm thick, overlying massive brown calcareous clay; (iv) reddish yellow brown loose sands are developed on the chert hills. Large amounts of chert fragments can appear at the surface or at depths of up to 30 cm with partially weathered chert appearing at about 50 to 75 cm.

The areas dominated by lateritic gravelly sand regoliths are commonly laterally separated from the calcareous and clay-rich regoliths by erosional breaks. However, in places, such breaks are unclear or absent; for example where spurs dominated by the lateritic regoliths extend from uplands to the adjacent valley floor. This is the case at the North Bounty pit. In the east wall of the pit, the outcropping lateritic profile at the south end is situated on the lower end of a spur. To the north, this profile is buried beneath calcareous clays. Here, the friable calcareous light brown clay merges at a depth of less than a metre to plastic non-calcareous clay. Beneath this is a laterite duricrust, which itself merges at depth to a coarsely mottled clay. This laterite duricrust also changes laterally to a mottled clay and represents the dominant substrate to the dark brown clays, although in places a light brown clay horizon, 30 cm thick, intervenes between these materials. Near the north-west corner of this pit, gravelly lenses (30 cm thick and about 100 cm long) are present at the interface between the dark brown plastic clay and the underlying mottled clay. This suggests that fluvial transport could have played a role in development of the upper parts of the regolith. Conversely, in other profiles (e.g. east wall of Bounty pit) plastic clay is continuous with the underlying weathered rocks (high-Mg basalt) implying it to be residual.

The Soil Pattern

The main elements of the soil pattern relate to the erosional modification of a deep intensively weathered regolith (Figure 3). Erosion has exposed deeper less weathered elements of this regolith and the country rock. In addition some of these materials have moved downslope as sediments or in solution resulting in further modification of the soil pattern.

Large areas of calcareous clays occur where erosion has removed the lateritic sandy soils. This has been particularly effective adjacent to areas drained by the clearly defined incised southward drainage. Local erosional catchments have developed on slopes, however, suggesting the erosion need not be directly related to drainage incision, but rather to specific slope conditions, the nature of which were not clarified in this study. Debris from the local catchments had accumulated as fans on the broad valley floors north of the valley divide. Such a catchment occurs between 35500-36000N where a large area of calcareous soil on the slopes that rise westward from the Bounty pit can be accounted for by local slope processes.

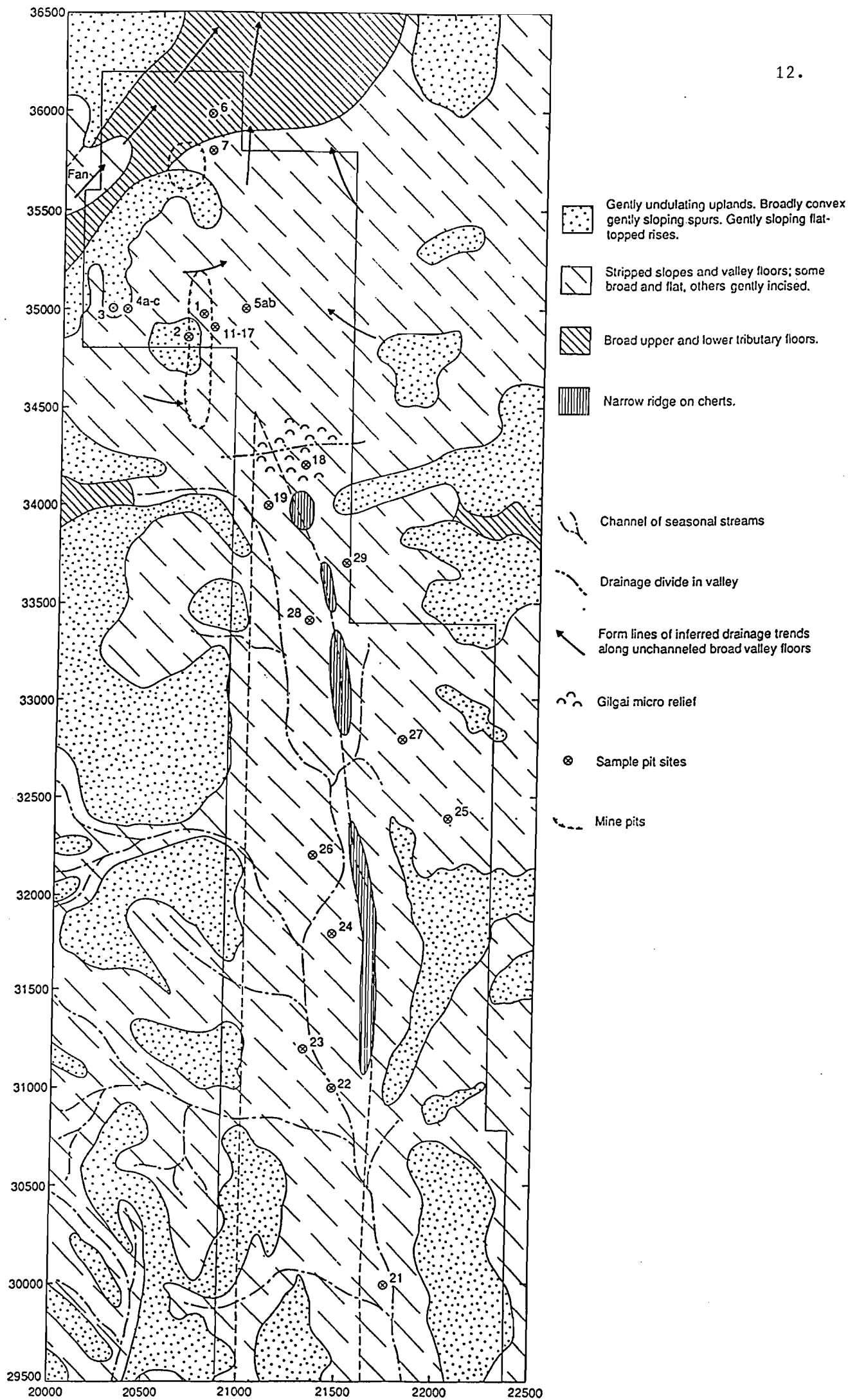
Some calcareous red earths have an associated gilgai micro-relief featuring a complex pattern of sink holes and low mounds (puffs). These are best developed in an area of a few hectares on the valley divide between the north and south drainages.

The most common substrate to the calcareous clays are non-calcareous dark red brown plastic clays, although there are significant areas where very friable clays directly occur over weathered rock. However a more precise statement of their relative distributions could only be obtained by more intensive field traversing.

The duplex soils appear north of 36000N on the broad valley floor of the northward drainage. Carbonate is present at about 30 to 40 cm but they

overlie non-calcareous plastic red clays. The flanking slopes are much less stripped and the sandy surface of this soil in part reflects the greater extent of intact sandy lateritic profiles. Similarly, the generally lower abundance of carbonates in these soils reflect the absence of extensive areas of calcareous clays on the adjacent slopes.

Figures 3 (opposite): Soil pattern for the Mt. Hope area. Profiles 8, 9 and 10 do not exist, and Profile 20 occurs off the map at 21725E 28500N



SAMPLING and ANALYTICAL METHODS

Samples from the augering programme were provided by Aztec Exploration Ltd. These consisted of soils that had been collected and composited over a depth of about a metre using a small vehicle-mounted RAB drill. They had been homogenized, split and pulverized. The "pulp rejects" resulting from the earlier analysis were then collected by CSIRO for the further geochemical analysis.

Soil profile sites were selected on the basis of unusual auger analytical data e.g. high Au values. Pits were dug using a back-hoe but had to be restricted to the areas of clay-rich soil because in the lateritic areas the soils were too hard and dry. The soils so exposed were photographed, described and systematically sampled to the bottom of the pit.

Coarse material was collected and wet sieved in the laboratory into coarse (>2mm) and fine (<2mm), magnetic and non-magnetic fractions. Leaf litter was also collected at each site together, with fresh vegetative material from *Melaleuca* spp. shrubs and *Eucalyptus* spp. trees.

Soil samples and lags were analysed by ICP for a variety of major and minor elements following an alkali fusion digest. Sodium and K were determined by AAS using the same digest; As was determined following single acid digest (for the auger pulps), and Au by either an aqua regia digest (for the auger pulps) followed by AAS or cyanide digestion (for the profile samples) followed by ICPMS. In addition, soil profile samples were analysed for Ga, Ge, Nb, Pb, Rb, Sr, Y, Zn, S and Se by XRF.

Vegetation and litter samples were analysed by ICP following ashing and fusion digest. Gold was analysed by GFAAS after DIBK extraction. Detailed descriptions of the methods are given in the earlier report (Lintern, 1989).

Statistical treatment of the results (e.g. correlation matrix, R-Q mode principal component analysis and cluster analysis) was effected using programs designed by E.C. Grunsky (CSIRO) and the BRGM (Bureau de Recherches Geologiques et Minieres). Similar programs are commercially available e.g. SYSTAT. Contouring of isochemical points for each component (the distribution maps) was performed after gridding and weighting the data points according to the kriging algorithm.

Raw data for the entire series are available on the disc in a variety of formats.

RESULTS and DISCUSSION

The results for each element and oxide are described and discussed in turn. Histograms and cumulative frequency plots are included for each element and oxide. A few outlying analyses of samples falling outside the chosen class range are not included in the histogram.

The results for the 1060 auger samples are contour plotted by elements and oxides in Figures 4 to 22.

Detailed results for the profiles, lag and biogeochemical studies will be interpreted separately and included in a later report.

Confidence limits are semi-quantitative values determined for each element by analysis and describe the level above which values are considered generally precise and accurate.

Elementary statistical parameters are summarized in Appendix Table 2.

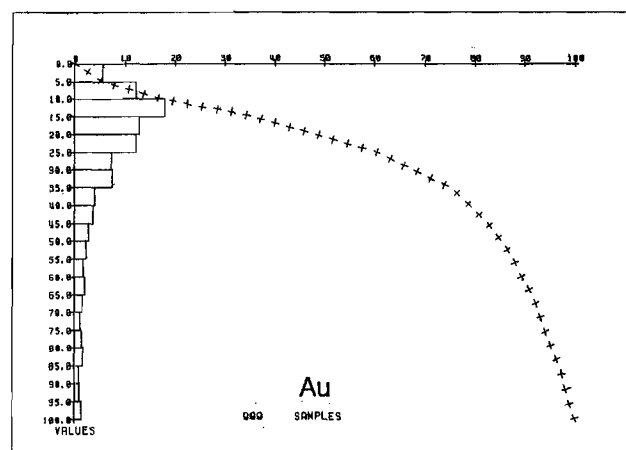
Au.

Mean value (ppb) 38

Standard deviation 64

Range 1 to 1020

Confidence limit 1

Components showing high positive correlation ($\alpha < 0.001$)MgO CaO Na₂O K₂OComponents showing high negative correlation ($\alpha < 0.001$)Al₂O₃ Fe₂O₃ TiO₂ Co V

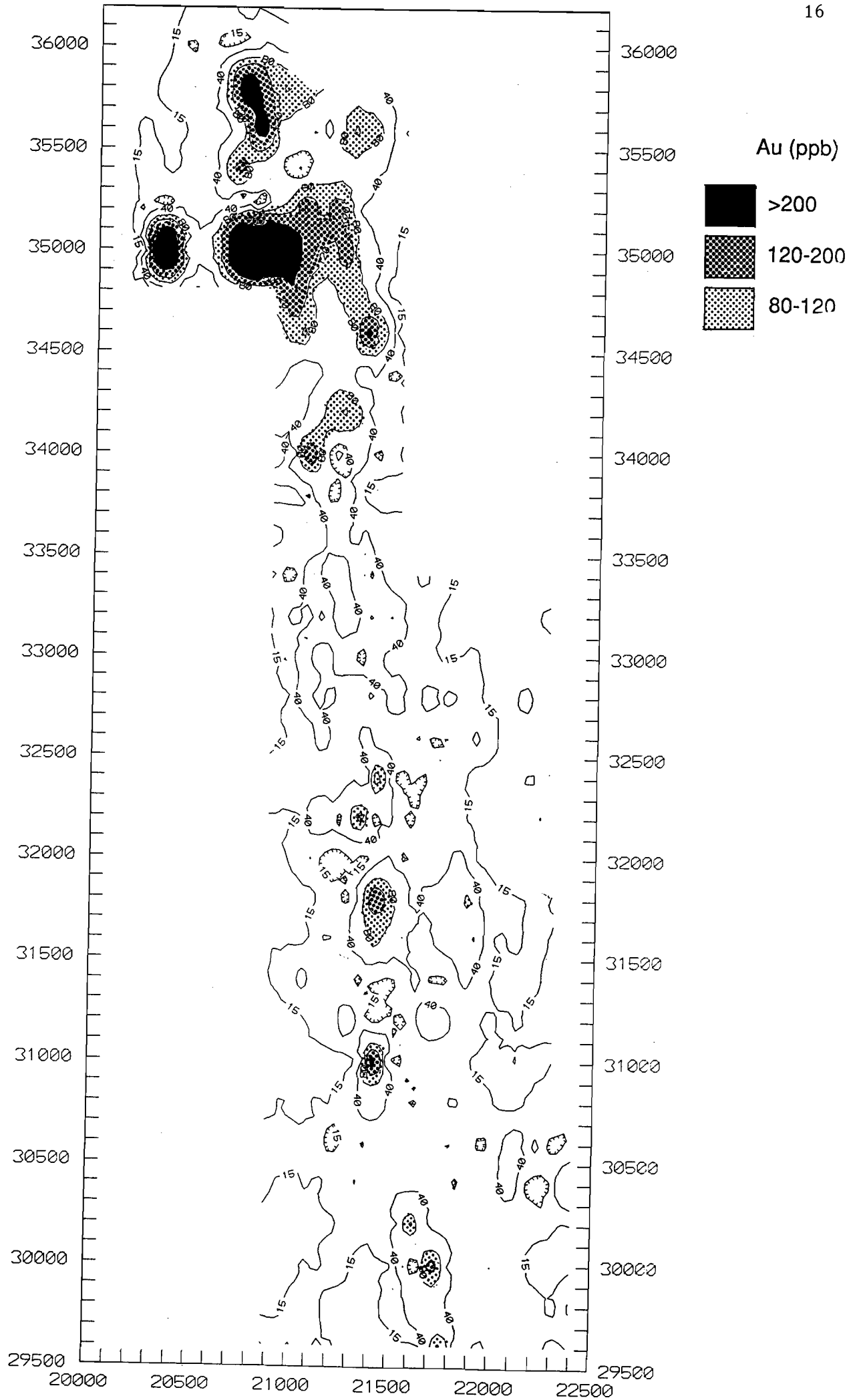
Gold values have a positively skewed distribution and a high standard deviation. The range of values is one of the highest for any of the components studied extending over at least four orders of magnitude.

Gold shows a statistically significant correlation with the alkali and alkaline earth metals but with little association with iron oxides (Appendix Figure 6).

The distribution map indicates a nearly continuous zone of Au enrichment following a linear north-south trend through the centre of the study area. There is a strong association between the occurrence of Au and the presence of underlying chert/BIF. The major soil anomaly is associated with the present Bounty Pit (20800E 35000N), with its size and shape suggesting considerable lateral dispersion. The remaining anomalies in the same area are associated with the North Bounty Pit (20800E 35800N) and the West Bounty Pit (20300E 35000N).

The anomalies are considered in greater detail in the section "Further Discussion". Of particular note, however, and discussed overleaf under As, is the occurrence of a Au concentration of 1.8 ppm in the fine magnetic fraction collected at Profile 24.

Figure 4 (opposite): Distribution of Au by soil auger sampling.



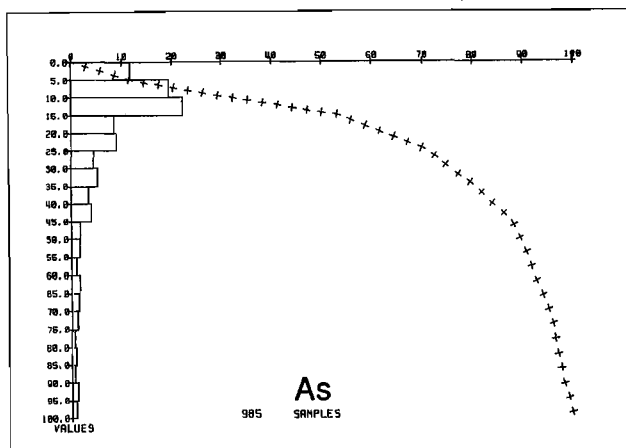
As.

Mean value (ppm) 34

Standard deviation 52

Range 1 to 570

Confidence limit 2

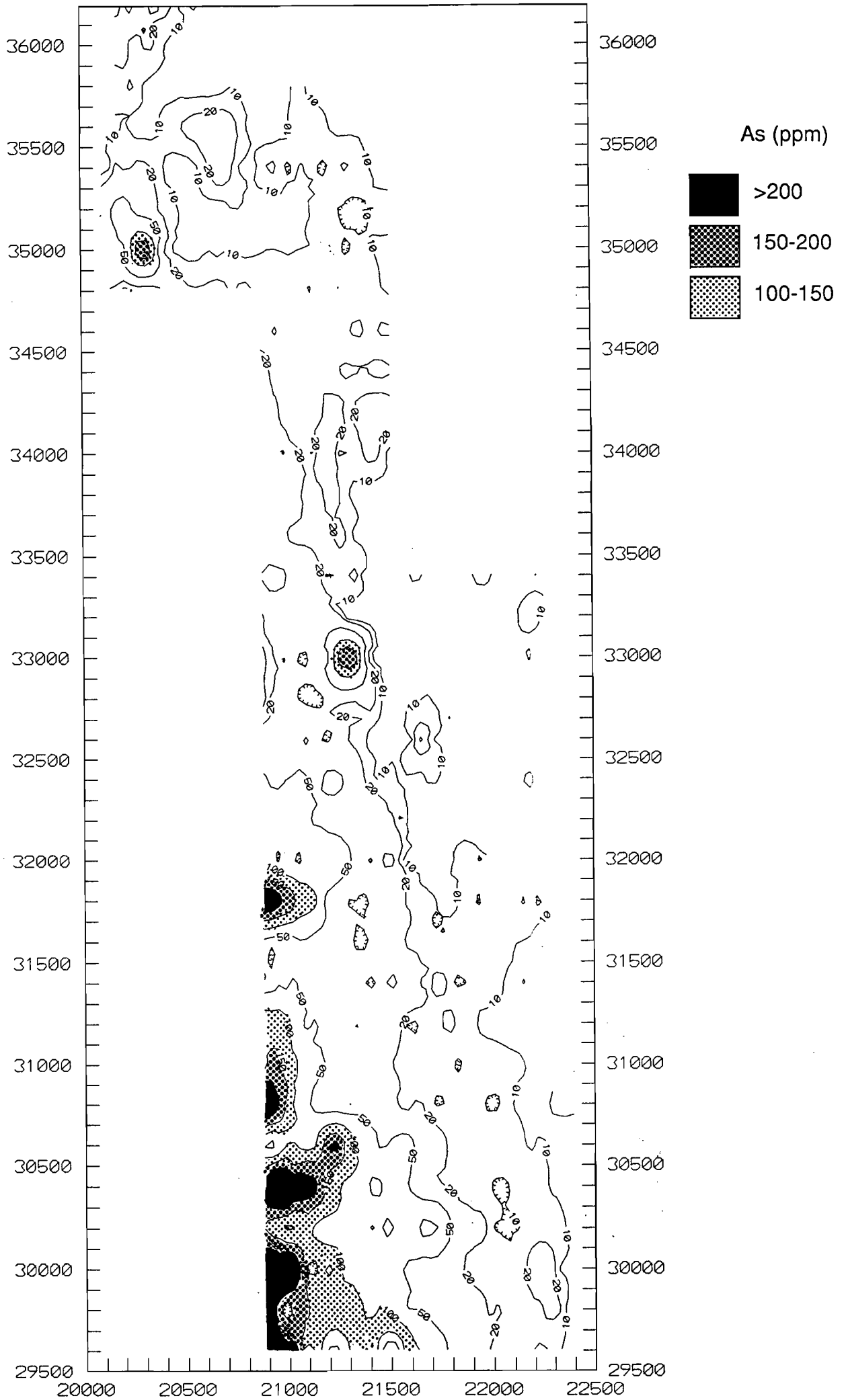
Components showing high positive correlation ($\alpha < 0.001$)Al₂O₃ Fe₂O₃ Co Cr V ZrComponents showing high negative correlation ($\alpha < 0.001$)SiO₂ MgO CaO Na₂O K₂O P₂O₅ Mn

The histogram and cumulative frequency plot suggest at least two populations of As. The high standard deviation value is due to the highly skewed nature of the distribution with a large proportion of the data (7%) falling outside the major size classes shown.

The distribution map indicates that As concentrations are low throughout much of the study area but are markedly enriched within the Fe₂O₃-rich lateritic soils in the south-west, which overlie basaltic and gabbroic rocks. The plot of As versus Fe₂O₃ can be seen in Appendix Figure 3. The results can be explained, at least in part, by the known tendency for As to concentrate with Fe₂O₃ in soils. Smaller areas of anomalously high As occur elsewhere in the study area the most notable of which are centred around (i) 20300E 35000N (over what is now the West Bounty Pit) and (ii) 21400E 33000N.

By plotting the As/Fe₂O₃ ratio, additional areas of interest are highlighted, the most significant of which is at 21500E 32000N. Profile 24 (21390E 31800N) was dug close to this anomaly and the fine magnetic lag material at this site contained 1.8 ppm Au. As arsenic is commonly considered an important pathfinder for Au, the anomalously high areas mentioned are of prime exploration significance.

Figure 5 (opposite): Distribution of As by soil auger sampling.



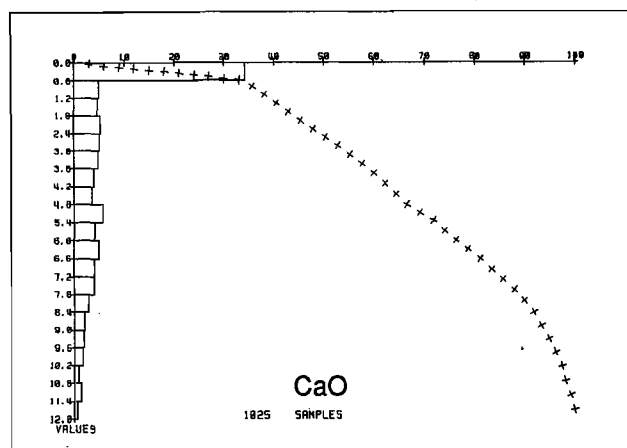
CaO.

Mean value (%) 3.7

Standard deviation 3.7

Range 0.01 to 18.63

Confidence limit 0.01

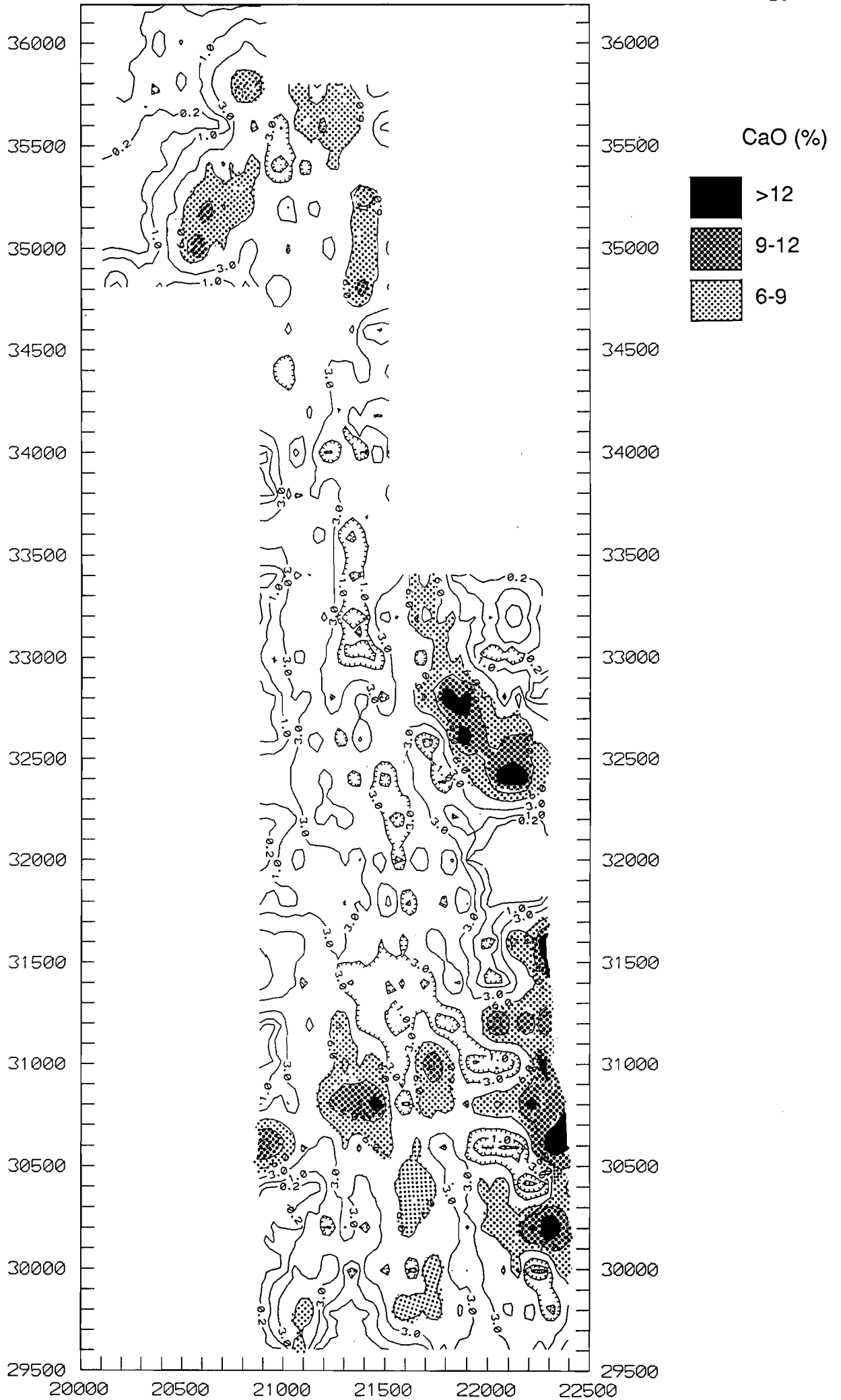
Components showing high positive correlation ($\alpha < 0.001$)MgO Na₂O K₂O P₂O₅ Au Ba Cu Mn NiComponents showing high negative correlation ($\alpha < 0.001$)SiO₂ Al₂O₃ Fe₂O₃ TiO₂ As Be Co Cr V Zr

Calcium and Mg, in these soils, occurs almost exclusively as pedogenic carbonate, dominantly calcite and dolomite. However, the samples were not analysed for CO₂ and results are reported as CaO.

The high standard deviation and highly skewed nature of the histogram is, like that for MgO, strong evidence for overlapping populations. The high correlations between CaO and other components are shown by the scattergrams in Appendix Figure 4.

The lowest CaO concentrations (<0.5%) occur in soils derived from the lateritic duricrusts and siliceous sedimentary rocks. The highest CaO concentrations (>0.5%) occur in the eastern portion of the study area in powdery calcareous earths overlying the tholeiitic basalts. Appreciable amounts of CaO also occur throughout the study area over a variety of rock types with local concentrations developing in some areas. Little CaO is found in the laterite. The Ca is probably derived from the immediately underlying bedrock. Plants and/or soil-water capillary processes may well play a role in the appearance of carbonate in the near surface environment. When calcite and dolomite are present in the same profile the former nearly always overlays the latter which suggests that surface reworking has taken place. Dolomite is more soluble than calcite in alkaline solutions and, therefore, more likely to precipitate second, so that a progressively downwards rather than upwards carbonate formation is postulated. The soil processes of colluviation, chemical dissolution and downslope deposition may cause localised concentrations in drainage areas.

Figure 6 (opposite): Distribution of CaO by soil auger sampling.



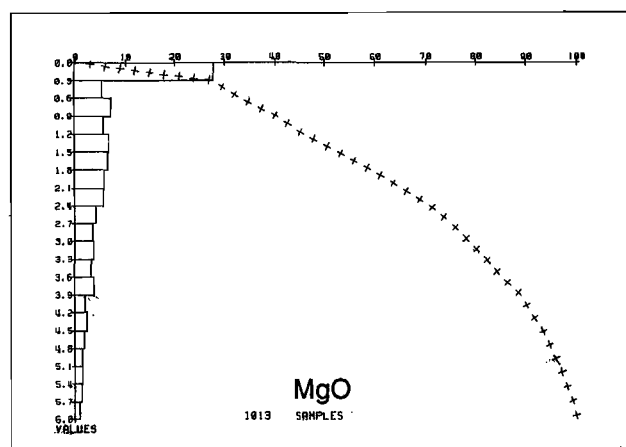
MgO.

Mean value (%) 2.0

Standard deviation 2.0

Range 0.01 to 11.54

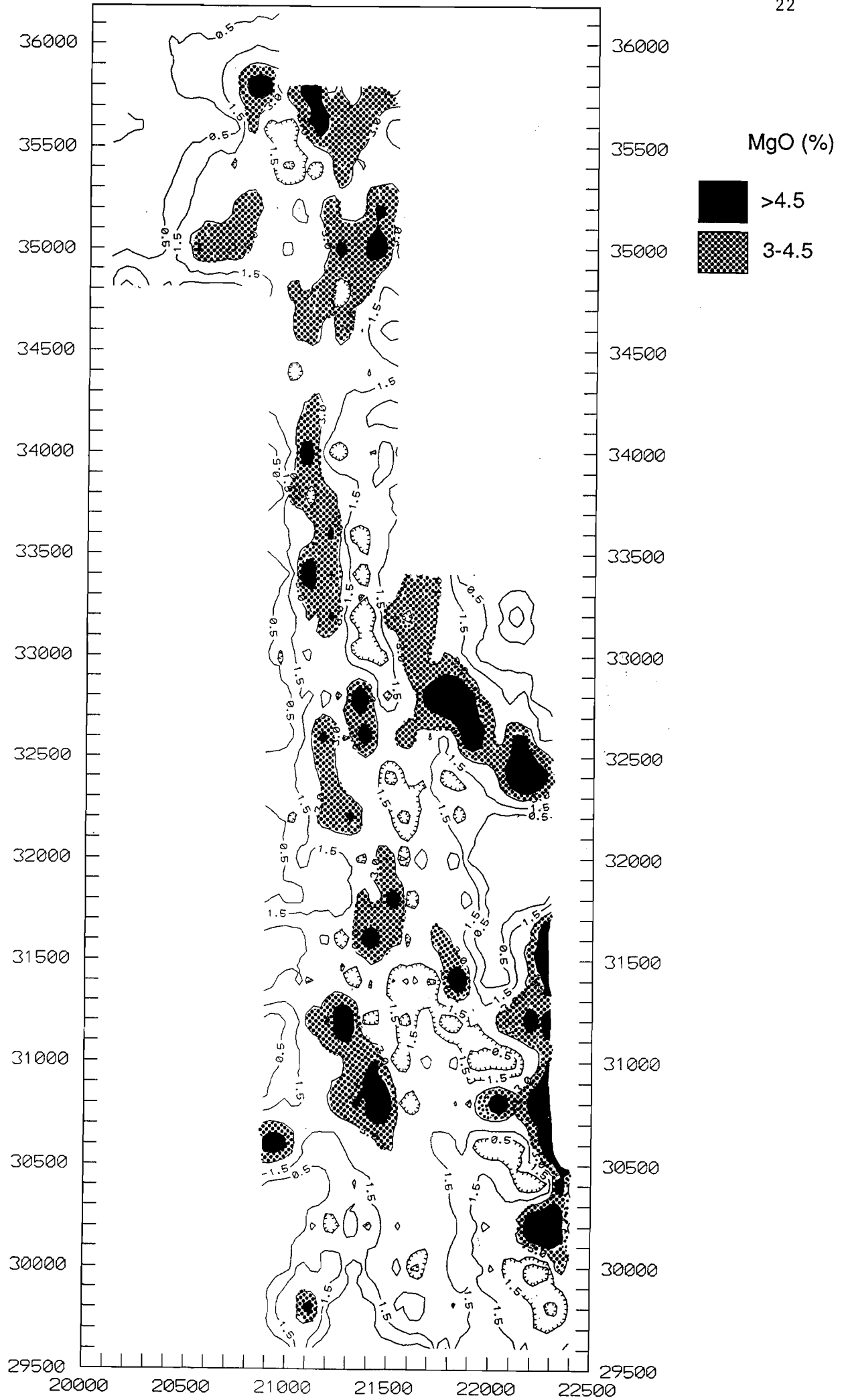
Confidence limit 0.01

Components showing high positive correlation ($\alpha < 0.001$)CaO Na₂O K₂O P₂O₅ Au Ba Cu Mn NiComponents showing high negative correlation ($\alpha < 0.001$)SiO₂ Al₂O₃ Fe₂O₃ TiO₂ As Cr V Zr

The histogram cumulative frequency plot, and very high standard deviation suggest the presence of several overlapping populations. Low MgO concentrations (<0.2%) at or near the detection limit are restricted to soils derived from lateritic duricrusts and sandstone/chert/siltstone units. It was found from the earlier study that soils containing MgO concentrations greater than about 0.5% are usually indicative of carbonate existing as dolomite within red clay-rich profiles. These soils represent approximately one third of the study area.

There is an association of the red clay-rich soils and MgO with an underlying high Mg basalt and peridotite-komatiite units. The appearance of MgO on the flanks of the eastern lateritic area support the view that some red clay-rich soils have formed as a result of colluviation processes. The laterites themselves do not contain any appreciable amounts of MgO but have been observed to be covered by a variable thickness of Mg- and Ca-rich calcareous soils.

Figure 7 (opposite): Distribution of MgO by soil auger sampling.



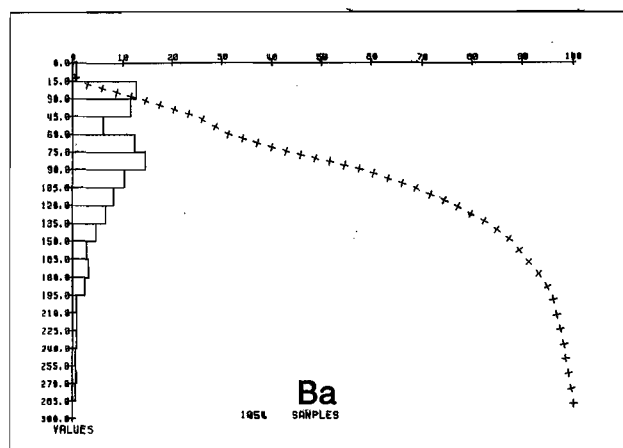
Ba.

Mean value (ppm) 93

Standard deviation 111

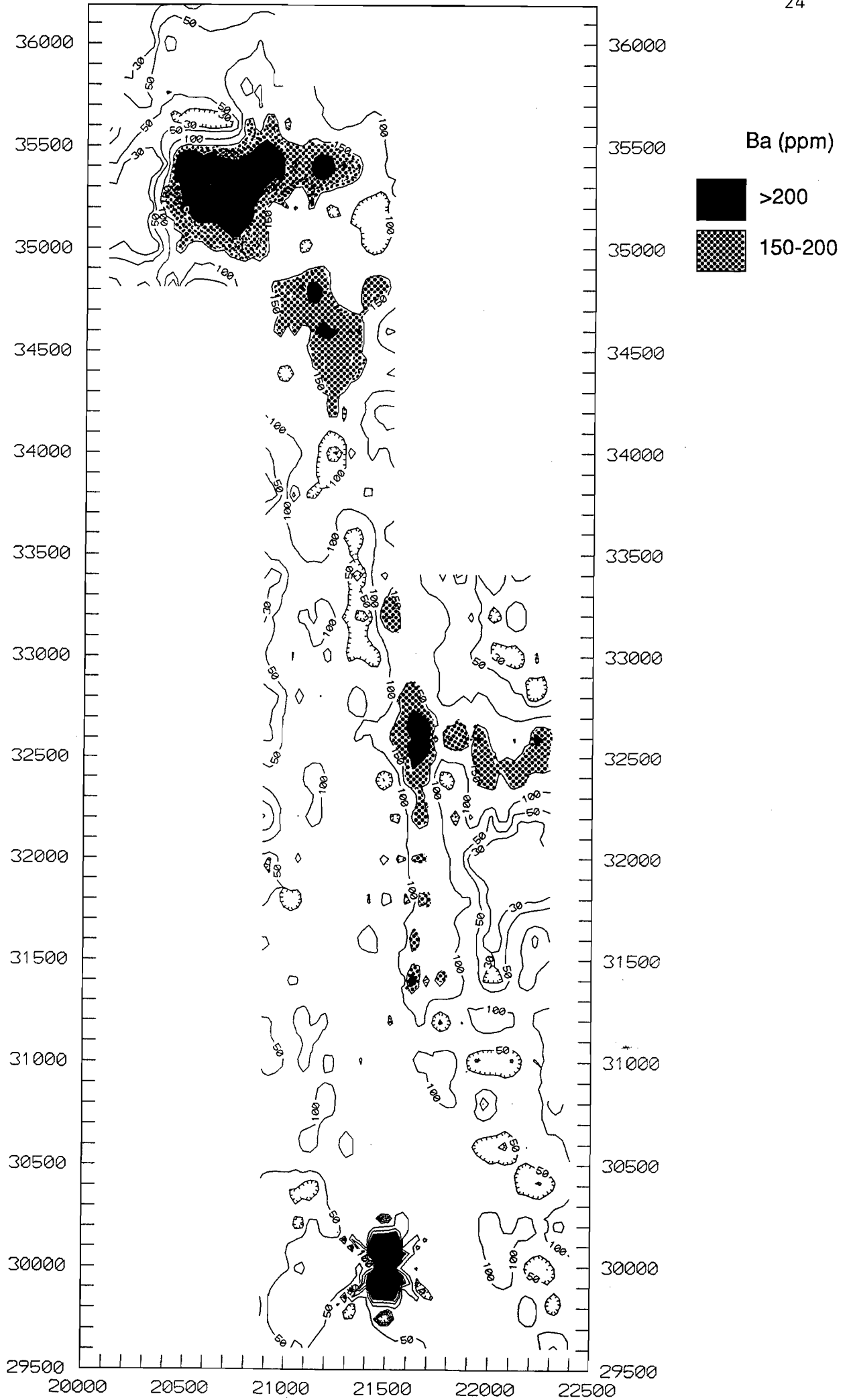
Range 10 to 3171

Confidence limit 10

Components showing high positive correlation ($\alpha < 0.001$)MgO CaO Na₂O K₂O P₂O₅ Co Cu MnComponents showing high negative correlation ($\alpha < 0.001$)Fe₂O₃ TiO₂ Cr V Zr

The histogram and high standard deviation for Ba demonstrate the presence of at least two populations. The distribution map suggests that the low value population group is associated with the lateritic soils whilst the high value with the calcareous soils. The correlation coefficients suggest a strong association between Ba and the alkali and alkaline earth metals: the relationship between Ba and CaO can be seen in the Appendix Figure 4. Barium and K have similar ionic radii and commonly replace one another in minerals such as orthoclase feldspars (e.g. hyalophane) and mica, the latter having been identified in the study area. The presence of Ba in the vicinity of the Bounty Pit may be due to a high S activity, resulting from weathering sulfides, leading to the precipitation of Ba as sparingly soluble barite. Barite has been identified (by SEM) near Au grains in a sample taken at 18.5 metres (04-1148) from within the Bounty pit. Alternatively, Ba may be associated with feldspars, which are locally abundant in near-surface material from this area. There are insufficient data to determine whether Ba is associated with the primary mineralization.

Figure 8(opposite):Distribution of Ba by soil auger sampling.



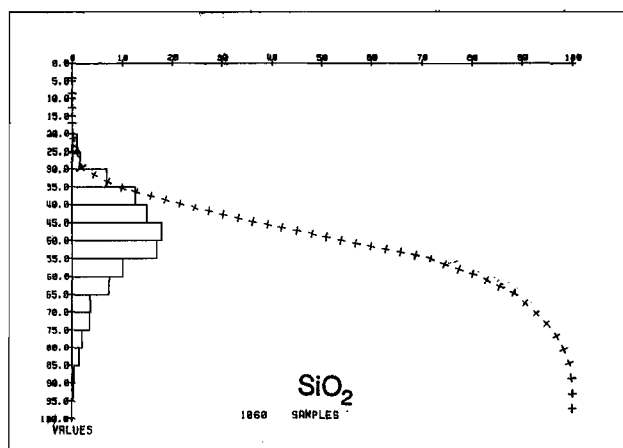
SiO₂

Mean value (%) 50

Standard deviation 12

Range 22.18 to 93.12

Confidence limit 0.1

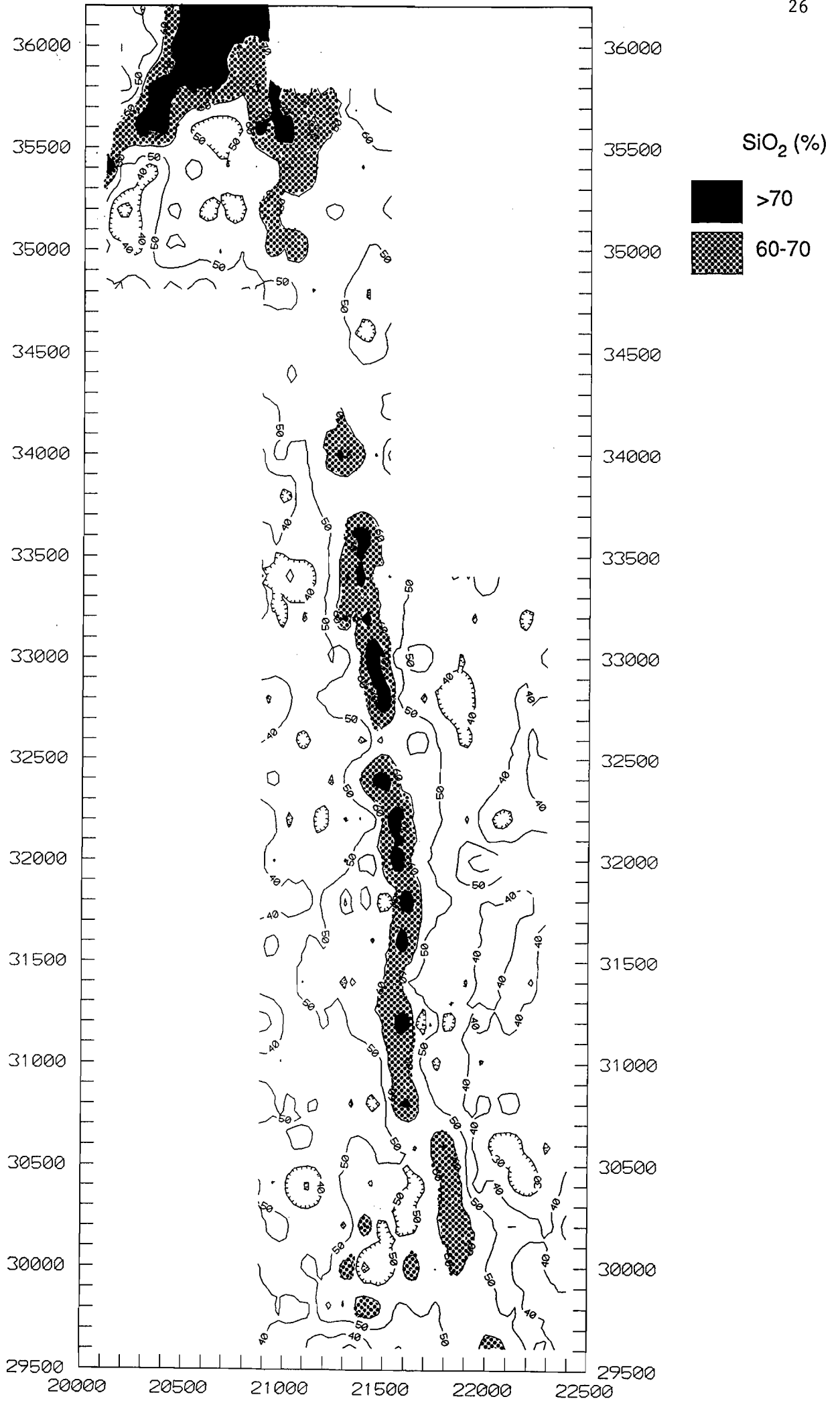
Components showing high positive correlation ($\alpha < 0.001$)K₂O Be NiComponents showing high negative correlation ($\alpha < 0.001$)Al₂O₃ Fe₂O₃ MgO CaO TiO₂ As Co Cr Cu Mn V Zr

The histogram and standard deviation show that the SiO₂ data is almost normally distributed, with some positive skewness.

Inspection of the distribution map for SiO₂ clearly shows a strong north-south trend extending over several kilometres of the study area. The high concentrations of SiO₂ are primarily related to siltstone, chert and sandstone units of the greenstone belt. Examination of Profile 24 (see Figure 3) and the surrounding area indicate that these rocks are close to or at the surface and are responsible for the high SiO₂ values. They also have low concentrations of Fe₂O₃, alkaline earths and most trace elements.

A strongly SiO₂-enriched area appears to be associated with duplex soils occurring within the broad, poorly developed drainage north of 35700N. Quartz-rich sands overlying and penetrating red clay-rich soils have previously been described from the area (Profile 7, Lintern, 1989). The origin of the quartz sands is not known but they appear to be transported.

Figure 9 (opposite): Distribution of SiO₂ by soil auger sampling.



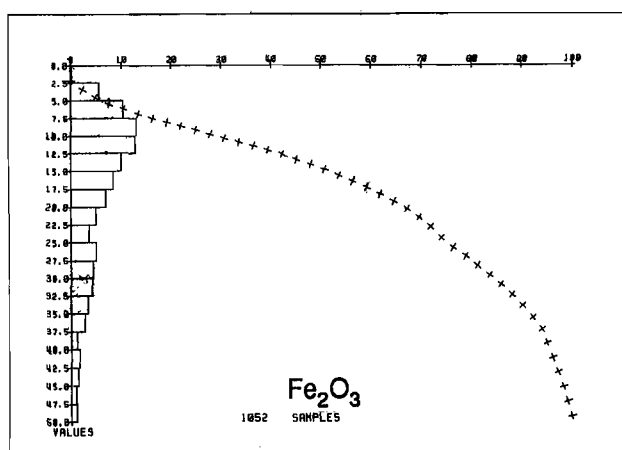
Fe₂O₃

Mean value (%) 18

Standard deviation 11

Range 2.14 to 54.40

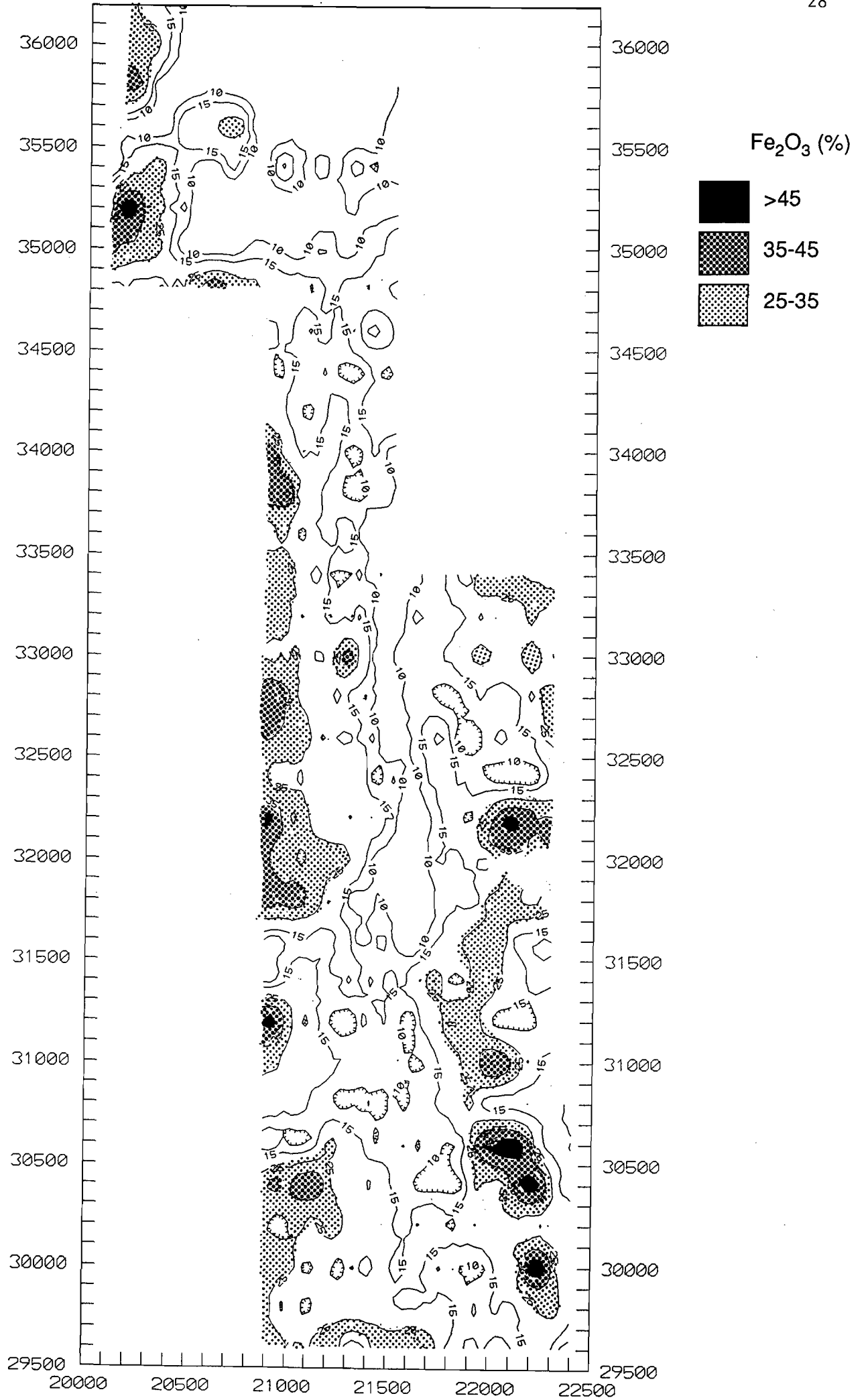
Confidence limit 0.1

Components showing high positive correlation ($\alpha < 0.001$)Al₂O₃ TiO₂ As Co Cr Cu V ZrComponents showing high negative correlation ($\alpha < 0.001$)SiO₂ MgO CaO Na₂O K₂O P₂O₅ Au Ba Mn

The high standard deviation, cumulative frequency plot, histogram and regional distribution of Fe₂O₃ suggest there to be three distinct populations; the highest concentrations represent the laterite unit, the intermediate concentrations represent the Ca- and Mg-rich carbonate unit and the lowest Fe₂O₃ content representing the sediment/sandstone/chert unit that extends in a narrow belt through the centre of the exploration lease. In the laterite unit, the areas highest in Fe₂O₃ may reflect the better preserved and/or deepest areas of laterite cover that have not been eroded or weathered to the same extent as adjacent areas.

The dominant iron minerals observed in the field, profile sampling and XRD analysis are hematite and goethite. These iron oxides are concentrated within predominantly residual lateritic material overlying basalts on the eastern and western boundaries of the exploration lease.

Figure 10 (opposite): Distribution of Fe₂O₃ by soil auger sampling.



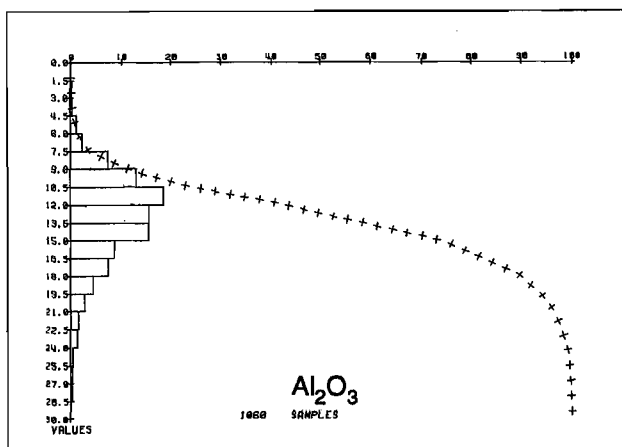
Al₂O₃

Mean value (%) 13.1

Standard deviation 3.7

Range 1.88 to 27.87

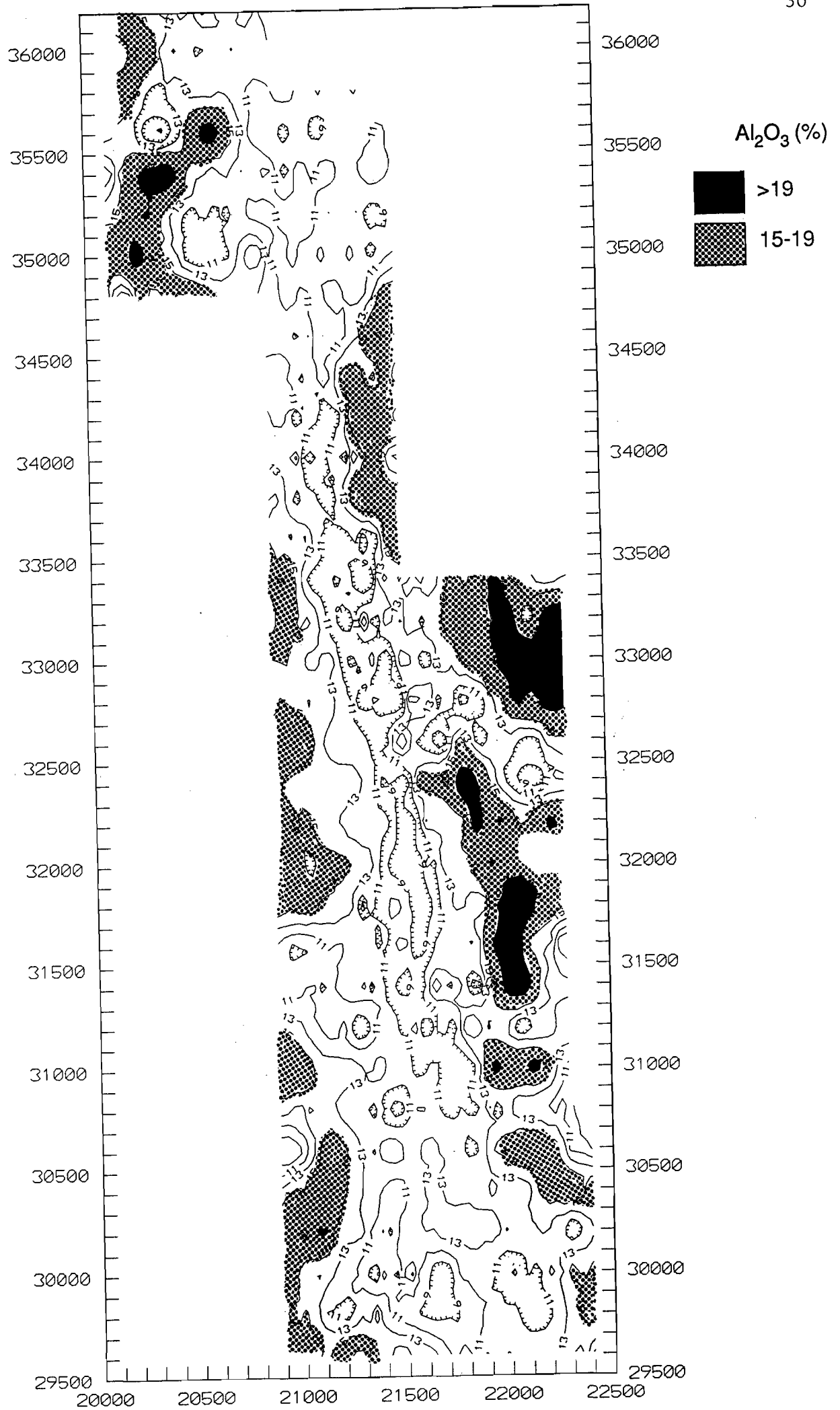
Confidence limit 0.1

Components showing high positive correlation ($\alpha < 0.001$)Fe₂O₃ TiO₂ As Co Cr Cu V ZrComponents showing high negative correlation ($\alpha < 0.001$)SiO₂ MgO CaO Na₂O K₂O Au Mn Ni

The Al₂O₃ data are almost normally distributed with a minor positive skewness. The regional distribution of Al₂O₃ is similar to that of Fe₂O₃ suggesting a strong association of Al with Fe. As for Fe₂O₃ the soils derived from the chert, siltstones and sandstones are especially depleted in Al₂O₃ whereas the red calcareous earths have intermediate concentrations. Additional support for the association comes from the high correlation coefficient between Fe₂O₃ and Al₂O₃. The Al₂O₃ concentrations appear to be particularly high in laterites overlying tholeiitic basalts in the eastern region of the lease although this may reflect the greater extent of lateritic material in this area. The minor elements showing high correlation with Al₂O₃ are probably associated more with the iron oxides.

The Al₂O₃ contents decrease gradually across the mapped boundaries of the lateritic duricrust, rather than declining abruptly, as for Fe₂O₃. There are at least three possible explanations for this phenomenon: (i) it may reflect the continuation of lateritic components beneath the immediate clay-rich covered surface (but still within the top metre), (ii) a weathering process involving the leaching and transportation of Al from the lateritic area and forming a larger halo around it, or most probably, (iii) the occurrence of Al₂O₃ as a major component of the clays in these soils.

Figure 11 (opposite): Distribution of Al₂O₃ by soil auger sampling.



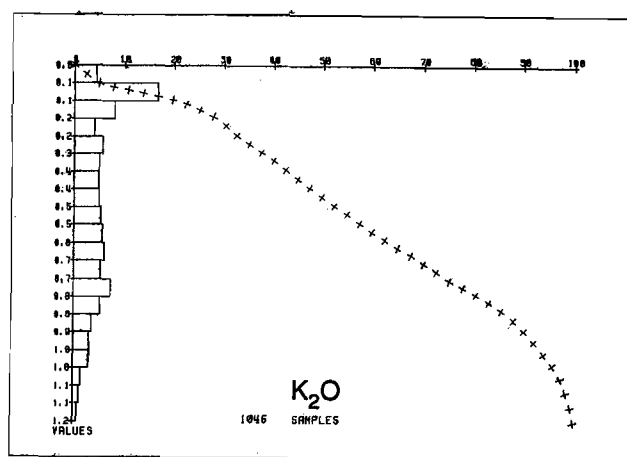
K₂O.

Mean value (%) 0.5

Standard deviation 0.3

Range <0.02 to 1.57

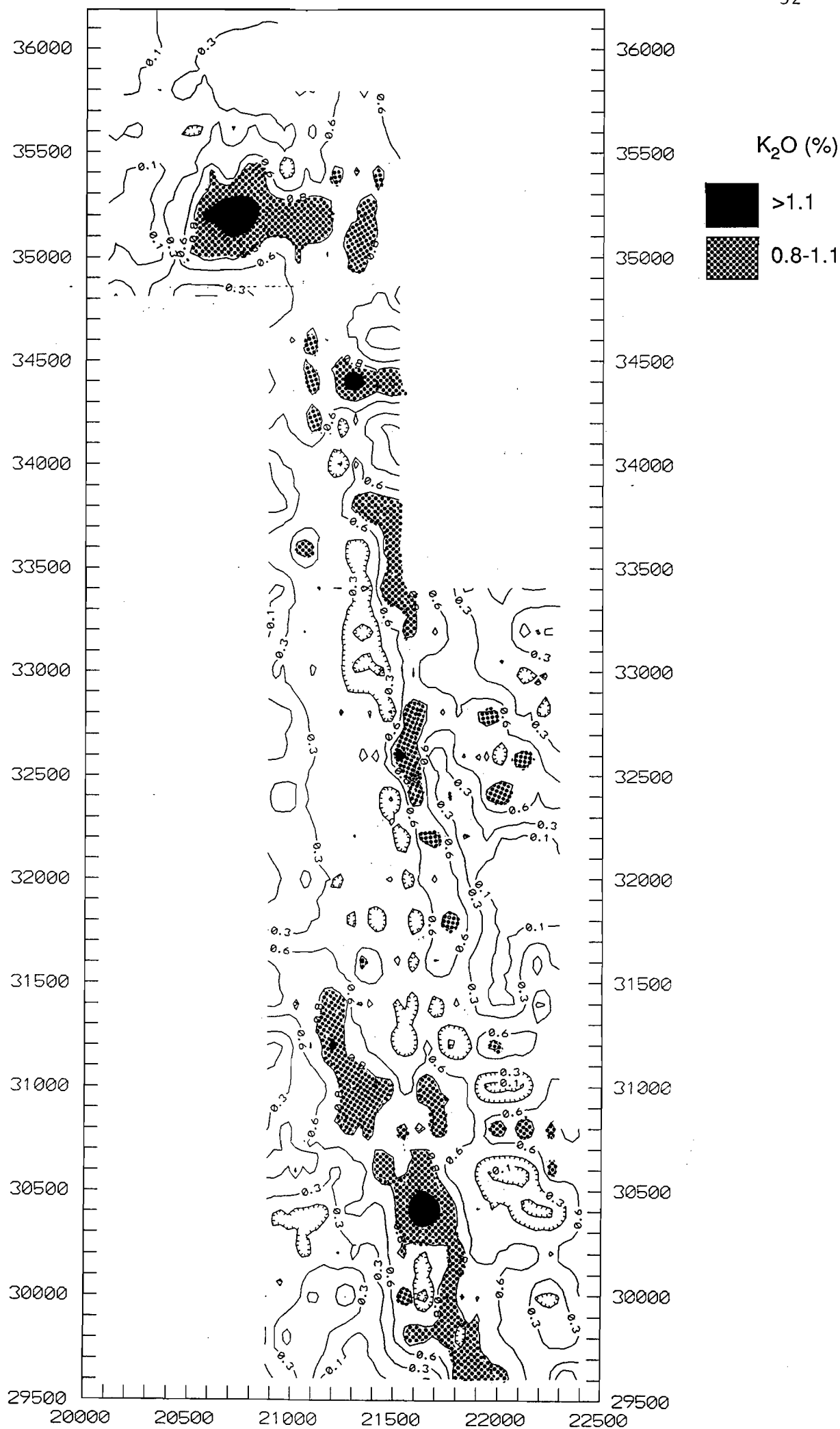
Confidence limit 0.02

Components showing high positive correlation ($\alpha < 0.001$)MgO Na₂O CaO P₂O₅ Au Ba Mn NiComponents showing high negative correlation ($\alpha < 0.001$)Al₂O₃ Fe₂O₃ TiO₂ As Co Cr V Zr

The histogram, cumulative frequency plot and high standard deviation value are indicative of an overlapping multi-population distribution.

Potassium is associated with the red clay-rich soils but, unlike Ca and Mg, it is not ubiquitous. Near the Bounty mine, illite has been identified in soil profiles and it is here that K₂O shows its greatest concentration and largest anomaly. Further south near Profile 20 mica, probably muscovite, was observed. The major K₂O anomalies show a similar pattern to those of Ba. There is little K₂O associated with the laterite soils but, as with the alkaline earth metals, there is an accumulation downslope from the lateritic areas. The high concentration of K₂O in the drainage in the south-west of the study area is not readily explained, but may be a result of the illuviation of micas from the flanking slopes.

Figure 12 (opposite): Distribution of K₂O for soil auger sampling.



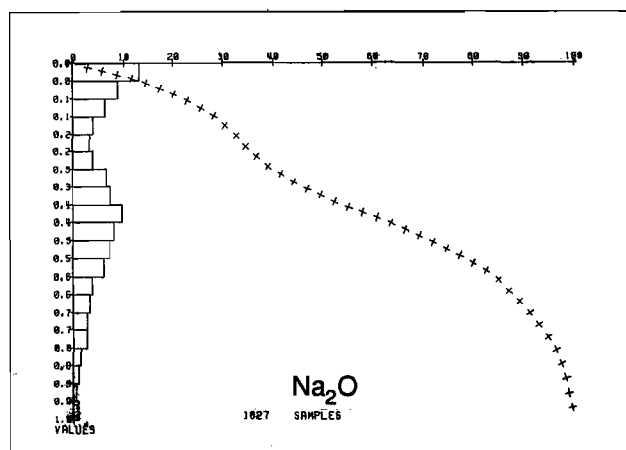
Na₂O.

Mean value (%) 0.4

Standard deviation 0.3

Range <0.02 to 1.58

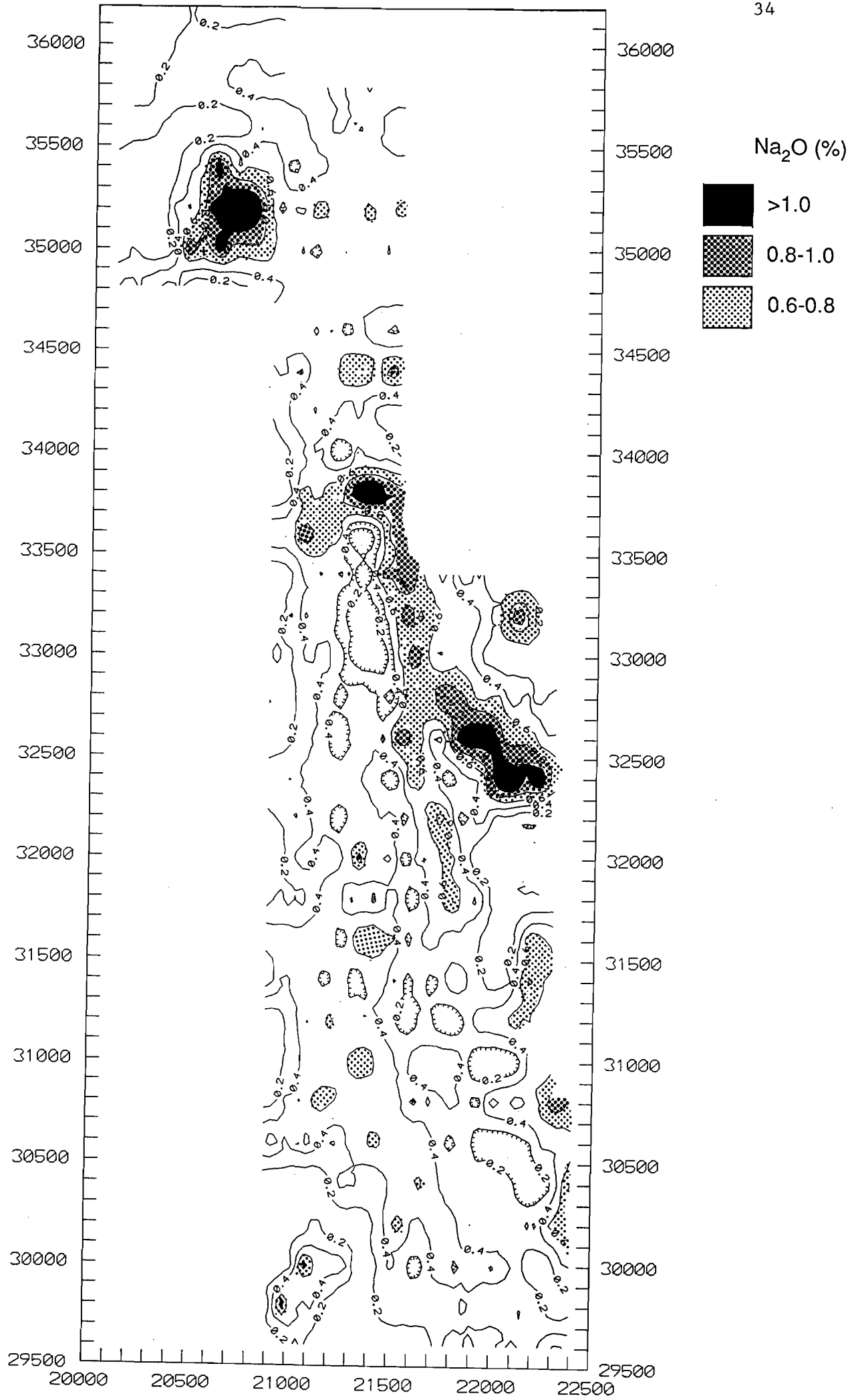
Confidence limit 0.02

Components showing high positive correlation ($\alpha < 0.001$)MgO K₂O CaO P₂O₅ Au Ba Cu Mn NiComponents showing high negative correlation ($\alpha < 0.001$)Al₂O₃ Fe₂O₃ TiO₂ As Cr V Zr

The cumulative frequency plot, histogram and high standard deviation suggest there to be at least two distinct populations. Low concentrations of Na₂O are associated with the lateritic soils, whereas higher values are associated with the calcareous soils. The distribution of Na₂O is very similar to that of K, with which it is strongly correlated ($r=0.7761$). The very high Na₂O concentration in soils close to the Bounty mine are probably associated, at least in part, with the occurrence of edenite (sodian amphibole) which has been identified by XRD in soil profiles.

The alkalis, alkaline earths and Mn all show high concentrations at about 22000E 32500N and may be associated with saprolitic material from outcropping or near-surface weathered tholeiitic basalt which was exposed in profile 25 nearby.

Figure 13 (opposite): Distribution of Na₂O in soil auger samples.



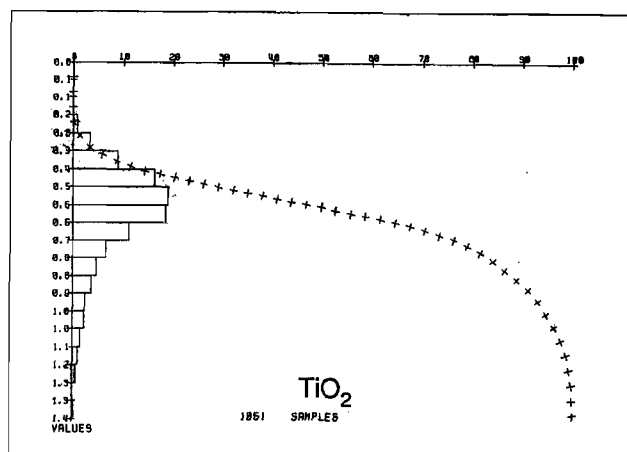
TiO₂

Mean value (%) 0.6

Standard deviation 0.2

Range 0.22 to 2.82

Confidence limit 0.01

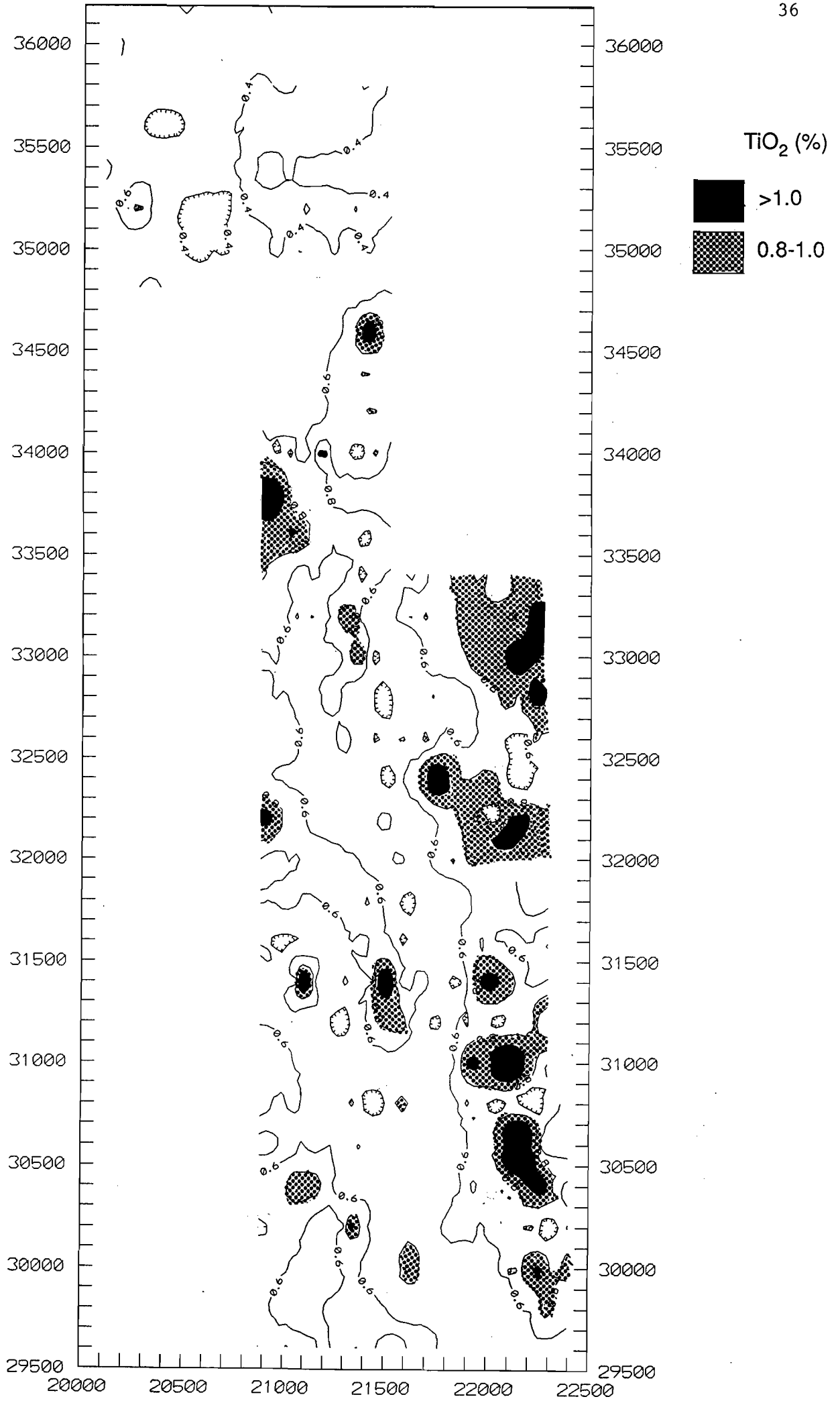
Components showing high positive correlation ($\alpha < 0.001$)Al₂O₃ Fe₂O₃ Co Cr Cu V ZrComponents showing high negative correlation ($\alpha < 0.001$)SiO₂ MgO CaO Na₂O K₂O P₂O₅ Au Ba

The histogram of the TiO₂ data shows it to have a near-normal distribution, but with some positive skew. This distribution is reflected in the low standard deviation.

Titanium minerals, expressed here as TiO₂, are most strongly concentrated in the lateritic soils and this is reflected in the high correlation with Fe₂O₃ and Al₂O₃. Rutile and anatase were occasionally found in sufficient quantities to be detected by XRD in soil profile samples.

The distribution map indicates that TiO₂ values are lowest in the most northern part of the study area. The low values may reflect either (i) the presence of the Binneringie dyke, (ii) the effect of transported material or (iii) an analytical artefact from the samples of the earlier pilot study. The resistate minerals are, as their name suggests, the most difficult to dissolve even by fusion techniques and so analyses are often prone to reporting artificially low values. Caution is required, therefore, in interpreting the Ti/Zr ratio in these data using the plots published by Hallberg (1984), whose analyses were based on XRF. The plot of the Ti/Zr ratio suggests that most samples plot in the andesitic field (Ti/Zr <60 but >12) with some samples occurring in the north of study area and in the sedimentary ridge having a distinctly more acidic origin (Appendix Figure 5). This can be explained, in part, by the presence of acidic granitoid xenoliths that are known to frequently occur in Proterozoic dykes (Hallberg, 1987).

Figure 14 (opposite): Distribution of TiO₂ by soil auger sampling.



Zr.

Mean value (ppm) 129

Standard deviation 35

Range 44 to 283

Confidence limit 20

Components showing high positive correlation ($\alpha < 0.001$) Al_2O_3 Fe_2O_3 TiO_2 As Be Co Cr VComponents showing high negative correlation ($\alpha < 0.001$) SiO_2 MgO CaO Na_2O K_2O P_2O_5 Ba Mn

Zirconium values are normally distributed.

Zirconium tends to be associated with the lateritic soils as indicated by the high correlation with Fe_2O_3 and Al_2O_3 . Zirconium commonly occurs as zircon and as such is highly immobile, thereby concentrating residually within lateritic material. Areas of high Zr do exist, however, within zones of calcareous clay-rich soils e.g. 21400E 34200N. As with TiO_2 , wet chemical dissolution techniques are not particularly recommended for total Zr analysis due to its resistant characteristic.

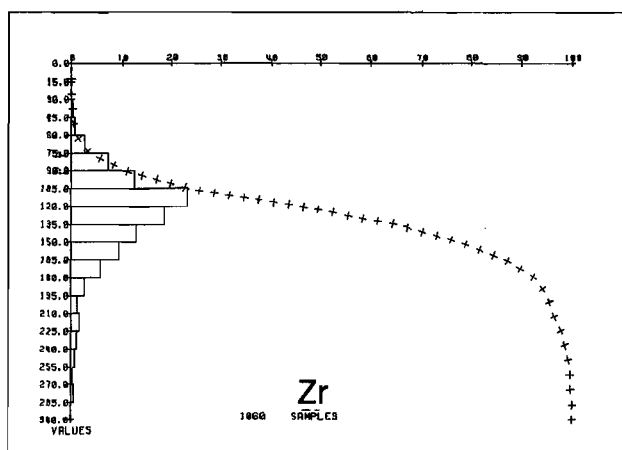
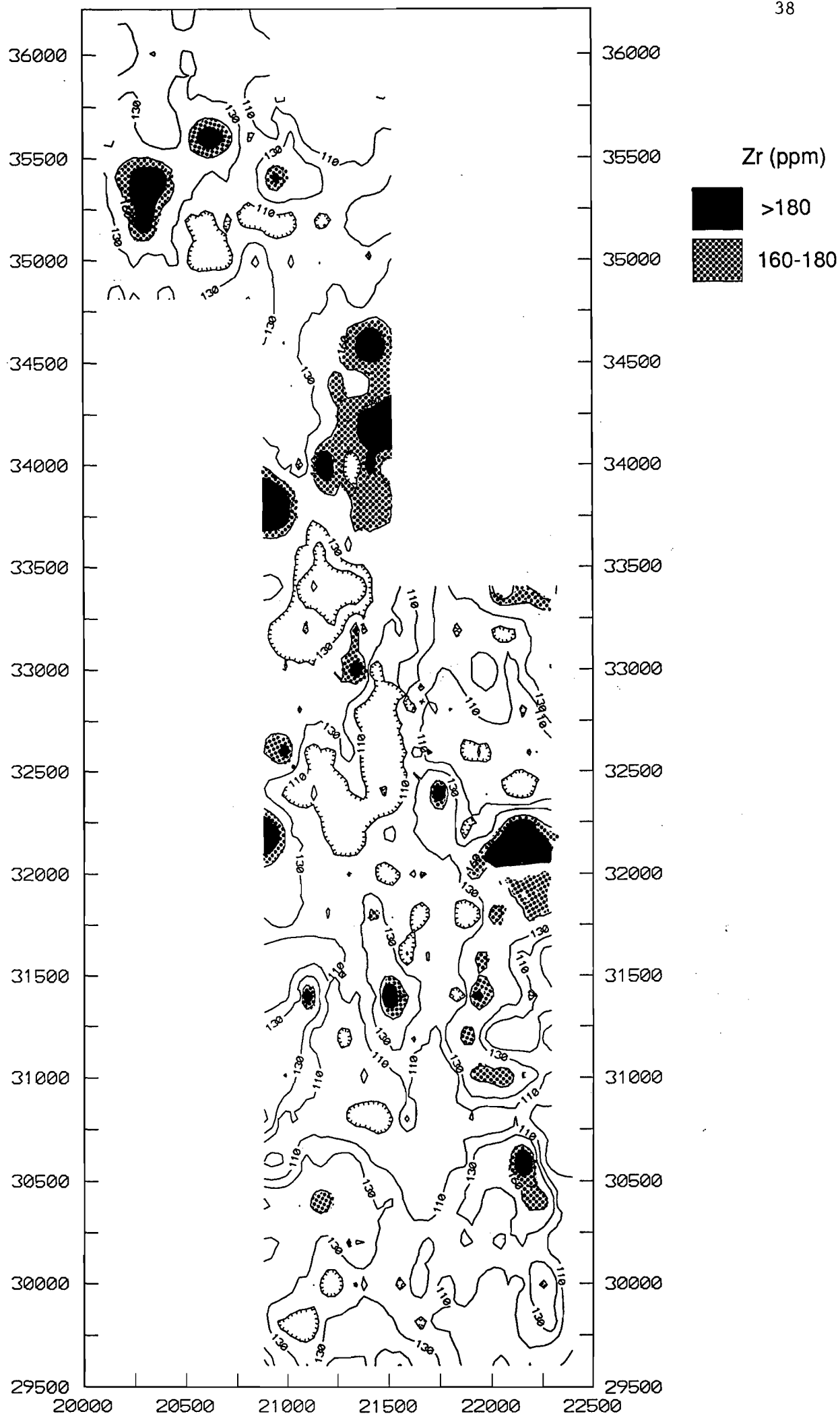


Figure 15 (opposite): Distribution of Zr by soil auger sampling.



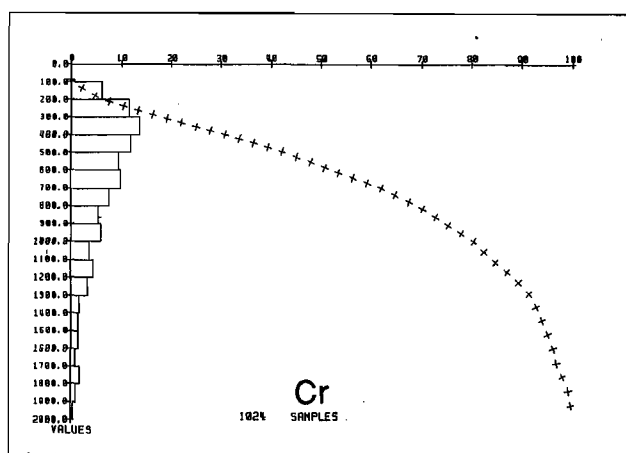
Cr.

Mean value (ppm) 728

Standard deviation 526

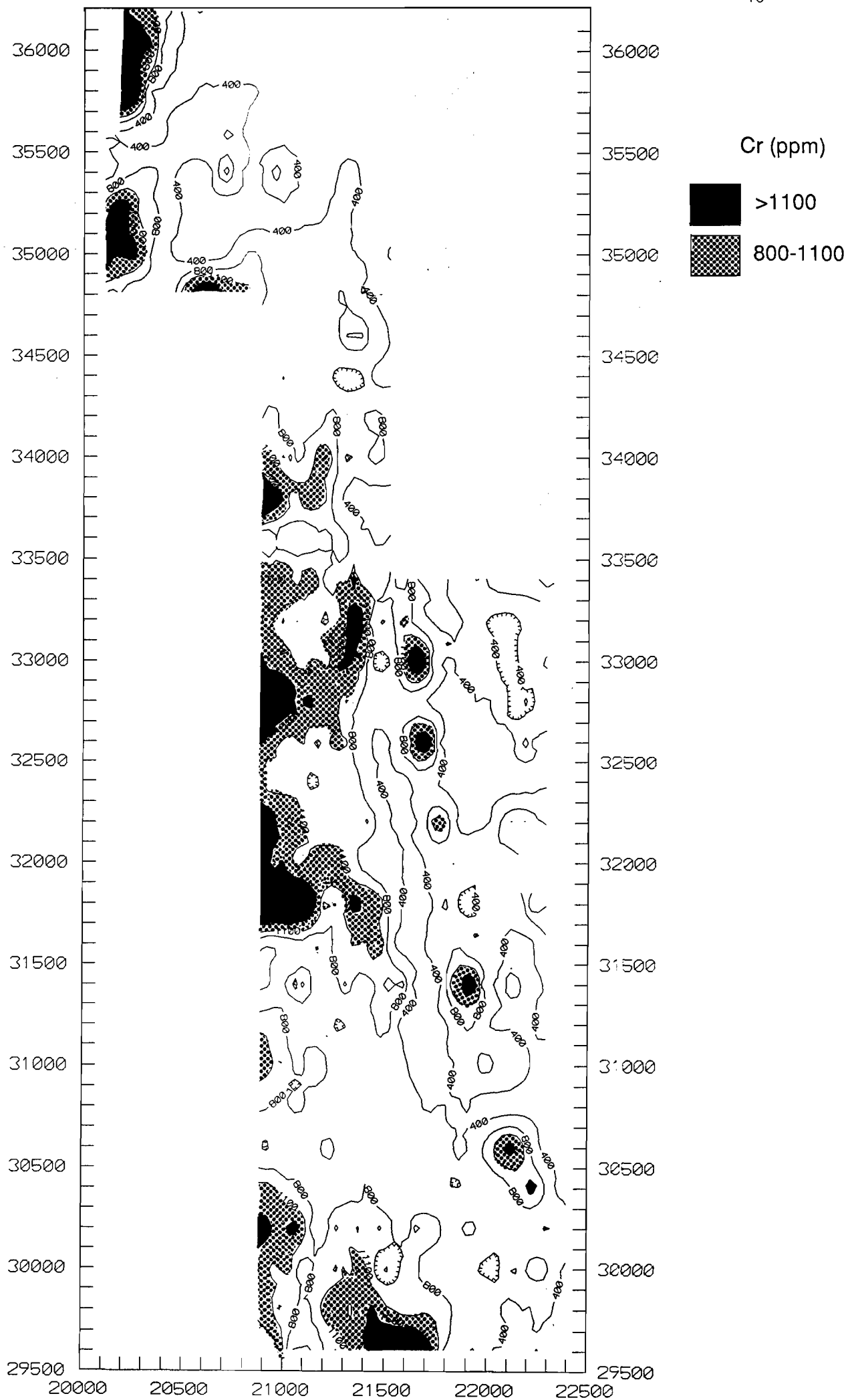
Range 104 to 4564

Confidence limit 10

Components showing high positive correlation ($\alpha < 0.001$) Al_2O_3 Fe_2O_3 TiO_2 As Co Ni V ZrComponents showing high negative correlation ($\alpha < 0.001$) SiO_2 MgO CaO Na_2O K_2O P_2O_5 Ba Mn

The Cr data are highly positively skewed and have a large standard deviation. This implies that there may be more than one control on the Cr distribution. A weak linear trend running approximately north-south and corresponding to ultramafic units (predominantly dunite) appears to be responsible for one group of high Cr values (e.g. samples centred around 21700E 32600N). Here, Cr probably occurs in the form of resistant chromites. Flanking the western border is a larger area of high Cr values corresponding to lateritic soils. Scavenging of Cr by iron oxides, derived from basic rocks, is thought to be responsible for this group.

Figure 16 (opposite): Distribution of Cr by soil auger sampling.



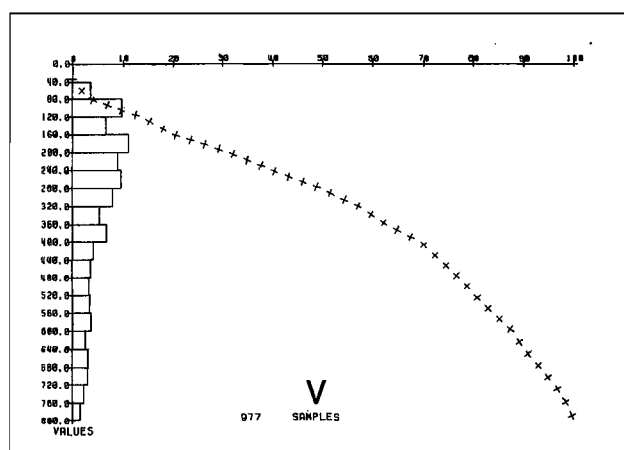
V.

Mean value (ppm) 378

Standard deviation 254

Range 43 to 1370

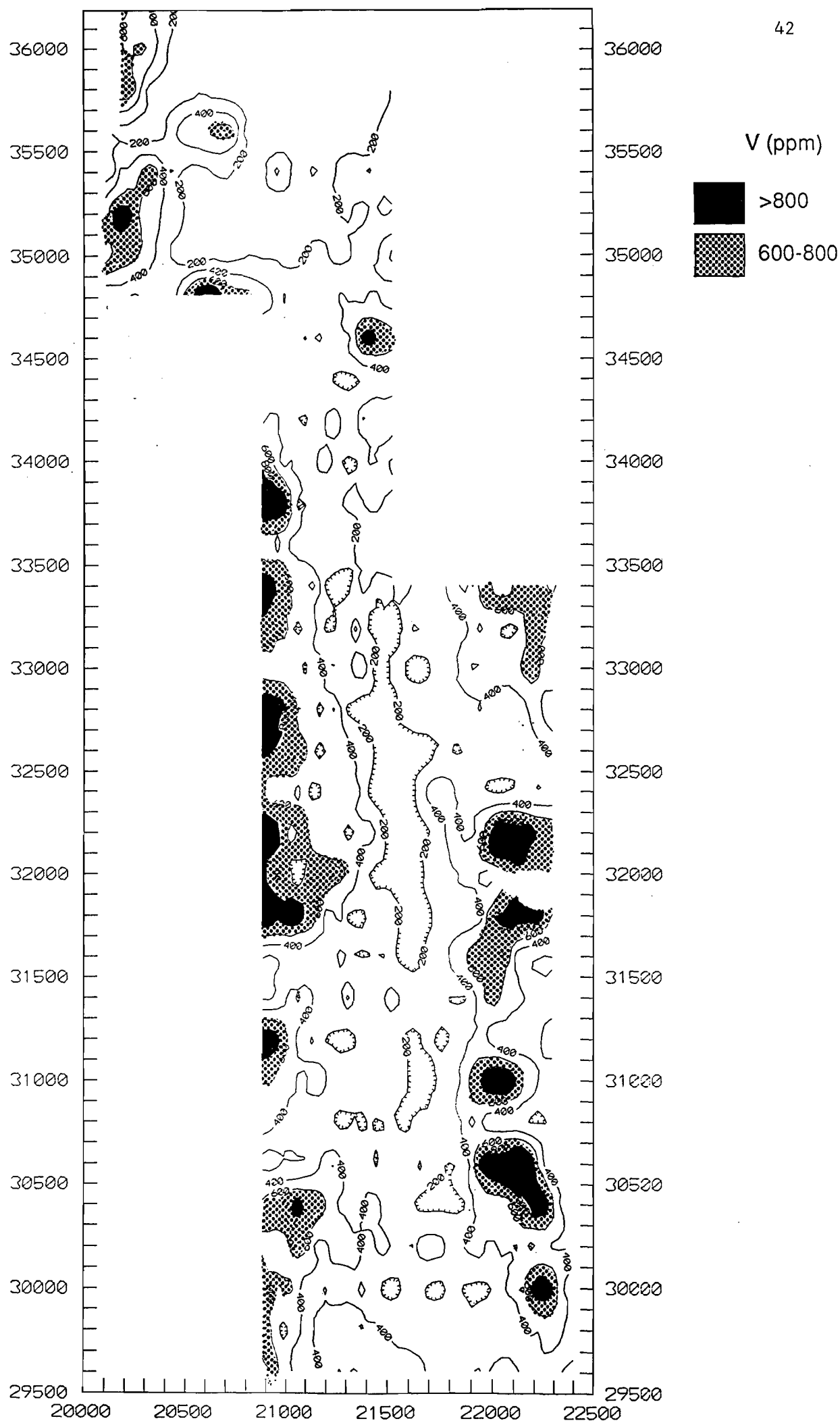
Confidence limit 20

Components showing high positive correlation ($\alpha < 0.001$) Al_2O_3 Fe_2O_3 TiO_2 As
Co Cr ZrComponents showing high negative correlation ($\alpha < 0.001$) SiO_2 MgO CaO Na_2O
 K_2O P_2O_5 Au Ba Mn Ni

Vanadium has a highly skewed and possibly multi-modal distribution. Vanadium and Fe_2O_3 are the most highly correlated of all the components examined in this study (Appendix Figure 5).

The concentration of V is dominated by iron oxides that flank the study area as lateritic gravels. It is also highly correlated with other components commonly associated with resistate minerals. The especially strong correlation of Fe_2O_3 and V (Appendix Figure 2), however, suggests more a relationship derived from the weathering of mafic minerals followed by iron oxide scavenging rather than its occurrence as a resistate mineral. The lowest V concentrations are associated with soils derived from siltstones and sandstones that run through the centre of the study area.

Figure 17 (opposite): Distribution of V by soil auger sampling.



Be.

Mean value (ppm) 0.9

Standard deviation 1.7

Range <3 to 26.1

Confidence limit 3

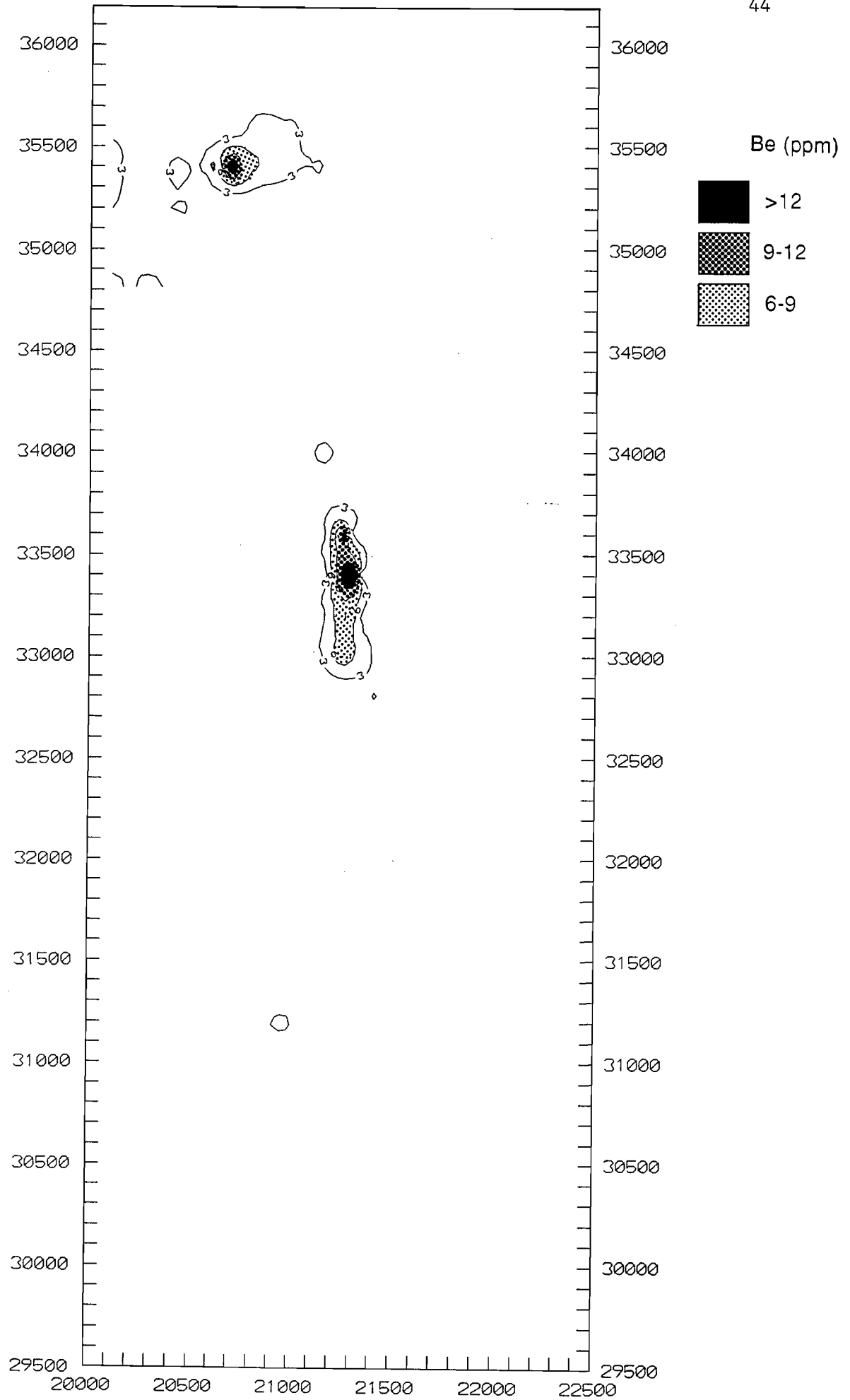
Components showing high positive correlation ($A < 0.001$) SiO_2 Zr

Components showing high negative correlation ($A < 0.001$) CaO

The histogram for Be has not been included since reliable data in excess of 3ppm has limited occurrence.

There are two Be anomalies in the study area (see opposite). The most northern anomaly at 20700E 35400N is associated with pegmatite and muscovite-rich granite. However, the larger anomaly, centred at 21300E 33400N, does not coincide with any known pegmatites. The anomaly was examined further by digging a soil profile and by pan concentrating the heavy fraction of a surface soil composite. The heavy mineral concentrate contained no detectable minerals characteristic of some pegmatites in the region (e.g. tourmaline). Nevertheless, the size and persistence of the Be anomaly are a little unusual and warrant further investigation.

Figure 18 (opposite): Distribution of Be by soil auger sampling.



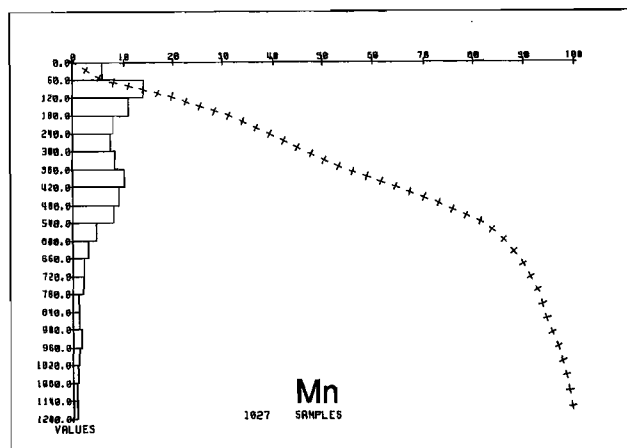
Mn.

Mean value (ppm) 398

Standard deviation 357

Range 12 to 3628

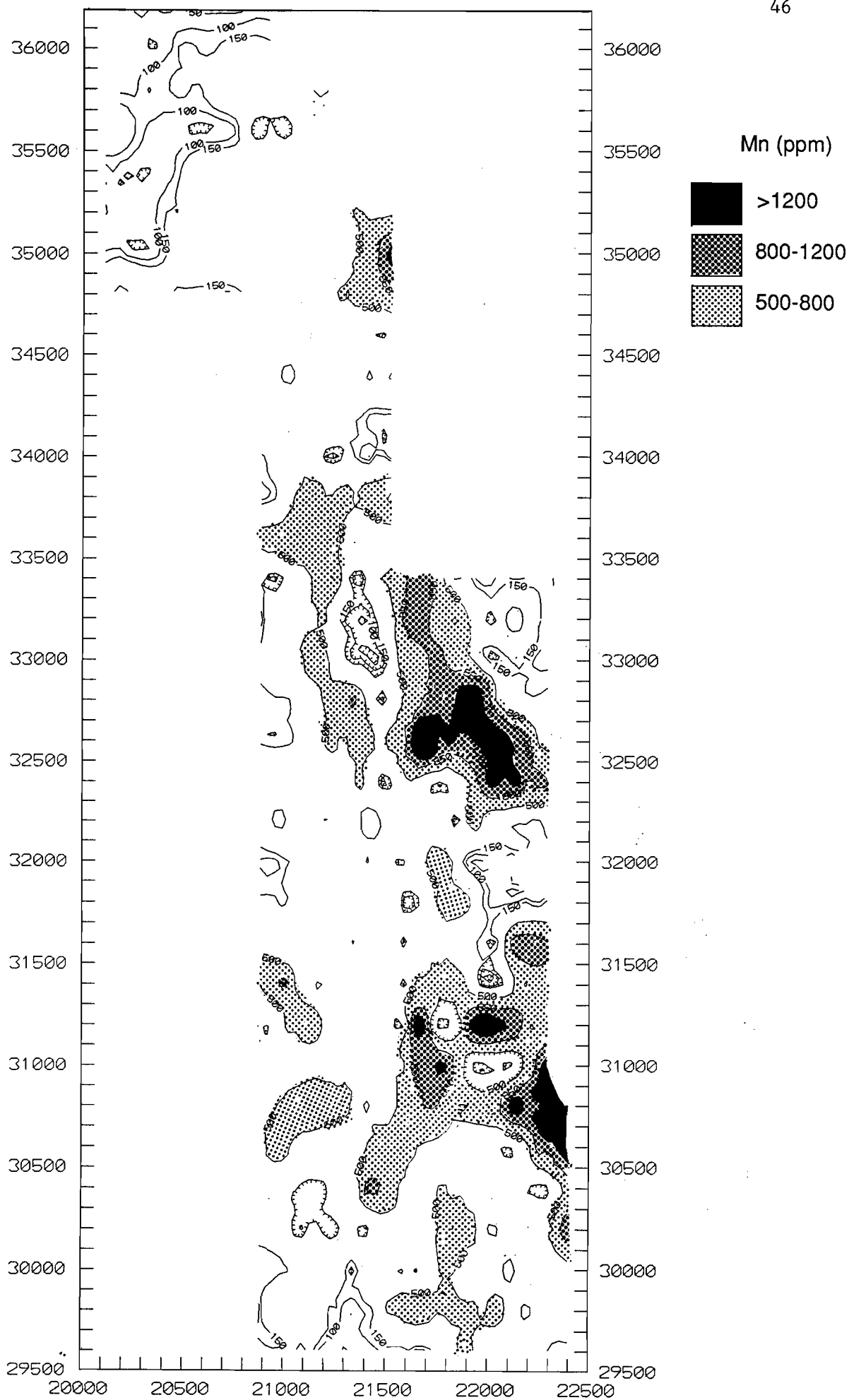
Confidence limit 50

Components showing high positive correlation ($\alpha < 0.001$)MgO CaO Na₂O K₂O P₂O₅ Ba Co Cu NiComponents showing high negative correlation ($\alpha < 0.001$)SiO₂ Al₂O₃ Fe₂O₃ As V Zr

The Mn distribution is markedly bi-modal and the data have a high standard deviation. The highest values recorded come from the eastern part of the study area, overlying tholeiitic basalts.

The regional distribution of Mn is very similar to that of the alkali and alkaline earth metals. This association is demonstrated by the CaO-Mn binary plot (Appendix Figure 4) and is reflected in the high correlation coefficient. Manganese minerals were not in sufficient concentration to be identified by XRD but probably exist as either carbonate or oxide. High concentrations (>1000 ppm) of Mn are associated with high concentrations (>100 ppm) of Co and, therefore, suggest the presence of MnO₂.

Figure 19 (opposite): Distribution of Mn by soil auger sampling.



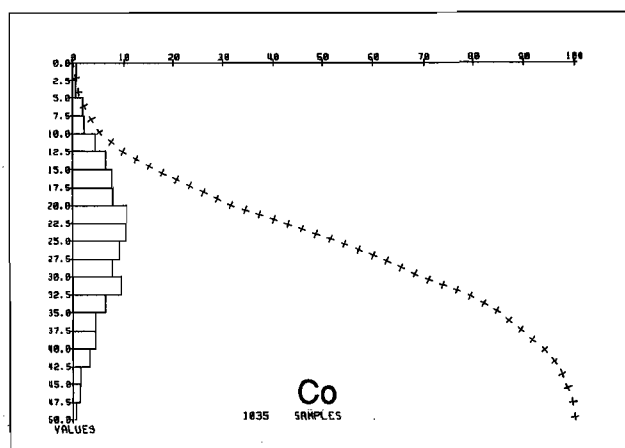
Co.

Mean value (ppm) 26

Standard deviation 14

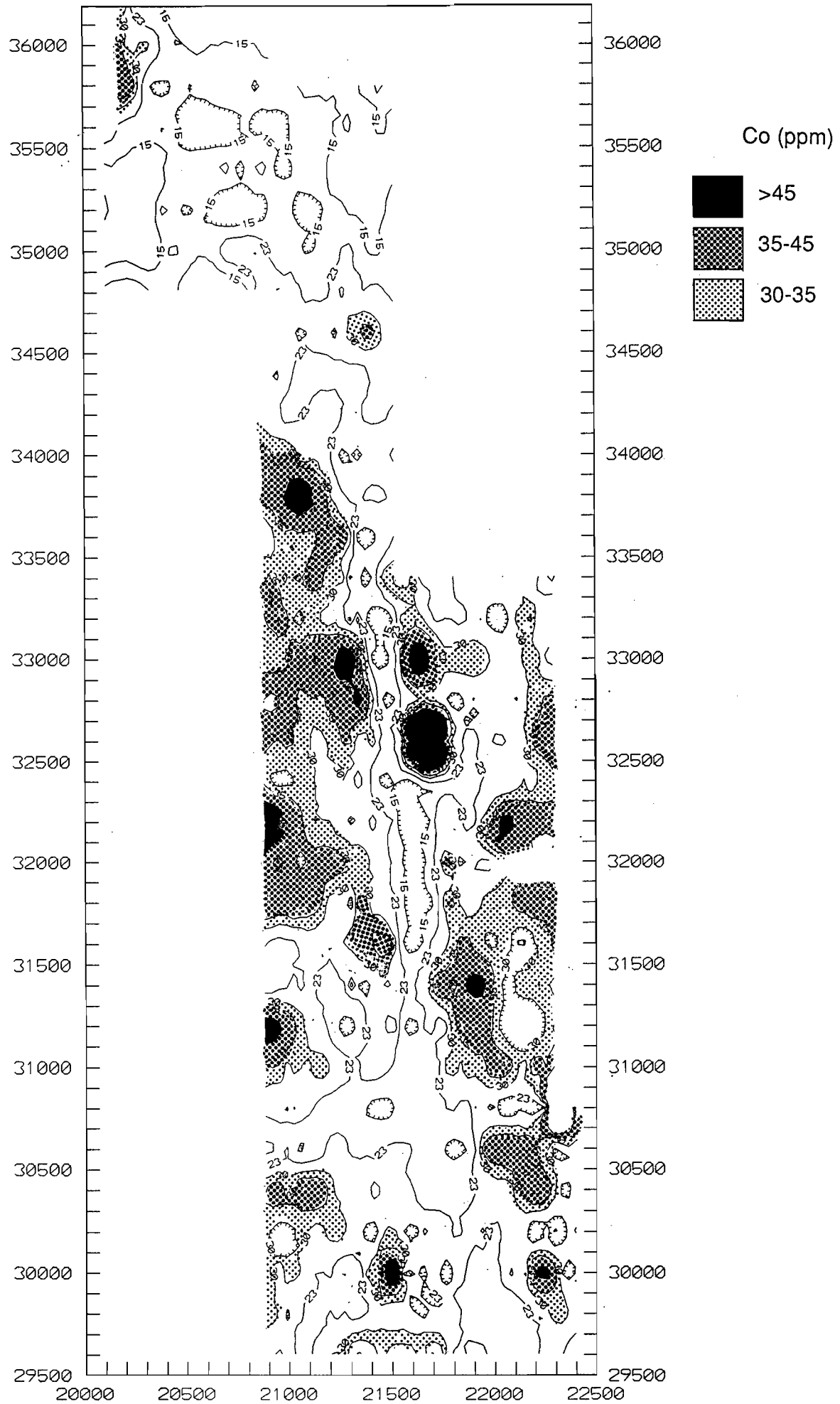
Range 0.5 to 202

Confidence limit 20

Components showing high positive correlation ($\alpha < 0.001$)Al₂O₃ Fe₂O₃ TiO₂ As Ba Cr Cu Mn Ni V ZrComponents showing high negative correlation ($\alpha < 0.001$)SiO₂ CaO K₂O P₂O₅

The histogram for the Co data indicates the values are normally distributed over a narrow range (the class intervals are 2.5 ppm). Cobalt shows a strong correlation with the transition metals but its overall distribution is controlled by iron oxides. In particular, the lateritic and clay-rich soils associated with weathered ultramafics (dunites) at 21700E 32600N have the highest concentrations of Co and are evidence for the predominantly residual nature of the soils in this part of the study area. The high Co area is spatially wider than that of Cr and suggests some lateral dispersion. Iron oxides are well known scavengers of transition metals and are probably responsible for the poor mobility of Co in this environment. The highest concentrations of Co (>100 ppm), however, are probably due to adsorption by Mn oxides (Appendix Figure 6).

Figure 20 (opposite): Distribution of Co by soil auger sampling.



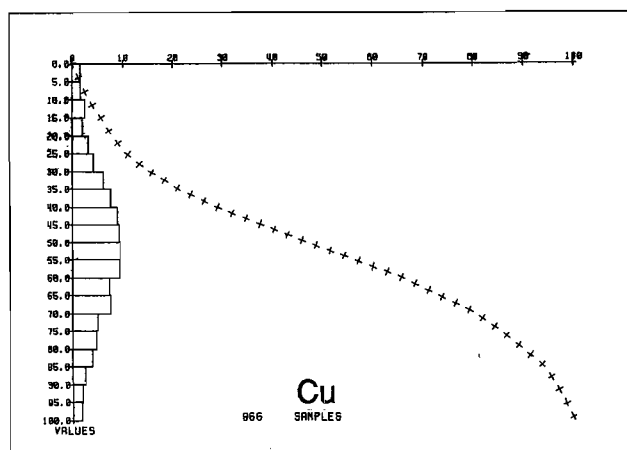
Cu.

Mean value (ppm) 59

Standard deviation 32

Range 0.5 to 228

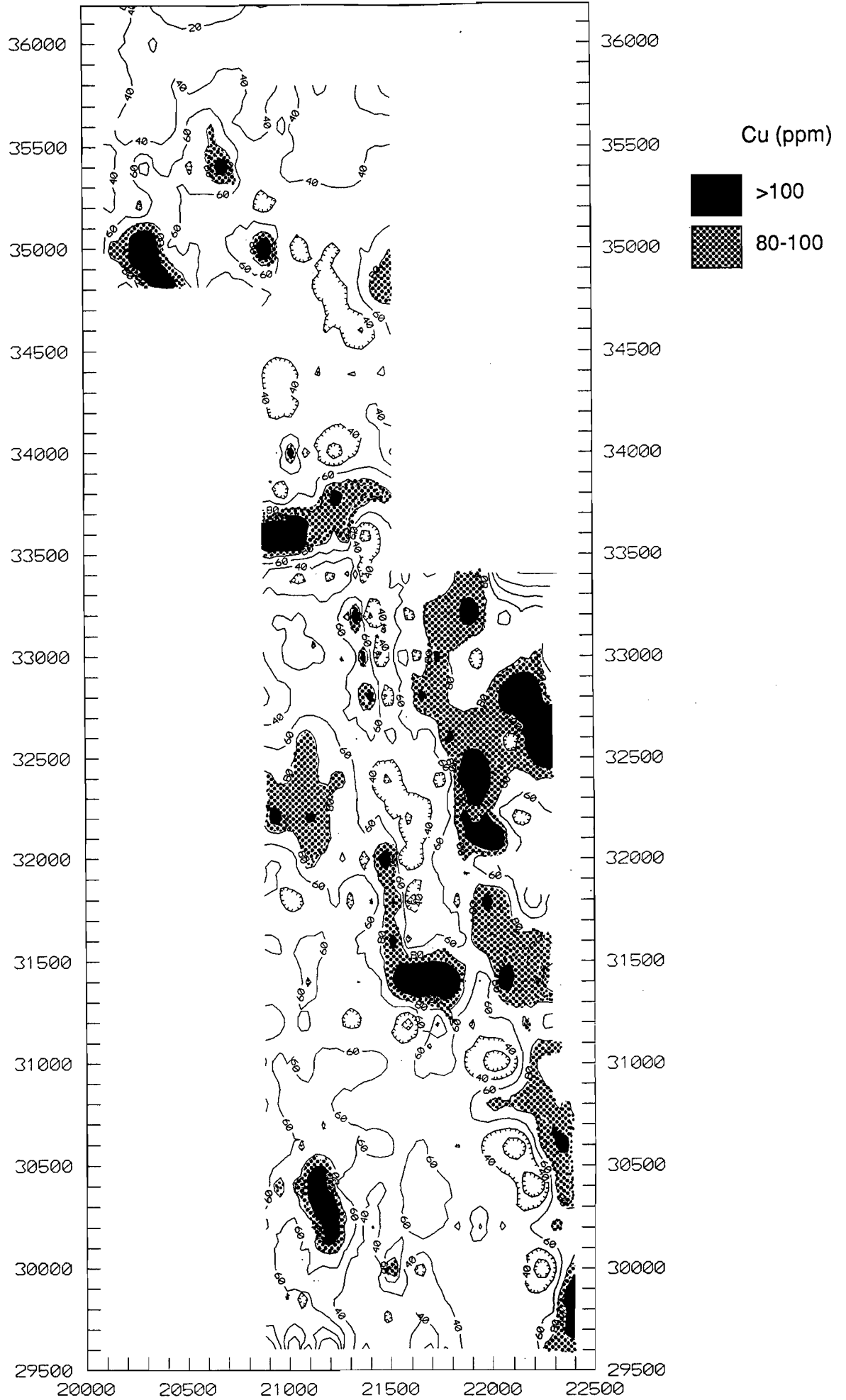
Confidence limit 10

Components showing high positive correlation ($\alpha < 0.001$)Al₂O₃ MgO CaO Na₂O TiO₂ P₂O₅ Ba Co MnComponents showing high negative correlation ($\alpha < 0.001$)SiO₂ Ni

The Cu data has a high standard deviation but is approximately normally distributed.

The Cu distribution does not specifically follow a particular lithology but concentrations are consistently higher in the eastern side of the study area where clay-rich soils derived from the tholeiitic basalts are located. Some linear trends that follow the chert may reflect minor sulphide units. The zone of high Cu concentrations extending ENE from 20900E 33600N appears to coincide with the subcrop of a cross-cutting Proterozoic dyke. Other high Cu concentrations are also close to the margin of dykes. Anomalously high Cu contents in some of the lateritic gravels is presumably due to scavenging by iron oxides. This includes the area associated with Au mineralization in the West Bounty Pit.

Figure 21 (opposite): Distribution of Cu by soil auger sampling.



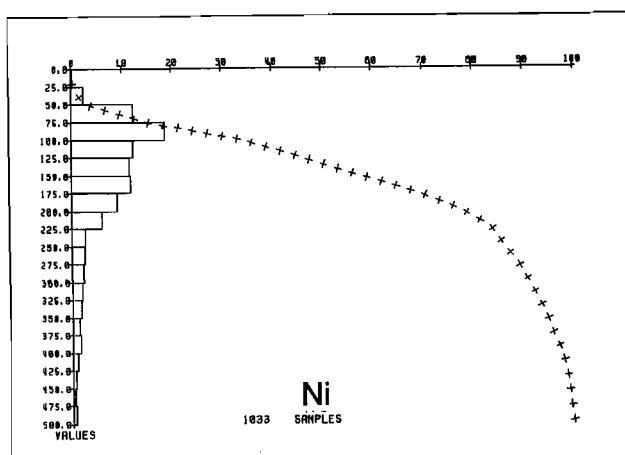
Ni.

Mean value (ppm) 170

Standard deviation 140

Range 12 to 2015

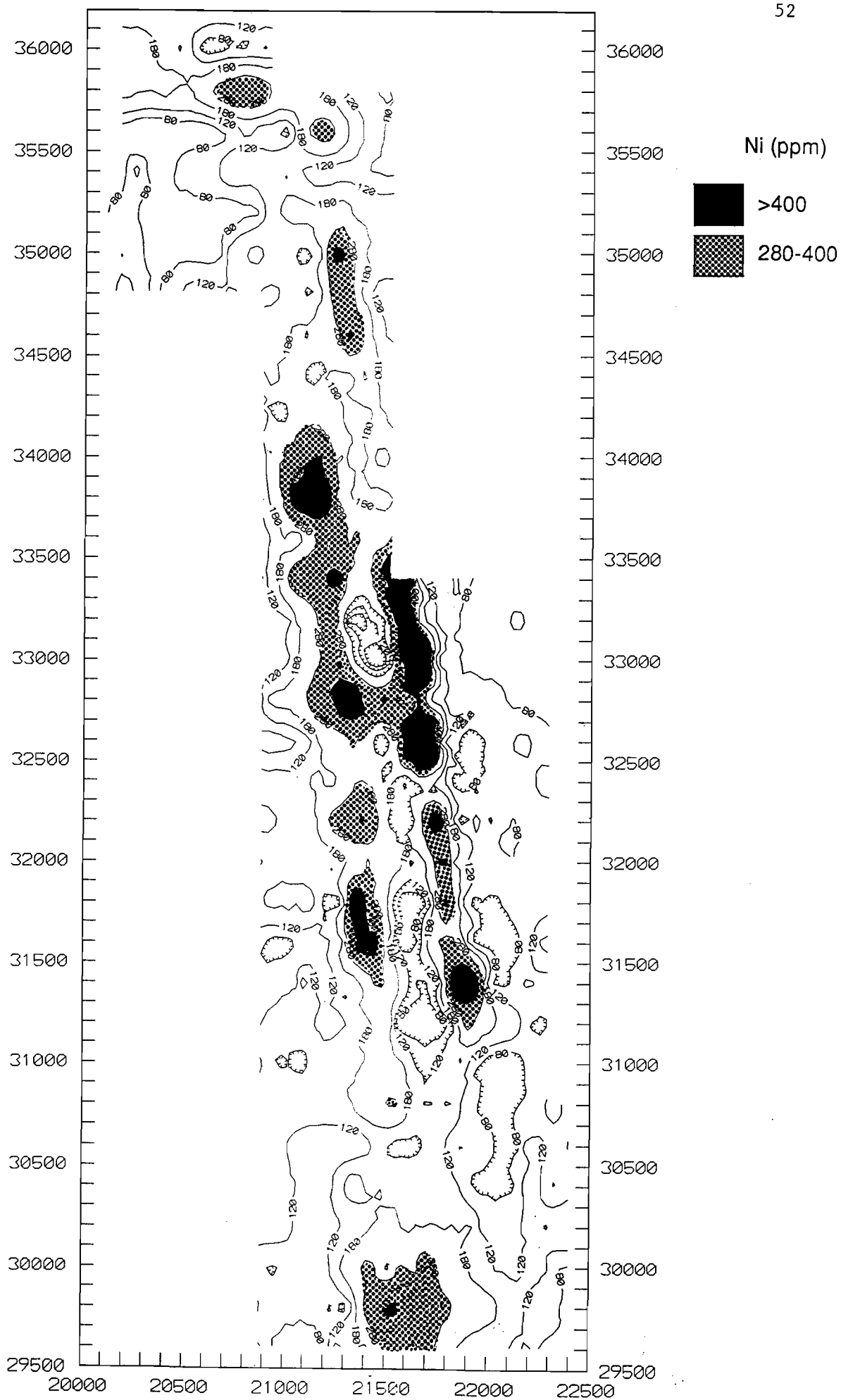
Confidence limit 20

Components showing high positive correlation ($\alpha < 0.001$)SiO₂ MgO Na₂O K₂O Co Cr MnComponents showing high negative correlation ($\alpha < 0.001$)Al₂O₃ Cu V

The distribution of Ni data is highly skewed and may indicate the presence of two populations with similar mean values.

High Ni concentrations are associated with silcretes and lateritic gravels overlying dunites and komatiites that flank the siltstone and sandstone units. These units follow a linear trend through the centre of the study area. Here, Ni concentrations appear to parallel those for Cu and Cr. Cobalt, with which Ni is correlated, shows similar but more localised concentrations in this area. The high nickel contents (e.g. 2015 ppm) are typical of enrichments occurring within laterite derived from weathering of Mg-silicates in ultramafic rocks.

Figure 22 (opposite): Distribution of Ni by soil auger sampling.



Further Discussion

Bounty Pit mineralization is associated with a shear occurring within a near vertical west dipping metamorphosed sediment described as chert/BIF. The sediment is sandwiched between metadolerite in the hanging wall and a komatiite- high Mg basalt-ultramafic sequence in the footwall. This lithological sequence extends the entire length (approximately north-south) of the study area. Gold mineralization occurs mainly in zones of silica-sulphide-carbonate alteration within the sediment.

Mineralization at the Bounty Pit has an average grade of 5 gpt from 0-60m, 8.9 gpt from 60-310m and continues below this. Near the surface, mineralization is about 20m in width, however, the soil auger anomaly (>80 ppb) extends downslope over 750m. An explanation for this phenomenon comes from a detailed examination of soil profiles in the vicinity. These profiles were deep enough to include samples at least to the depth of the soil auger sampling program. There is minimal lateritic cover over mineralization presumably due to erosion or chemical weathering. Soils predominantly consist of a heavy homogeneous clay loam containing friable pedogenic carbonate. The earlier study demonstrated that the Au in the soil is intimately associated with this carbonate (Figure 23). In addition, its position and structure suggest that it is actively accumulating. The nature of the Au-alkaline earth relationship points to a chemical rather than a purely mechanical dispersion mechanism. Presumably, solutions containing Ca, Mg and Au are dissolving and later precipitating the metals at approximately the same time. The origin of the solution is probably meteoric (rain) since the water-table is tens of metres below the surface, whereas the origin of the solutes is clearly the narrow mineralized surface zone. Re-working of the Au, alkali and alkaline earth metals in the soil profile then takes place, facilitated by vegetation via plant uptake and leaf litter fall. Dilution of the Au anomaly increases with distance away from and downslope of mineralization and, therefore, explains the shape of the displaced "mushroom" shaped Bounty Pit anomaly (Figure 24).

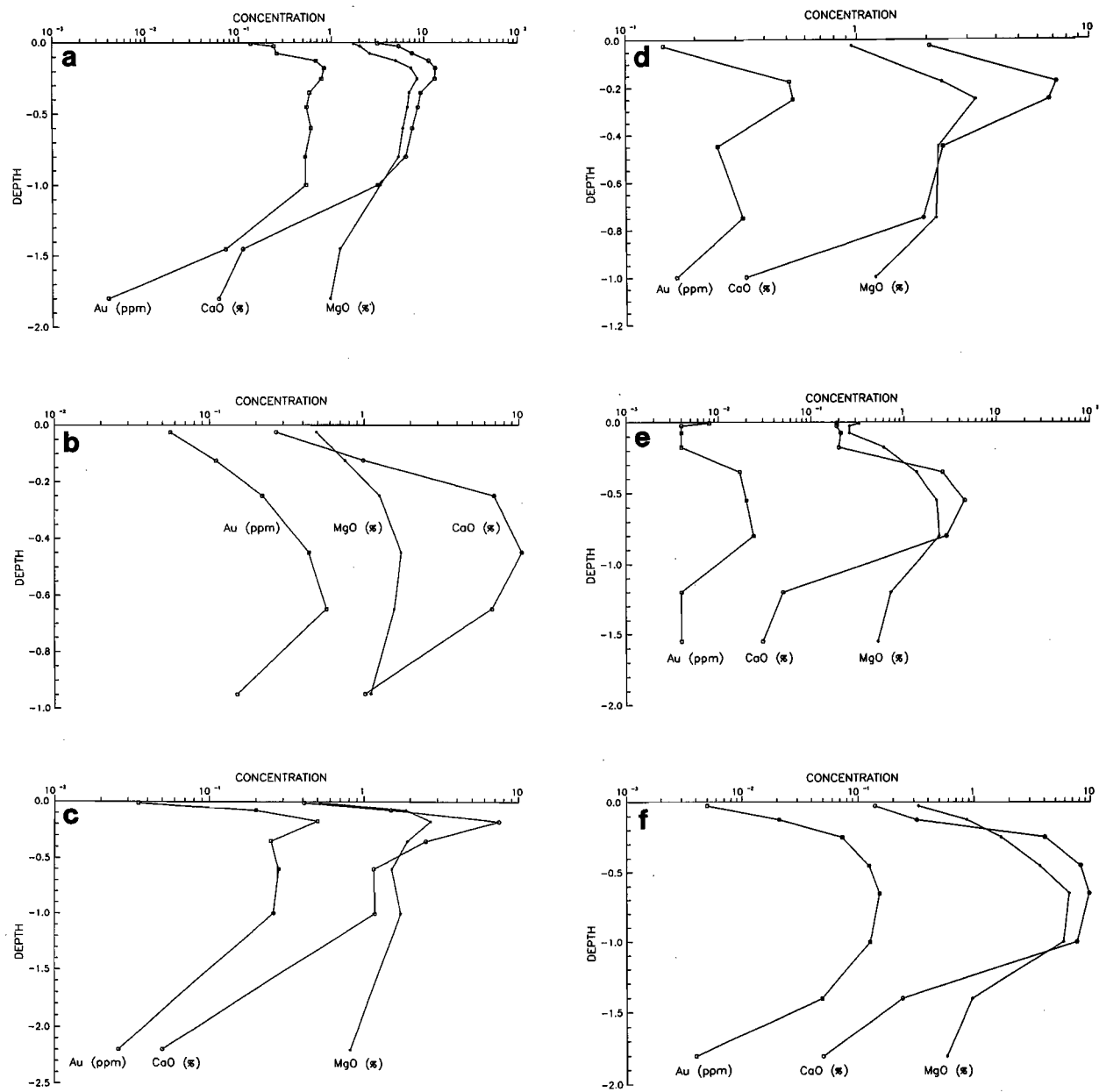


Figure 23: Depth v concentration for CaO, MgO and Au in carbonate-rich profiles: a) pit 1; b) pit 4; c) pit 5(a); d) pit 5(d); e) pit 6; f) pit 7. (From Lintern, 1989).

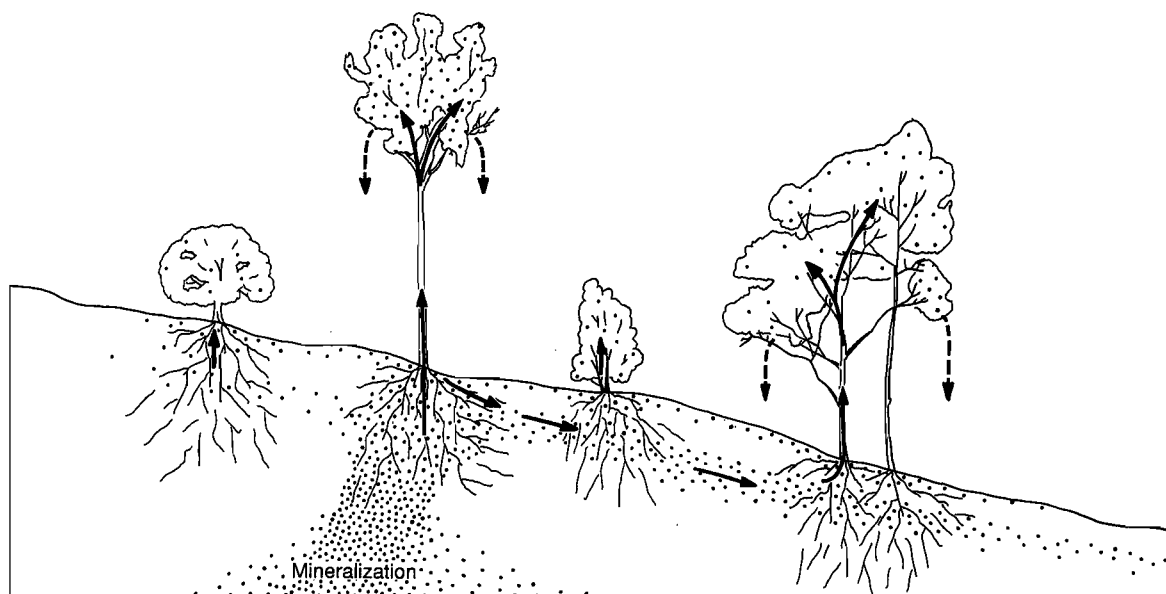


Figure 24: Schematic dispersal pattern of Au (dots) proposed for the Bounty Pit anomaly.

Further from mineralization, the pattern of concentration in the carbonate horizon continues, but the Au contents progressively decline. This is not necessarily the case for the alkaline earth metals. Although there is carbonate alteration associated with primary mineralization, alkaline earth metals are abundant in the country rocks, mainly in silicate minerals, and on weathering also give rise to carbonate accumulation in soils. There are difficulties, therefore, when interpreting Au/CaO ratios over a broad area since this does not take into account the dilution effect caused by carbonates originating from a non-mineralized source. Nevertheless, a plot of Au/CaO ratio for CaO concentrations greater than 1% is useful since it emphasizes anomalies relatively high in Au for the amount of carbonate (CaO) present (Appendix Figure 1). The anomalies present in the ratio map not coincident with Au anomalies occurring in the distribution map represent additional areas requiring further investigation.

The West Bounty Pit anomaly, in contrast with the Bounty Pit anomaly, occurs within lateritic gravels. Drilling suggests it to be associated with quartz

stringers within tholeiitic basalts. These veins, however, are only weakly mineralized, although the strength of the soil anomaly, whilst spatially smaller, is comparable to that found at the Bounty Pit. At least two possible explanations for the anomaly exist, they are : (i) that the anomaly in the lateritic gravels represents a strong accumulation of Au derived from quartz mineralization; the size of the anomaly may indicate that there are other veins yet to be located, or the now weathered portions of the veins were more strongly mineralized; or (ii) that the anomaly is a remnant of a more extensive anomaly over the Bounty Pit, now, largely eroded; if this is the case the original laterite cover over the Bounty Pit may have had even higher Au values.

The North Bounty Pit anomaly is slightly weaker than the previous two. Mineralization is associated with the same sediments as those found at Bounty. The two Pits are separated by the Binneringie dyke. Like the Bounty Pit anomaly, the Au is associated with carbonate but is displaced downslope from the known mineralization. This may be a topographic effect or indicative of further mineralization at depth. The identification of further soil anomalies in the area may lead to the discovery of Au mineralization associated with quartz stringers.

Of the remaining Au anomalies, several have been examined in further detail by excavating small pits using a back-hoe. These are to be described in a later report. They all show a strong Au-carbonate association but the underlying mineralization, as indicated by available drilling, is weaker than that at Bounty and North Bounty. Nevertheless, each soil anomaly can be related to mineralization in bedrock. The size and strength of each anomaly does not, however, reflect known underlying Au concentration; for example, the anomaly at 21420E 31000N (peak of 380 ppb and 400 metres in length >40 ppb) has insignificant underlying Au (3 drillholes with 5m <200 ppb) whereas a similar soil anomaly at 21420E 31800N (peak of 250 ppb and 500 metres >40 ppb) has moderate Au mineralization (2 drillholes with 30m averaging 700 ppb). Further detailed drilling may be required to find the source of the anomalies.

FURTHER STATISTICAL ANALYSIS

Introduction and methods.

The data were analyzed using two multivariate methods. These were (1) R-Q mode principal component (PC) analysis and (2) cluster analysis.

(1) R-Q mode PC analysis.

R-Q mode PC analysis is a form of PC analysis (see Davis, 1986, p.584) that extracts linear components which represent systematic variations within a data set. The advantage of this technique, over standard methods of PC analysis, is that it scales the data such that the scores of the variables (also referred to as factor scores) and the scores of the soil samples can be projected onto the same axes. This allows the simultaneous examination of relationships between the samples and the variables. The number of significant PCs is usually less than the number of variables, so it is a compact way of expressing the variation of the data by combining variables that are linearly related. The loadings represent the weight that each variable contributes to a particular factor. In some cases, these factors represent systematic differences in geochemistry and often reflect geological weathering processes. In other cases, however, particularly for the less significant factors, the linear relationships between variables may have no apparent meaning.

(2) Cluster analysis.

Cluster analysis divides the data into "natural groups" based on their statistical differences. The analysis commences by generating random seeds within the multidimensional data space which initially define group centres. The procedure then iteratively assigns each soil sample into a specific group based on its Euclidian (or multidimensional) distance from the group centres. The iterations continue until the calculated Mahalanobis distances (the distances between group centres) are minimized and the group centres become stable. The technique is very sensitive to outliers and the initial ordering of the data can affect the results. Despite some instability in the group centre solutions, significant groups are robust enough that the group centres stabilize even though outliers may be eliminated or the initial order of the data is changed.

The P_2O_5 and Be data have been eliminated from R-Q mode PC and cluster analysis since they frequently occur at or near their detection limit.

Results and Discussion.

The minor element concentrations are highly variable and many range over several orders of magnitude. Advanced types of statistical treatment assume the data sets are normally distributed, or nearly so, so logarithmic transformation was performed to improve normality. The success of the improvement can be measured, in part, as following transformation, the correlation coefficient between most minor and major elements noticeably increased (Table 1). In particular, the correlation coefficients between Au, Mn and Ba showed a stronger affinity with the major alkalis and alkaline earths; correlation coefficients between Au, Mn and Ba also increased significantly.

	Eigenvalues	% Contribution	Cumulative % contribution
1	7.35	40.88	40.88
2	3.21	17.87	58.75
3	1.73	9.64	68.40
4	1.15	6.43	74.83
5	.99	5.50	80.34
6	.70	3.89	84.23
7	.65	3.62	87.86
8	.46	2.58	90.45
9	.38	2.13	92.58
10	.34	1.92	94.51
11	.24	1.34	95.85
12	.19	1.11	96.96
13	.15	.85	97.82
14	.11	.64	98.47
15	.09	.51	98.98
16	.08	.49	99.48
17	.05	.28	99.76
18	.04	.23	100.00

Table 2: Eigenvalues, % contribution, cumulative % contribution for Mt. Hope Soils subset of entire data series (logarithmic transforms) excluding P₂O₅ and Be.

R-Q mode PC analysis.

Eigenvalues generated by R-Q mode PC analysis showed that almost 95% of the variability observed in the data are accounted for by a combination of the first ten factors (Table 2).

	SiO ₂	Al ₂ O ₃	Fe ₂ O ₃	MgO	CaO	Na ₂ O	K ₂ O	TiO ₂	As	Au	Ba	Co	Cr	Cu	Mn	Ni	V	Zr
SiO ₂	1.00	-.41	-.64	-.15	-.24	.02	.10	-.31	-.22	.08	.02	-.37	-.32	-.35	-.15	.12	-.63	-.11
Al ₂ O ₃	-.41	1.00	.43	-.48	-.45	-.23	-.30	.45	.11	-.13	-.09	.12	.18	.29	-.27	-.26	.49	.41
Fe ₂ O ₃	-.64	.43	1.00	-.47	-.44	-.55	-.59	.48	.36	-.16	-.20	.44	.63	.05	-.23	-.09	.92	.54
MgO	-.15	-.48	-.47	1.00	.84	.59	.53	-.37	-.19	.19	.20	-.01	-.30	.12	.50	.22	-.43	-.55
CaO	-.24	-.45	-.44	.84	1.00	.56	.58	-.36	-.19	.14	.19	-.13	-.38	.17	.52	.02	-.40	-.59
Na ₂ O	.02	-.23	-.55	.59	.56	1.00	.77	-.21	-.26	.13	.33	-.03	-.39	.22	.50	.15	-.51	-.39
K ₂ O	.10	-.30	-.59	.53	.58	.77	1.00	-.32	-.24	.12	.30	-.18	-.43	.08	.47	.11	-.57	-.42
TiO ₂	-.31	.45	.48	-.37	-.36	-.21	-.32	1.00	.05	-.18	-.14	.30	.24	.13	-.09	-.08	.55	.56
As	-.22	.11	.36	-.19	-.19	-.26	-.24	.05	1.00	-.03	-.10	.16	.39	.09	-.17	-.03	.30	.13
Au	.08	-.13	-.16	.19	.14	.13	.12	-.18	-.03	1.00	.09	-.10	-.06	.03	-.03	.08	-.18	-.05
Ba	.02	-.09	-.20	.20	.19	.33	.30	-.14	-.10	.09	1.00	.17	-.19	.15	.18	.07	-.25	-.10
Co	-.37	.12	.44	-.01	-.13	-.03	-.18	.30	.16	-.10	.17	1.00	.41	.18	.37	.44	.35	.12
Cr	-.31	.18	.63	-.30	-.38	-.39	-.43	.24	.39	-.06	-.19	.41	1.00	-.09	-.22	.34	.60	.39
Cu	-.35	.29	.05	.12	.17	.22	.08	.13	.09	.03	.15	.18	-.09	1.00	.23	-.10	.01	-.08
Mn	-.15	-.27	-.23	.50	.52	.50	.47	-.09	-.17	-.03	.18	.37	-.22	.23	1.00	.24	-.24	-.39
Ni	.12	-.26	-.09	.22	.02	.15	.11	-.08	-.03	.08	.07	.44	.34	-.10	.24	1.00	-.16	-.03
V	-.63	.49	.92	-.43	-.40	-.51	-.57	.55	.30	-.18	-.25	.35	.60	.01	-.24	-.16	1.00	.54
Zr	-.11	.41	.54	-.55	-.59	-.39	-.42	.56	.13	-.05	-.10	.12	.39	-.08	-.39	-.03	.54	1.00

	SiO ₂	Al ₂ O ₃	Fe ₂ O ₃	MgO	CaO	Na ₂ O	K ₂ O	TiO ₂	As	Au	Ba	Co	Cr	Cu	Mn	Ni	V	Zr
SiO ₂	1.00	-.40	-.66	.16	-.00	.15	.24	-.36	-.22	.17	.15	-.40	-.30	-.24	-.11	.12	-.66	-.07
Al ₂ O ₃	-.40	1.00	.47	-.43	-.37	-.25	-.32	.54	.05	-.29	-.29	.21	.21	.27	-.25	-.26	.49	.45
Fe ₂ O ₃	-.66	.47	1.00	-.52	-.42	-.49	-.54	.56	.43	-.34	-.42	.47	.68	.05	-.17	-.02	.93	.50
MgO	.16	-.43	-.52	1.00	.92	.89	.87	-.41	-.12	.44	.79	-.03	-.37	.29	.74	.32	-.49	-.55
CaO	-.00	-.37	-.42	.92	1.00	.85	.86	-.36	-.11	.42	.77	.04	-.38	.32	.80	.22	-.39	-.56
Na ₂ O	.15	-.25	-.49	.89	.85	1.00	.87	-.26	-.19	.35	.82	.05	-.41	.33	.74	.26	-.45	-.43
K ₂ O	.24	-.32	-.54	.87	.86	.87	1.00	-.35	-.17	.36	.78	-.05	-.44	.25	.75	.25	-.52	-.45
TiO ₂	-.36	.54	.56	-.41	-.36	-.26	-.35	1.00	.04	-.38	-.29	.44	.31	.05	-.08	-.07	.61	.54
As	-.22	.05	.43	-.12	-.11	-.19	-.17	.04	1.00	-.01	-.17	.16	.51	.05	-.12	.11	.40	.18
Au	.17	-.29	-.34	.44	.42	.35	.36	-.38	-.01	1.00	.38	-.19	-.15	.07	.16	.23	-.35	-.16
Ba	.15	-.29	-.42	.79	.77	.82	.78	-.29	-.17	.38	1.00	.07	-.37	.24	.67	.26	-.44	-.29
Co	-.40	.21	.47	-.03	.04	.05	-.05	.44	.16	-.19	.07	1.00	.36	.19	.30	.27	.41	.12
Cr	-.30	.21	.68	-.37	-.38	-.41	-.44	.31	.51	-.15	-.37	.36	1.00	-.12	-.25	.40	.65	.45
Cu	-.24	.27	.05	.29	.32	.33	.25	.05	.05	.07	.24	.19	-.12	1.00	.36	-.00	.05	-.13
Mn	-.11	-.25	-.17	.74	.80	.74	.75	-.08	-.12	.16	.67	.30	-.25	.36	1.00	.29	-.18	-.42
Ni	.12	-.26	-.02	.32	.22	.26	.25	-.07	.11	.23	.26	.27	.40	-.00	.29	1.00	-.09	-.00
V	-.66	.49	.93	-.49	-.39	-.45	-.52	.61	.40	-.35	-.44	.41	.65	.05	-.18	-.09	1.00	.48
Zr	-.07	.45	.50	-.55	-.56	-.43	-.45	.54	.18	-.16	-.29	.12	.45	-.13	-.42	-.00	.48	1.00

Table 1: Correlation matrix for all components excluding P₂O₅ and Be before (top) and after (bottom) logarithmic transformation.

The Factors.

Factor 1: This accounts for most of the variability (more than 40%) and reflects the degree of compositional variation of the soils. The most important element groups are the major alkalis and alkaline earths, and the iron oxides (Table 3) i.e. the calcareous and the lateritic soils. There is a strong inverse relationship between a lateritic group (Al₂O₃, Fe₂O₃, TiO₂, Cr, V and Zr) and a calcareous group (MgO, CaO, Na₂O, K₂O, Au, Ba and Mn).

	1	2	3	4	5	6	7	8	9	10
SiO ₂	.384	-.626	.234	-.393	.132	.288	.180	.119	.107	.027
Al ₂ O ₃	-.544	.289	-.483	-.128	.383	.108	-.034	-.172	-.376	.134
Fe ₂ O ₃	-.769	.535	.068	.130	-.042	-.137	.021	-.037	.066	-.132
MgO	.905	.301	.067	.042	.026	-.028	.068	-.082	.024	.051
CaO	.860	.396	-.025	.134	-.023	-.137	.048	-.047	.010	.035
Na ₂ O	.853	.358	-.083	-.119	.091	-.007	.121	-.052	-.074	.044
K ₂ O	.883	.256	-.031	-.088	.062	-.013	.199	-.108	-.041	.060
TiO ₂	-.582	.410	-.268	-.445	.009	-.098	.086	.075	.231	.336
As	-.313	.305	.474	.472	.200	.204	.444	.193	-.058	.149
Au	.491	-.036	.325	.152	.534	-.371	-.364	.207	.035	.134
Ba	.794	.321	-.002	-.180	.126	-.128	.143	.086	-.116	-.275
Co	-.203	.713	.058	-.251	-.290	.115	-.169	.451	-.194	-.033
Cr	-.609	.371	.594	-.009	.026	.062	-.036	-.180	-.039	-.025
Cu	.203	.503	-.381	.220	.366	.496	-.227	.029	.243	-.122
Mn	.670	.597	-.087	-.061	-.224	-.033	.049	-.024	.156	.014
Ni	.228	.328	.711	-.340	-.032	.204	-.260	-.230	-.013	.054
V	-.759	.525	-.004	.140	-.025	-.178	.068	-.106	.120	-.031
Zr	-.644	.071	.095	-.446	.444	-.151	.205	.022	.090	-.224

Table 3: Principal Component R-Scores for Mt. Hope Soils subset of entire data series (logarithmic transforms) excluding P₂O₅ and Be. Columns are eigenvectors, rows are variables.

Factor 2: A further 18% of the variation is accounted for by the second factor. The most important major elements of this factor are Si and Fe, and minor elements include Co and Mn. This factor highlights the differences between those soil types overlying the sediments, and the other two major soil types (the calcareous and lateritic).

Factor 3: This factor accounts for over 10% of the variation. Samples with a high third factor are either (1) rich in Al₂O₃ or (2) have significant amounts of Ni, Cr and As. The latter group includes soils developed over ultramafic rocks.

Factor 4: This factor, accounting for over 6% of the variation, is dominated by samples high in As, but not in SiO₂, TiO₂, Zr or Ni. It represents the soils in the lower south-west of the study area which are particularly enriched in As.

Factor 5: This factor has the highest score for Au with Zr, Cu and Al₂O₃ also scoring highly. It accounts for over 5% of the variation. The significance of the element association is unclear but may be weakly related to the occurrence of Au in lateritic soils.

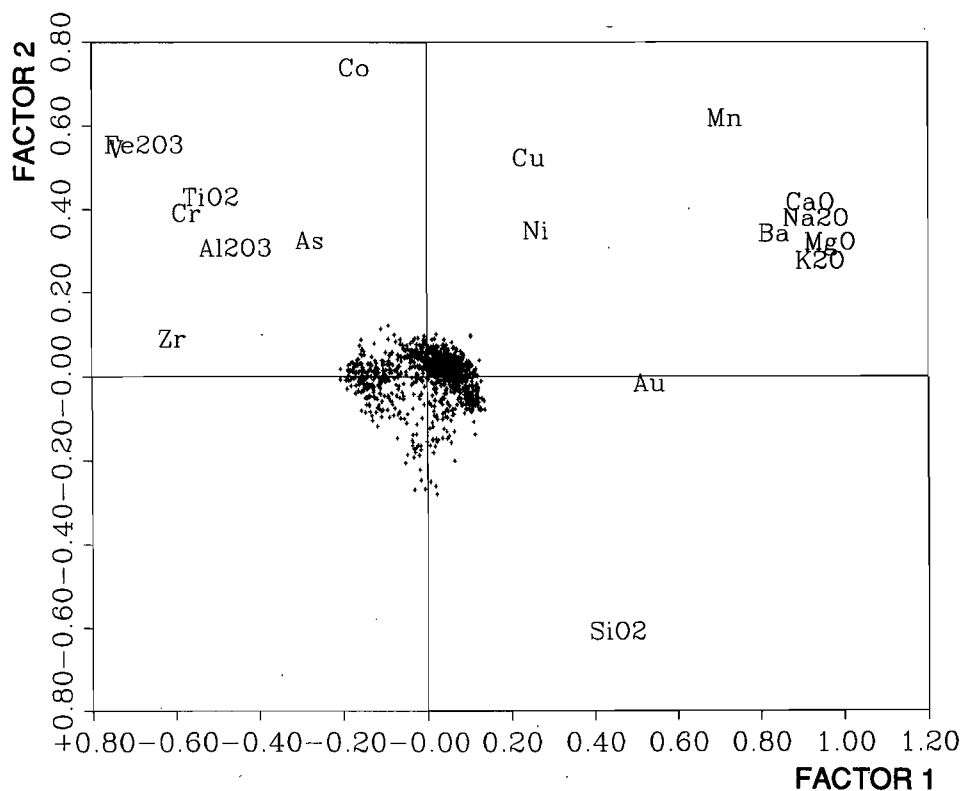


Figure 25: Factor 1 versus factor 2 for Mt. Hope Soils subset of entire data series (logarithmic transforms) excluding P_2O_5 and Be.

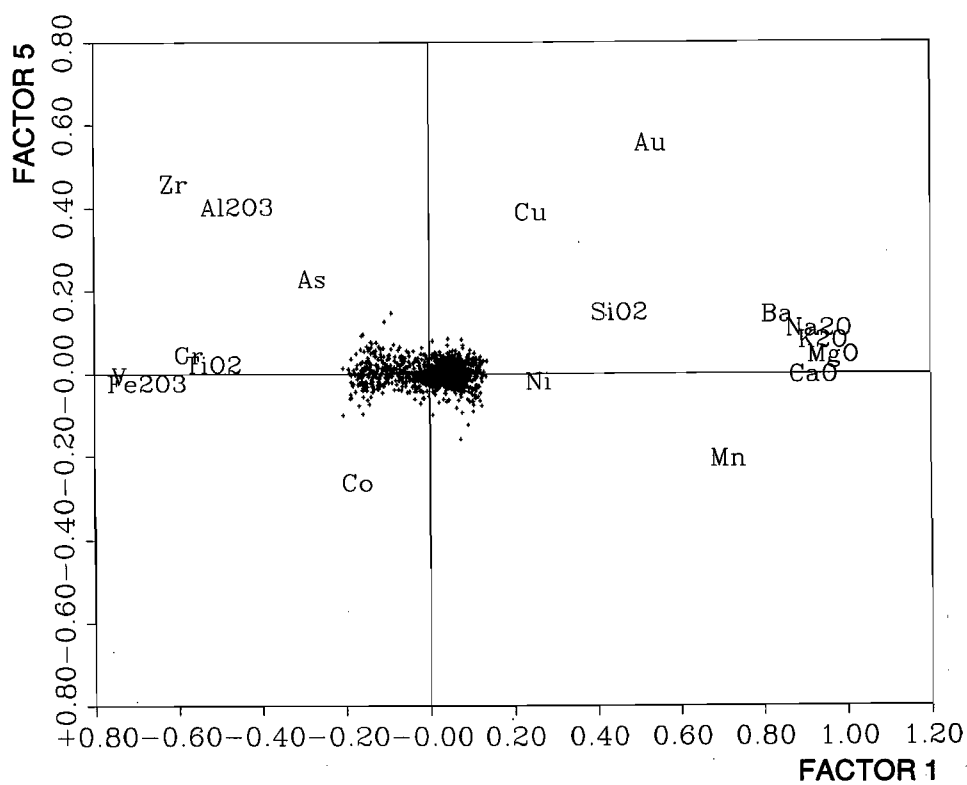


Figure 26: Factor 1 versus factor 5 for Mt. Hope Soils subset of entire data series (logarithmic transforms) excluding P_2O_5 and Be.

The relationship between soil samples and variables is illustrated by plotting the factor scores of the variables and samples onto the factor axes. The plot of factor 1 versus factor 2 divides the samples into three major compositional groups dominated by SiO_2 , Fe_2O_3 , and the major alkalis and alkaline earths (Figure 25). These correspond to siliceous, lateritic and calcareous soils, respectively. There is no strong relationship between Au enrichment and distinct major compositional characteristics as determined by factor 1 (Figure 26). Factor plots, however, are an over-simplification, since the factors are projected onto a plane when they actually are multidimensional.

Cluster analysis.

To detect and describe the presence of further groups, cluster analysis was used. Cluster analysis of the entire logarithmically transformed data set (excluding P_2O_5 , Au and Be) produced in excess of 50 cluster groups. (Gold was omitted in order to identify any independent cluster groups in Au-anomalous areas). The interpretation was simplified by truncating the number of cluster groups displayed to 10 (Figure 27). After examination of the cluster analysis hierarchical tree, comparing basic statistics (Table 4) of the cluster groups and considering their spatial associations (Figure 27) certain soil samples show groupings and have been linked into larger units or geochemical "Domains". Most cluster groups correspond to soils developed over different lithologies, suggesting that these soils have a strong residual character. Some cluster groups, however, overlie or transgress different geological units and hence may represent soils that have chemically transported constituents or have been mechanically transported.

The Geochemical Domains.

Features of individual geochemical Domains (I to VIII) are discussed below:

(a) Domain I consists mainly of samples from cluster group 9 which are high in SiO_2 with appreciable amounts of alkalis and alkaline earths. This domain is generally poor in As, Ba, Co, Cr, Cu, Mn, V and Zr but not Ni. Cluster group 10 samples that occur to the north of this domain are in duplex soils and are much higher in SiO_2 , poorer in the major alkalis and alkaline earths, and very poor in As, Ba, Co, Cr, Cu, Mn, V and Zr but not Ni.

Comparison of arithmetic means

Group	Obs.	SiO2	Al2O3	Fe2O3	MgO	CaO	K2O	Na2O	TiO2	As	Ba	Co	Cr	Cu	Mn	Ni	V	Zr
10	44	80.1	8.6	5.5	0.17	0.10	0.15	0.09	0.47	7	40	10	362	17	73	136	104	108
9	123	62.9	11.1	6.4	2.38	4.34	0.63	0.48	0.44	9	123	16	311	42	294	144	117	113
4	204	47.2	14.3	14.7	2.29	5.11	0.63	0.59	0.66	16	140	26	417	79	635	118	299	122
8	147	47.6	10.3	11.1	4.08	8.09	0.72	0.53	0.47	25	103	21	445	61	593	139	240	96
3	156	50.2	11.4	14.2	3.37	5.06	0.66	0.52	0.53	26	120	32	846	55	542	349	280	119
7	114	48.4	12.7	24.2	1.38	2.56	0.39	0.34	0.63	59	81	33	1122	60	404	214	520	126
2	105	39.4	17.7	33.1	0.04	0.06	0.07	0.04	0.63	88	26	27	1311	67	89	112	702	151
6	87	50.4	13.9	26.2	0.23	0.23	0.14	0.12	0.77	71	54	29	1190	53	152	169	555	166
1	50	35.8	16.5	39.9	0.03	0.09	0.08	0.05	1.05	13	31	38	1076	34	147	91	902	187
5	30	43.1	21.4	21.9	0.26	0.25	0.16	0.18	0.99	6	39	27	433	86	162	66	522	128

Comparison of standard deviation

Group	Obs.	SiO2	Al2O3	Fe2O3	MgO	CaO	K2O	Na2O	TiO2	As	Ba	Co	Cr	Cu	Mn	Ni	V	Zr
10	44	5.2	3.3	2.7	0.15	0.13	0.09	0.08	0.18	4	20	4	181	16	57	108	39	25
9	123	8.4	1.6	2.3	1.73	3.32	0.30	0.26	0.07	6	66	4	121	12	133	76	46	17
4	204	8.1	2.6	6.5	1.56	3.61	0.27	0.28	0.13	21	220	9	189	30	437	50	128	25
8	147	8.2	1.8	3.3	2.33	3.47	0.21	0.17	0.07	24	41	15	183	24	421	59	73	19
3	156	7.8	2.2	5.2	1.43	2.15	0.22	0.19	0.08	23	51	20	381	19	331	244	118	20
7	114	9.0	2.3	6.5	0.83	1.86	0.17	0.13	0.12	48	33	7	369	24	171	113	157	20
2	105	7.8	3.1	8.6	0.04	0.04	0.06	0.03	0.13	105	8	14	688	40	37	48	207	26
6	87	11.6	3.4	9.2	0.18	0.37	0.08	0.09	0.35	71	42	11	572	39	116	85	225	41
1	50	6.9	2.7	7.0	0.04	0.05	0.03	0.03	0.35	11	9	6	658	42	58	35	169	35
5	30	5.1	2.9	6.7	0.22	0.31	0.13	0.14	0.13	6	22	7	162	32	83	14	182	25

Comparison of geometric means

Group	Obs.	SiO2	Al2O3	Fe2O3	MgO	CaO	K2O	Na2O	TiO2	As	Ba	Co	Cr	Cu	Mn	Ni	V	Zr
10	44	79.9	7.9	5.1	0.12	0.07	0.13	0.06	0.44	5	36	8	324	13	59	93	98	105
9	123	62.2	11.0	6.1	1.77	2.63	0.55	0.42	0.43	8	108	15	288	40	265	126	110	112
4	204	46.4	14.1	13.5	1.89	3.73	0.57	0.53	0.65	10	117	25	377	74	511	110	272	119
8	147	46.8	10.2	10.6	3.48	7.27	0.69	0.50	0.46	18	98	19	404	58	514	129	229	94
3	156	49.5	11.2	13.3	3.09	4.41	0.62	0.49	0.53	18	113	29	785	51	493	298	255	117
7	114	47.5	12.5	23.3	1.19	1.86	0.35	0.32	0.62	44	76	32	1065	56	370	191	495	125
2	105	38.6	17.4	31.9	0.03	0.05	0.07	0.04	0.62	44	24	21	1136	57	81	102	669	148
6	87	49.0	13.4	24.6	0.18	0.14	0.13	0.09	0.72	46	45	26	1060	42	123	150	512	161
1	50	35.1	16.3	39.3	0.02	0.08	0.07	0.04	1.02	9	30	37	961	15	135	86	885	184
5	30	42.8	21.2	20.8	0.18	0.15	0.13	0.13	0.98	4	35	26	400	81	145	65	492	125

Comparison of geometric deviation

Group	Obs.	SiO2	Al2O3	Fe2O3	MgO	CaO	K2O	Na2O	TiO2	As	Ba	Co	Cr	Cu	Mn	Ni	V	Zr
10	44	1.07	1.53	1.46	2.33	2.22	1.83	2.21	1.41	2.15	1.60	1.92	1.59	2.40	1.89	2.59	1.41	1.27
9	123	1.15	1.16	1.38	2.27	3.32	1.76	1.67	1.17	1.70	1.62	1.33	1.47	1.36	1.59	1.69	1.42	1.17
4	204	1.20	1.20	1.51	1.83	2.51	1.67	1.67	1.21	2.58	1.58	1.33	1.57	1.42	1.97	1.45	1.56	1.24
8	147	1.20	1.21	1.35	1.77	1.64	1.37	1.35	1.18	2.29	1.37	1.49	1.58	1.38	1.62	1.45	1.35	1.24
3	156	1.18	1.22	1.42	1.52	1.88	1.51	1.51	1.16	2.70	1.36	1.43	1.44	1.47	1.47	1.68	1.55	1.20
7	114	1.21	1.21	1.32	1.69	2.44	1.58	1.51	1.18	2.09	1.37	1.24	1.37	1.48	1.54	1.59	1.38	1.17
2	105	1.22	1.18	1.31	2.74	1.71	1.45	1.85	1.22	3.43	1.37	2.41	1.73	1.78	1.56	1.53	1.38	1.18
6	87	1.27	1.32	1.45	2.10	2.38	1.51	2.02	1.42	2.58	1.69	1.55	1.64	2.00	1.91	1.64	1.50	1.27
1	50	1.22	1.18	1.20	3.07	1.63	1.38	1.67	1.29	2.46	1.29	1.19	1.56	5.44	1.51	1.42	1.21	1.20
5	30	1.12	1.15	1.39	2.49	2.58	1.80	2.35	1.14	2.52	1.59	1.29	1.51	1.43	1.59	1.22	1.42	1.23

Table 4: Comparison of arithmetic means, standard deviation, geometric means and geometric variation for the ten cluster groups.

(b) Domain II consists of cluster groups 6 and 2 and represents iron-rich lateritic soils, occurring over gabbro and dolerite in the western edge of the study area. It is rich in the minor elements Ba, Co, Cu, Mn, Ni, Zr but especially so in As, Cr and V. Cluster group 6 has higher concentrations of carbonate-related elements than cluster group 2 and possibly represents topographically-controlled local accumulations of soil carbonate.

(c) Domain III is comprised of cluster groups 1 and 5. It represents iron-rich lateritic soils that occur on the eastern side of the study area. It is similar to Domain II but it may be distinguished from it by lesser As and V concentrations. Cluster group 5 contains greater concentrations of carbonate-related elements than cluster group 1 and is analogous to cluster group 6 of Domain II but contains significantly lesser concentrations of As, Ba, Cr, Co, Cu, Mn, Ni, V and Zr.

(d) Domain IV consists of a homogeneous mixture of cluster groups 3 and 7. It represents calcareous soils that occur over the flanks and valleys of the lateritic uplands in the western portion of the study area (Domain II). It has concentrations of alkaline earths an order of magnitude greater than those found in Domain II. The concentrations of As, Ba, Cr, Co, Cu, Ni, V and Zr are similar to those found in Domain II. Manganese, though, is markedly higher in Domain IV. Samples of cluster group 3 have richer alkaline earths concentrations than those of cluster group 7.

(e) Domain V consists, predominantly, of cluster group 3. It occurs over ultramafic rocks. Samples here are particularly rich in Ni.

(f) Domain VI consists predominantly of cluster group 8 with a few of cluster group 7. Cluster group 8 samples are the richest in Ca, Mg and K. Cluster group 7 is richer in Cr than cluster group 8. The south part of Domain VI cuts across the known stratigraphy and may either correspond to a drainage or a diagonal fault.

(g) Domain VII occurs in a north-south orientation along the length of the study area and consists of cluster groups 9 and 10. It corresponds with soils overlying siltstones and sandstones. These groups are poor in As, Ba, Co, Cr, Cu, Mn, V and Zr but not Ni and are very rich in SiO_2 .

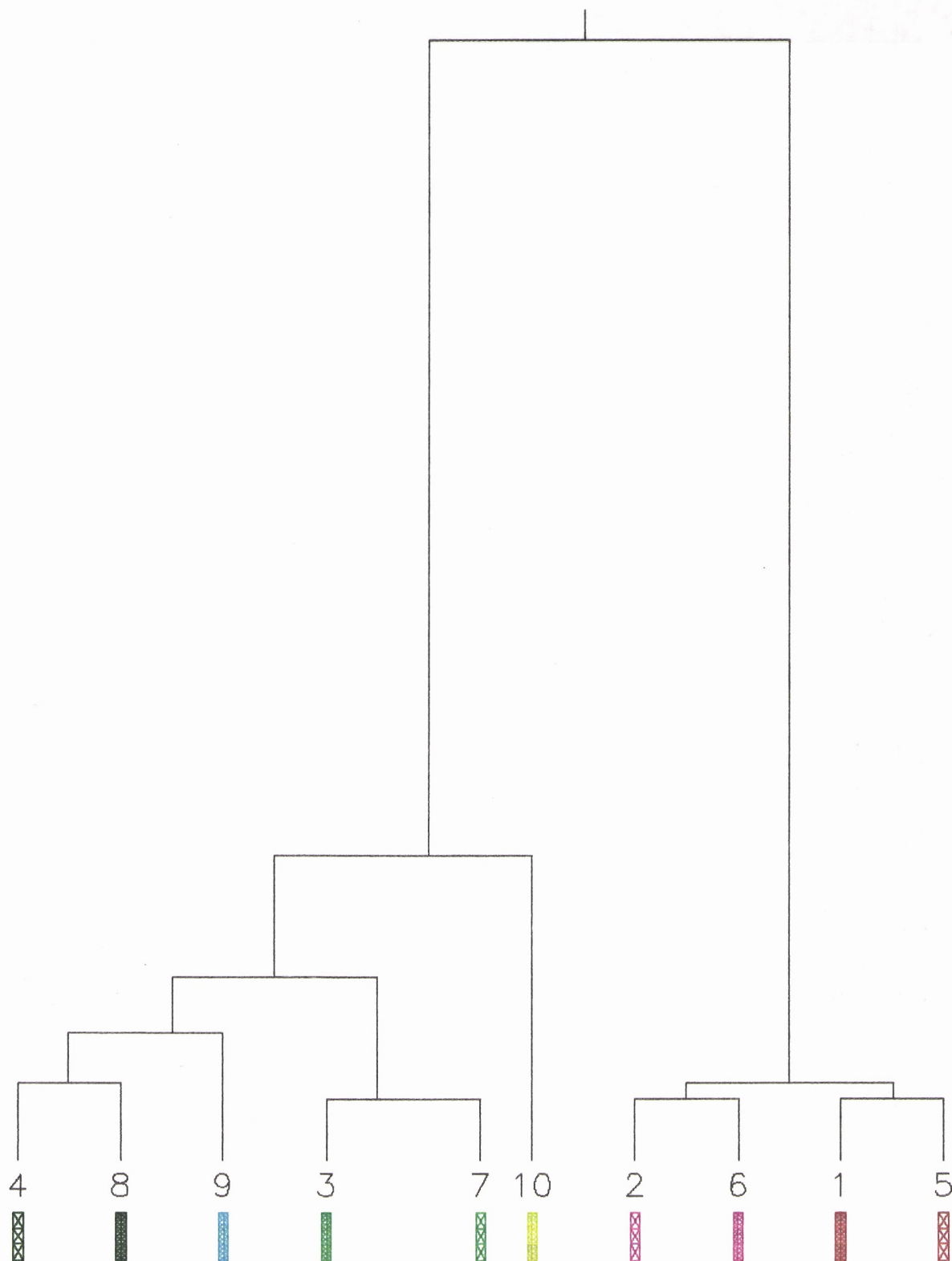
(h) Domain VIII consists of cluster group 4 and comprises carbonate soils in the eastern half of the study area. Soils east of the siltstone/sandstone ridge (Domain VII) tend to be richer in alkaline earths than those to the west and, also, have higher MgO/CaO ratios which may indicate the presence of dolomite. This Domain is characterised by very rich, but variable, concentrations of Ba, Cu and Mn.

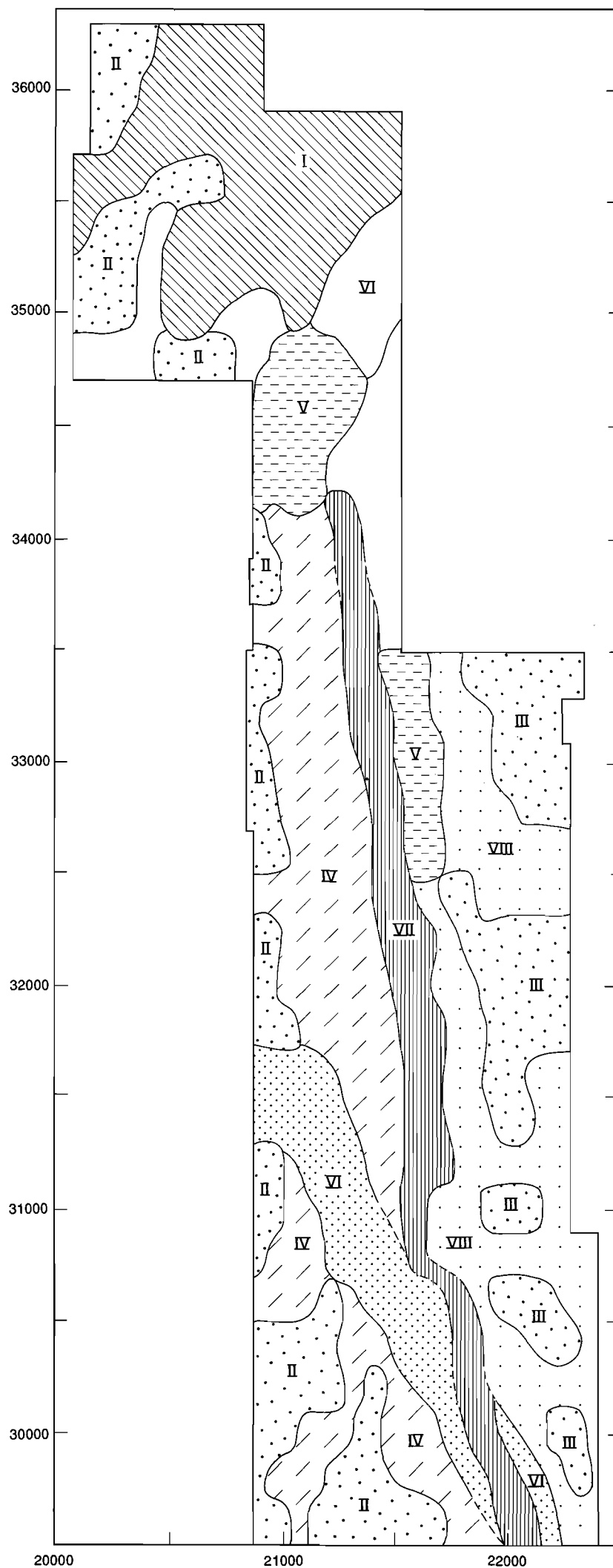
Implications for exploration

The residual nature of many of these soils is important for exploration since Au mineralization is likely to be overlain by a residual Au anomaly. Any such anomalies would require follow-up drilling. Some soil domains that cross cut the stratigraphy appear to be transported. Here, soil anomalies should be interpreted with caution.

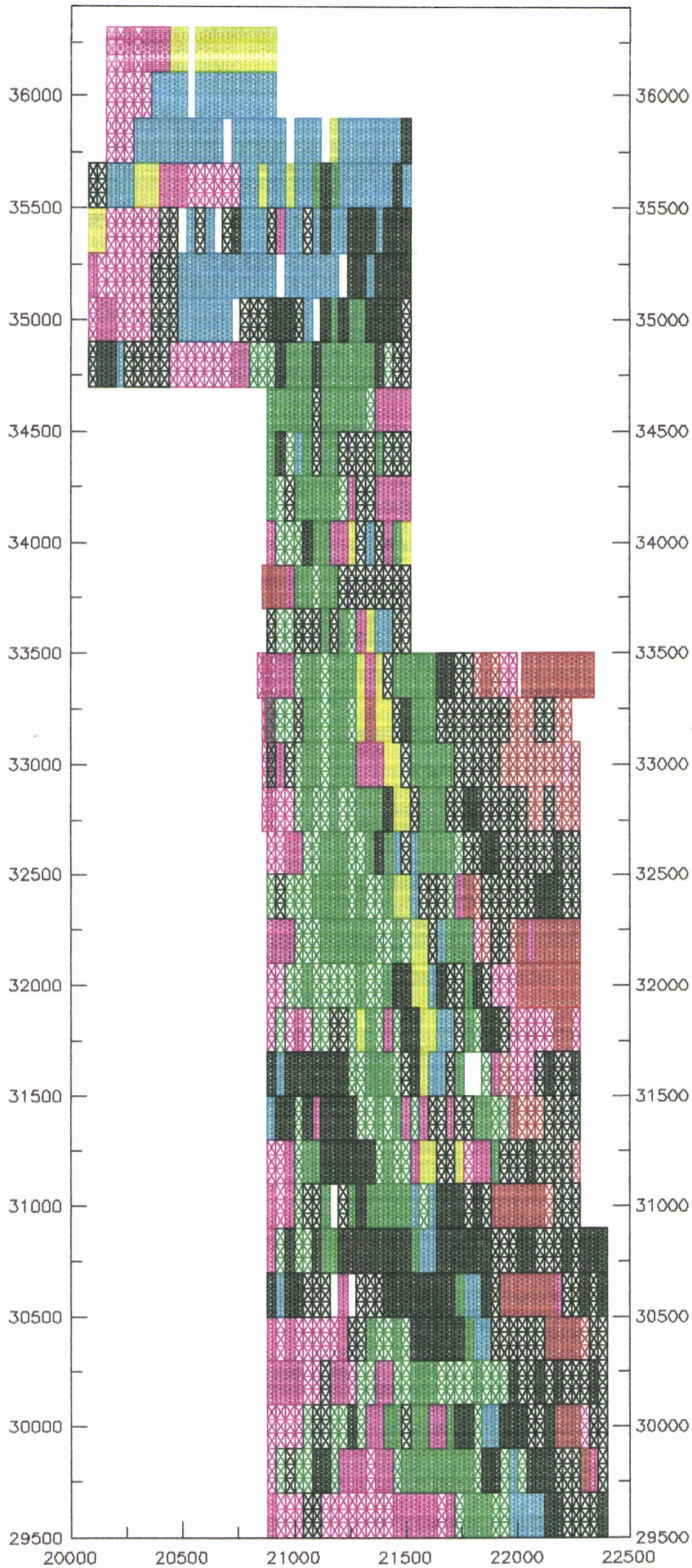
The Bounty Pit soil anomaly includes cluster groups 2, 4, 6, 7 and 9 which, as a whole, encompass a wide variety of element compositions. This large number of different cluster groups suggest that cluster analysis alone is not an appropriate technique to define all Au soil anomalies in the Mt Hope area as it is not sufficiently specific. Nevertheless, the technique is particularly useful in providing (i) information on the derivation of soils, e.g. residual or transported, and (ii) a method for classifying soils based on geochemistry which may provide a lead to the identification of underlying geology. Furthermore, with this information, the explorationist may delineate areas under transported overburden, which are not appropriate for conventional interpretation and may require, for example, bedrock sampling in order to assess the true potential of an area. It may also be possible, with caution, to apply the experience gained in this study to recognise subtle geochemical information in adjoining and more distal areas.

Figure 27: Cluster group and geochemical Domain (overlay) plots for the entire data series (logarithmic transforms) except P_2O_5 , Au and Be (opposite). The legend below describes the relationship and location of the cluster groups (1 to 10). See text for the geochemical Domain (I to VIII) descriptions.





GEOCHEMICAL
DOMAINS



SUMMARY

Examination of the geochemical distribution, soil and geology maps has shown broad associations between element concentrations, soil types and underlying geology. Late features, such as drainages, also leave their imprint on the geochemistry. Various techniques have been used to examine the data. Although no striking exploration targets were found, the study has shown that certain areas may be worthy of further investigation. These are summarised below:

- a) all the Au soil anomalies for which there has been insufficient drilling;
- b) the anomalies indicated by a high Au/CaO ratio (Appendix Figure 1);
- c) the large As anomaly in the south-west of the study area;
- d) the area in the vicinity of Profile 24 which has a high As/Fe₂O₃ ratio as well as 1.8 ppm Au in a magnetic, fine-fraction sub-sample;
- f) the larger Be anomaly;
- g) the apparent relationship between high Cu values and the contacts of some dykes.

ACKNOWLEDGEMENTS

We would like to thank CSIRO staff for their support in compiling this report. Particular, thanks go to P. Combes who was able to fuse almost twice the original number of samples planned for the study area. Thanks also go to C.R. Steel for drafting, D.J. Gray for computer support, J.W. Wildman and G.D. Longman for the ICP analyses, A.K. Howe for the AAS analyses and Analytical Services, Perth for the As analyses. Some of the statistical programs and review of the "Further Statistical Analysis" section were provided by E.C. Grunsky (CSIRO). We are particularly grateful to Aztec Mining Co. Ltd. who provided welcome hospitality whilst we were at Mt. Hope. Thanks also go to I.D.M. Robertson for critical comment of the manuscript.

REFERENCES

- Chin, R.J., Hickman, A.H. and Thom, R., 1984. Explanatory notes on the Hyden 1:250,000 geological sheet, Western Australia. West. Australian Geol. Survey.
- Davis, J.C., 1986. Statistical and data analysis in geology. 2nd edition. John Wiley and Sons, Brisbane, 646pp.
- Hallberg, J.A., 1984. A geochemical aid to igneous rock type identification in deeply weathered terrain. *J.Geochem.Explor.*, 20: 1-8.
- Hallberg, J.A., 1987. Postcratonization mafic and ultramafic dykes of the Yilgarn Block. *J.Geochem.Explor.*, 34: 135-149.
- Johnstone, M.H., Lowry, D.C. and Quilty, P.G., 1973. The geology of southwestern Australia - A review. *J. Roy. Soc. W. Aust.*, 56: 5-22.
- Lintern, M.J., 1989. Study of the distribution of gold in soils at Mt. Hope, Western Australia. Division of Exploration Geoscience Restricted Report No.24R. CSIRO, Floreat Park, W.A., Australia, 36pp.

APPENDIX(overleaf)

Figure 1: Au (ppb) over CaO (%) ratio plot (for CaO>1%).

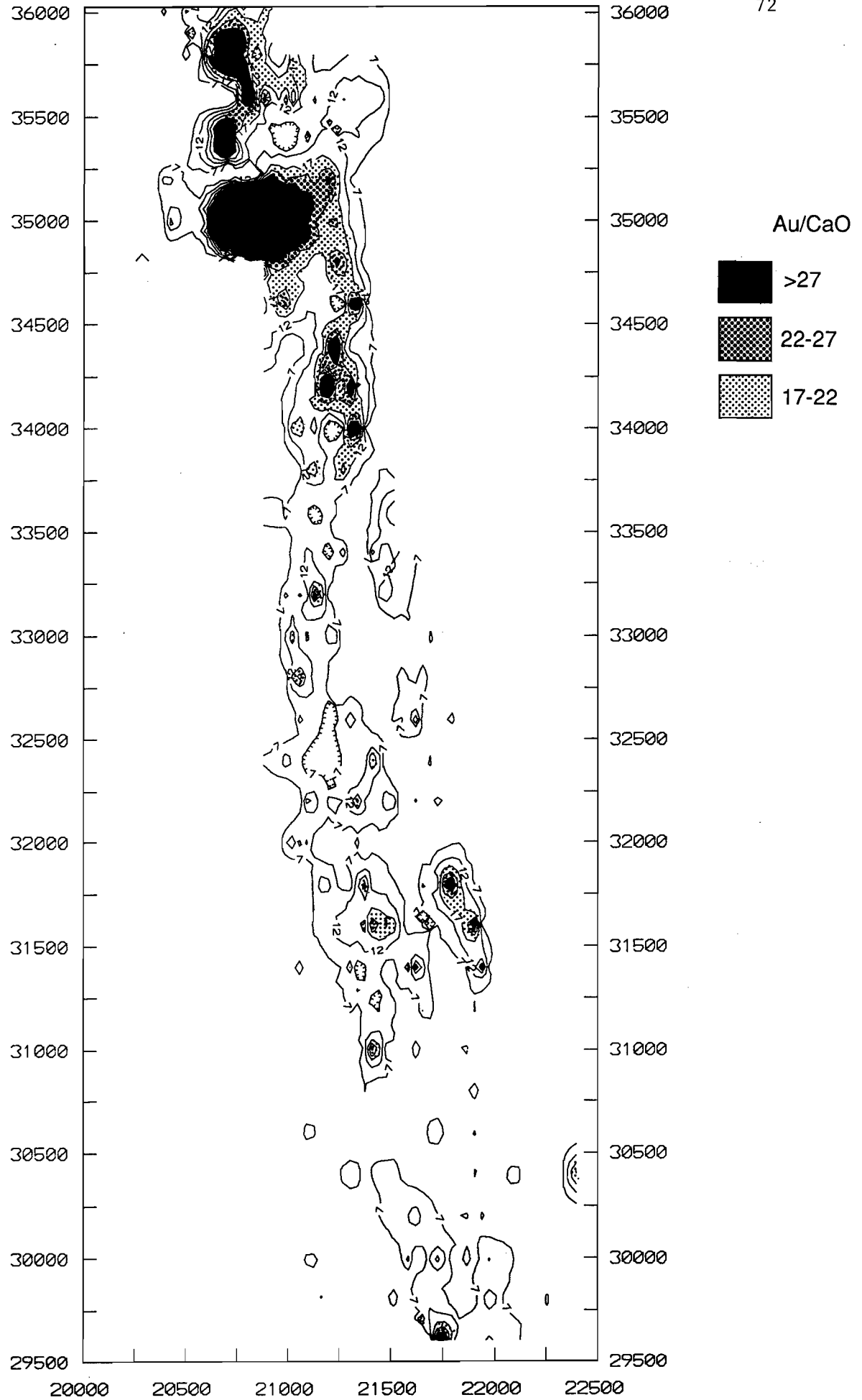


Figure 2: Binary plots for Fe_2O_3 and elements and oxides with which it shares strong correlation coefficients.

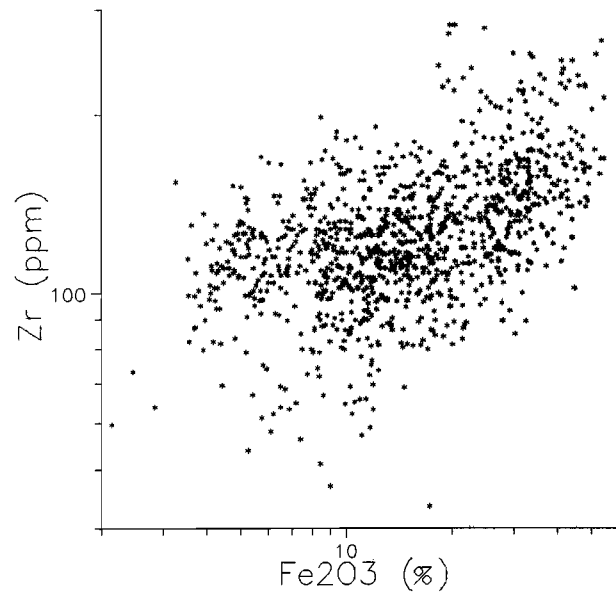
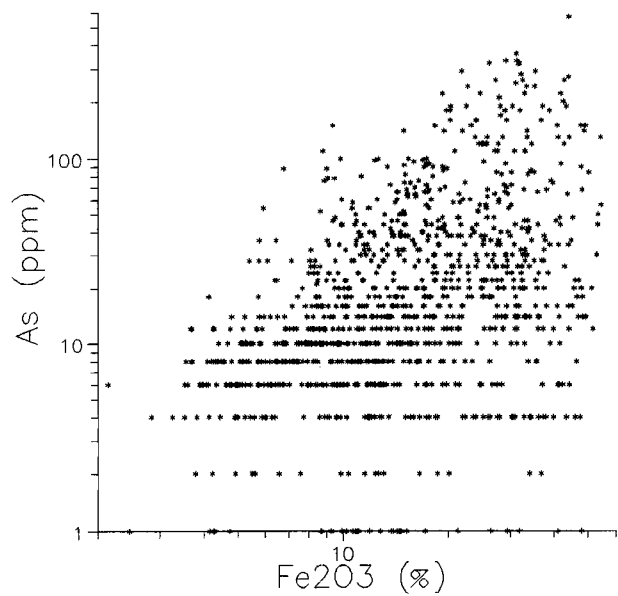
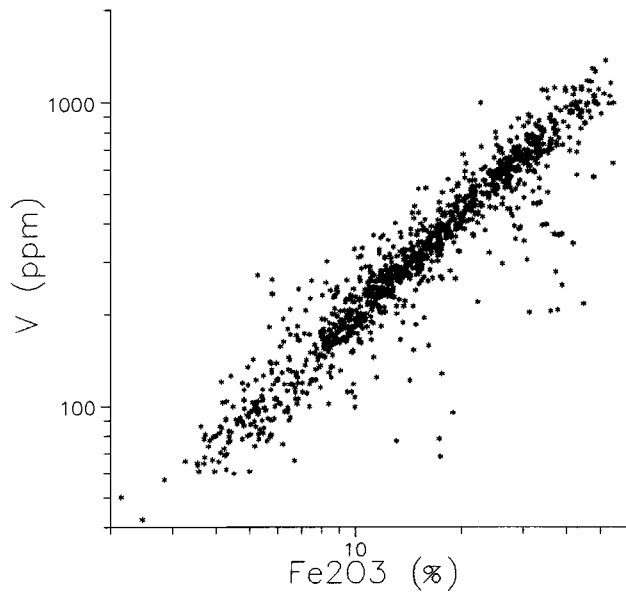
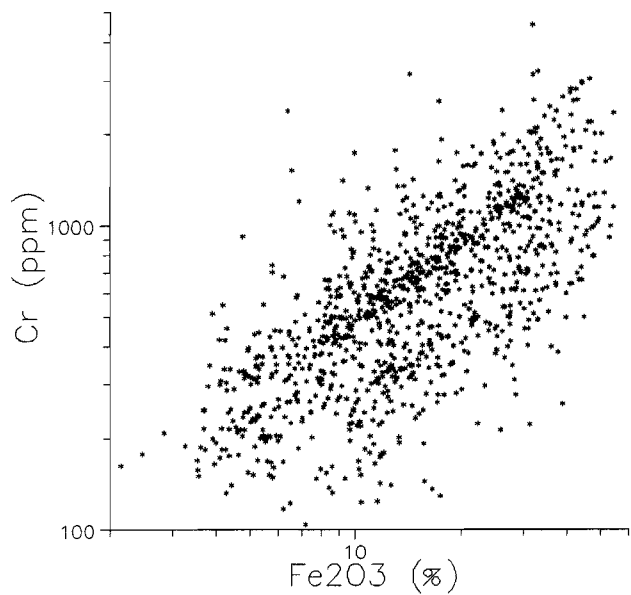
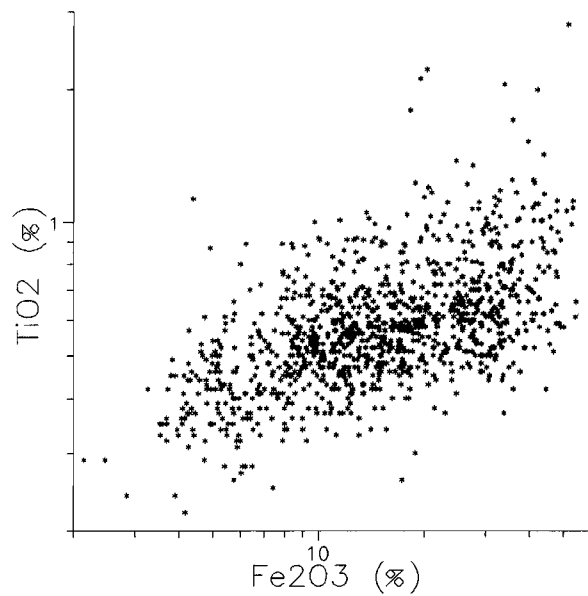
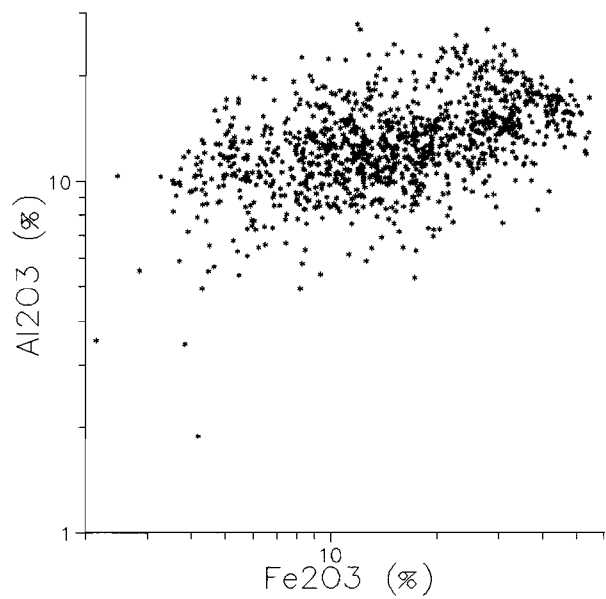


Figure 3: As (ppm) over Fe_2O_3 (%) ratio plot.

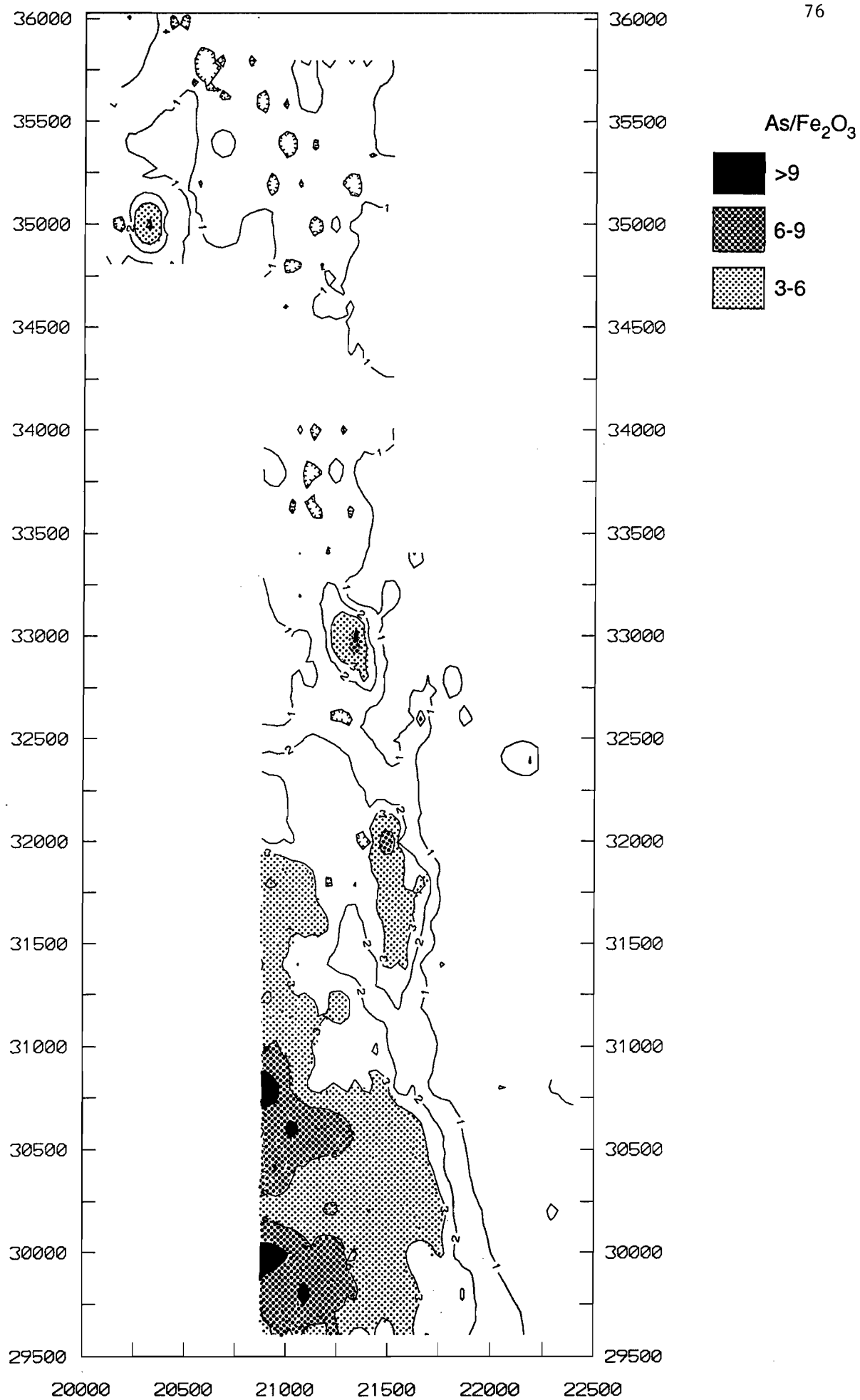


Figure 4: Binary plots for CaO and elements and oxides with which it has a strong correlation coefficient.

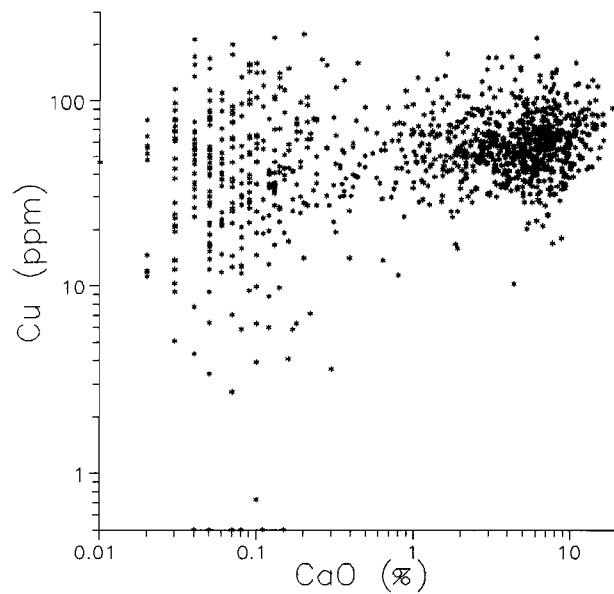
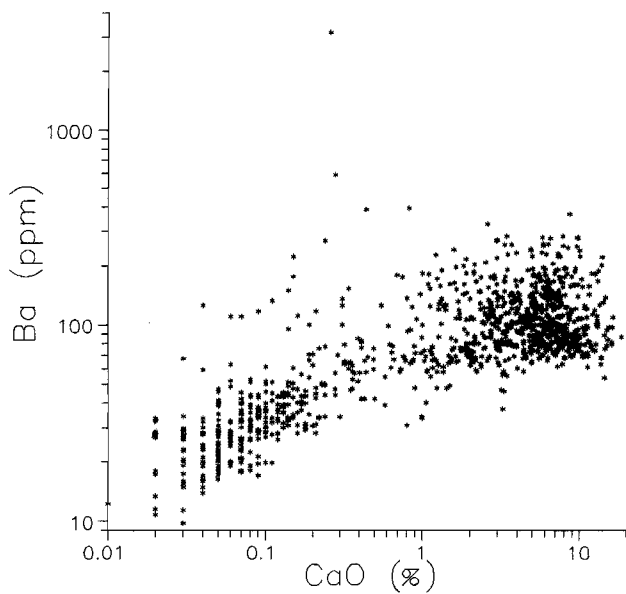
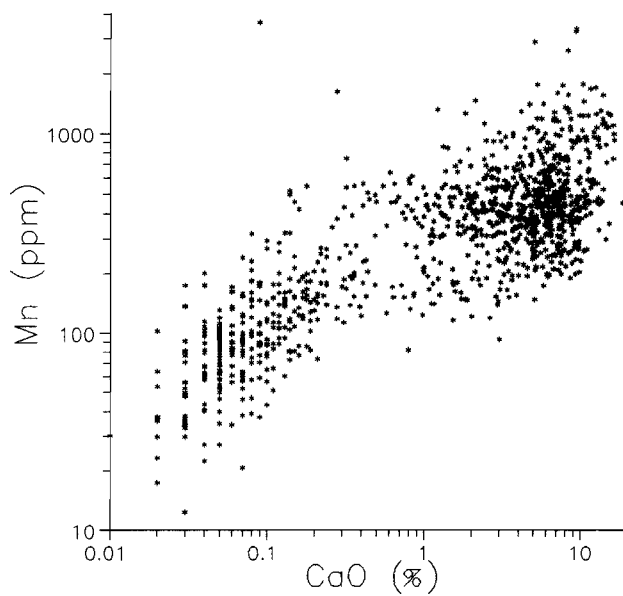
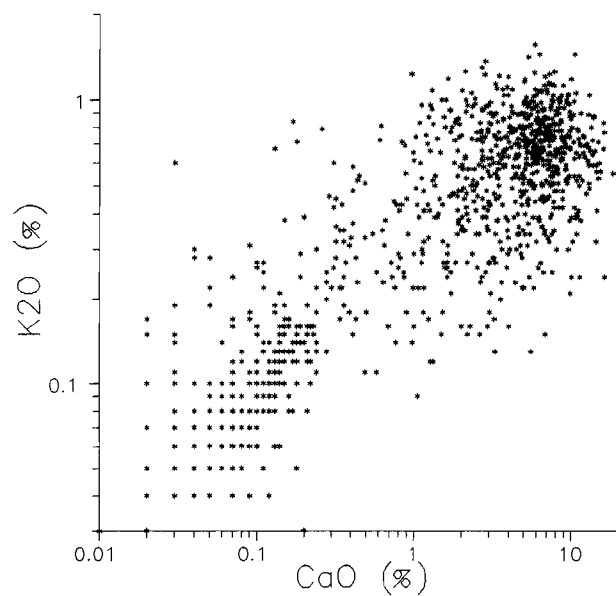
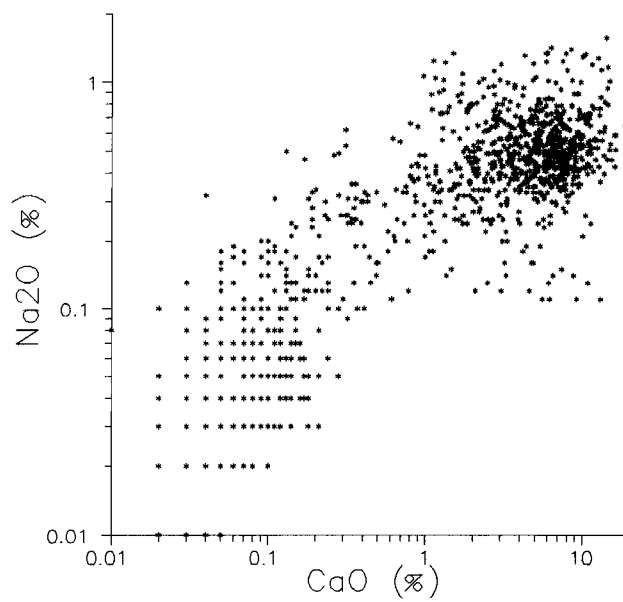
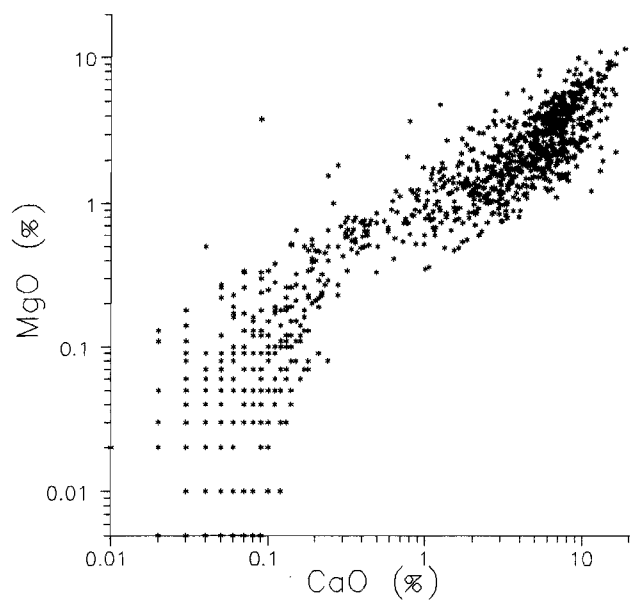


Figure 5: Ti (ppm) over Zr (ppm) ratio plot.

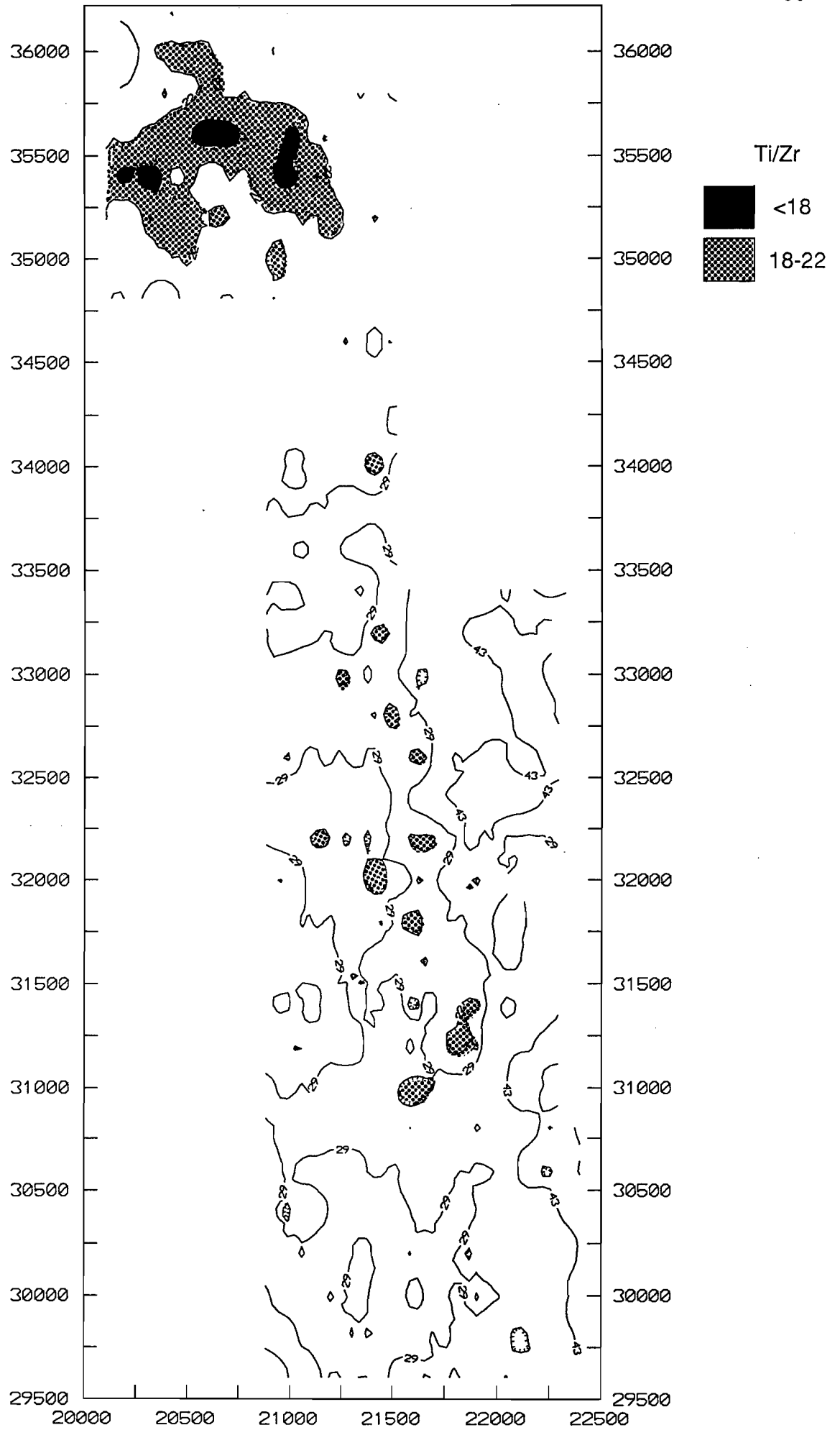


Figure 6: Selected binary plots.

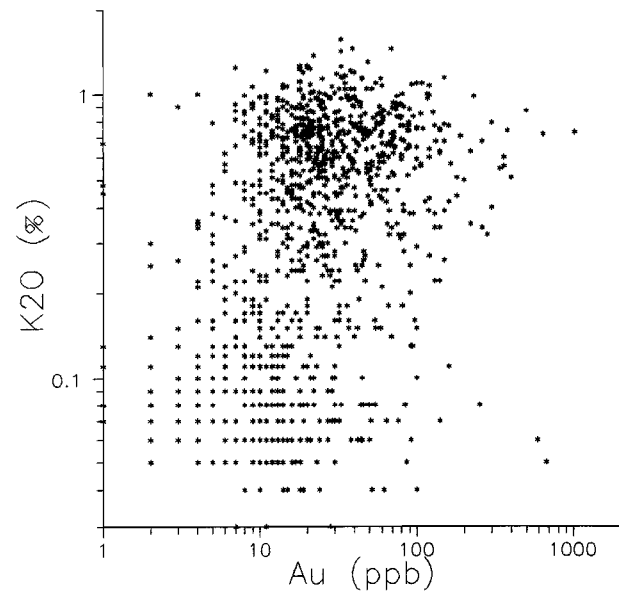
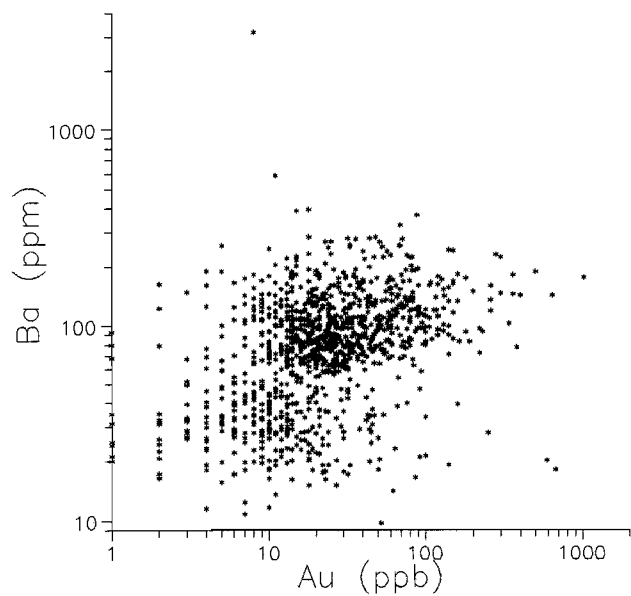
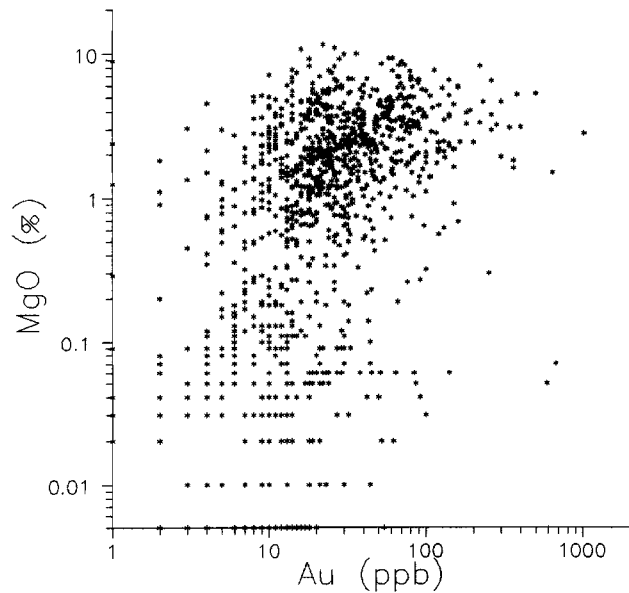
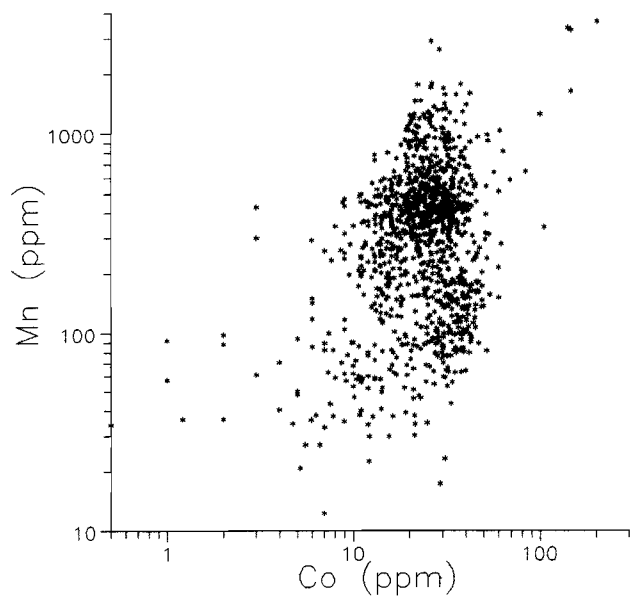
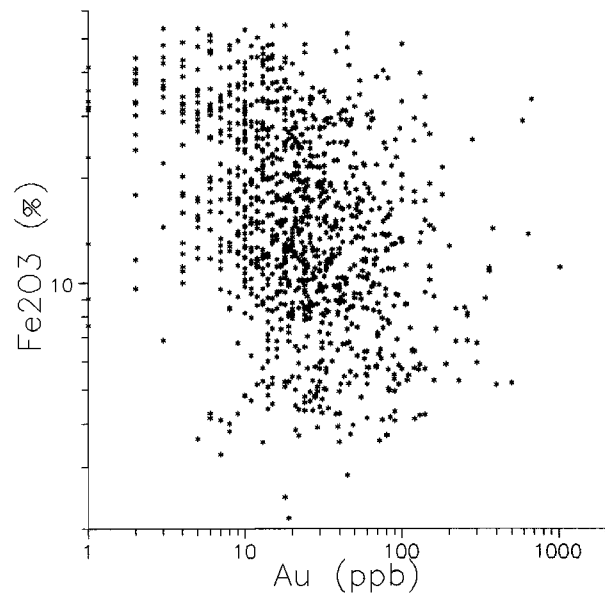
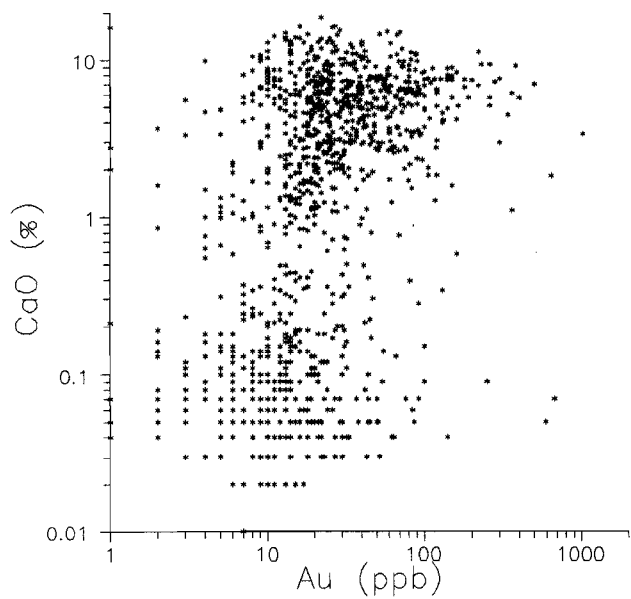


Table 1: Elementary statistical parameters.

Variable	Number of obs.	Minimum value	Maximum value	Arithmetic mean	Standard deviation	Coefficient of variation	Geometric mean	Geometric deviation
SiO ₂	1060	22.2	93.1	49.8	12.3	0.25	48.3	1.28
Al ₂ O ₃	1060	1.9	27.9	13.2	3.7	0.28	12.6	1.34
Fe ₂ O ₃	1060	2.1	54.4	18.0	11.2	0.62	14.7	1.91
HgO	1060	<0.1	11.5	2.0	2.0	1.01	0.8	6.09
CaO	1060	<0.1	18.6	3.7	3.7	1.01	1.2	7.09
Na ₂ O	1060	<0.1	1.6	0.4	0.3	0.73	0.2	3.04
K ₂ O	1060	<0.1	1.6	0.5	0.3	0.69	0.3	2.62
TiO ₂	1060	0.2	2.8	0.6	0.2	0.37	0.6	1.37
P	1060	<0.1	0.2	0.0	0.0	0.80	0.0	1.94
As	1060	1.0	570.0	33.6	51.8	1.54	16.8	3.17
Au	1060	1.0	1020.0	38.1	63.8	1.68	22.0	2.72
Ba	1060	9.8	3171.0	92.9	110.9	1.19	73.3	1.99
Be	1060	<0.1	26.1	1.0	1.7	1.78	0.1	11.69
Co	1060	<1.0	202.0	26.0	13.8	0.53	22.7	1.92
Cr	1060	104.0	4564.0	728.6	526.9	0.72	580.7	1.96
Cu	1060	<1.0	228.0	58.7	32.1	0.55	47.5	2.60
Mn	1060	12.3	3628.0	397.6	357.5	0.90	279.6	2.44
Ni	1060	11.8	2015.0	169.8	140.2	0.83	138.1	1.84
V	1060	42.5	1370.0	378.4	253.8	0.67	299.8	2.03
Zr	1060	43.5	283.0	128.5	35.3	0.27	123.8	1.31